Enemalta
Air dispersion modelling of stack emissions

Second phase final report

Authors

Calori G., Tinarelli G., Radice P., Costa M., Pozzi C., Finardi S.

Report ARIANET R2015.12

Authors: Calori G., Tinarelli G., Radice P., Costa M., Pozzi C., Finardi S.

Customer:

Enemalta Corporation
Central Administration Building, Church Wharf,
Marsa MRS 1000, Malta

Reference number: GN/DPS/T/3015/2012

Non-technical summary

Scope: Electricity for the Maltese Islands is provided by Enemalta Corporation, the state-owned energy utility, which as of 2013 operated two power stations: Marsa (MPS) and Delimara (DPS), with a total installed electrical capacity of 720 MW, provided by a mix of conventional steam units, gas turbines and a new combined cycle diesel engines block at DPS. In March 2015 MPS has been shut down and put on cold standby, pending final decommissioning, while in April 2015 a 200 MW submarine interconnection to the European grid has been inaugurated commissioned and handed over to Enemalta. Enemalta carried out an air dispersion modelling study for DPS in 2011 as part of the IPPC obligations. However, the revised Delimara IPPC permit requires that this dispersion model is updated to reflect changes in the combustion plants and the installation of the cable interconnector. This study is a 2-stage process re-assessing, using dispersion models, the likelihood of current and future emissions from DPS causing exceedances of the limit and/or target values as established in the Ambient Air Quality Regulations of 2010 (Legal Notice 478, 2010), and to assess the likelihood of such emissions causing exceedances of any applicable guideline values for vanadium, especially but not limited to the most sensitive receptor(s) in the prevailing wind direction within a 15 km radius.

Methodology: The dispersion of pollutants is simulated through a state-of-the-art 3D dynamic modelling system, allowing to take into account terrain features, including the presence of the sea, real-time meteorological data, the contributions from all main sources present in the domain as well from long-range transport, including natural sources. The models are fed by hourly meteorological data and, for what concerns power plants emissions, by hour-by-hour emission rates actually recorded by the continuous emission monitoring systems installed at the stacks, according to IPPC prescriptions. The DPS impact is assessed on the basis of the meteorology of three years (2010-2011-2012). The 3D modelling framework also considers the contributions from other relevant emission sources inside Malta as well from natural sources and long-range transport.

Measurements: For what concerns the power plants, the information with the maximum level of detail on the characteristics of their operating units and the flue gas emitted concentrations has been collected from Enemalta and employed for the model application. On most stacks, continuous emission monitoring systems (CEMS) are installed to measure hourly concentrations of flue gases, and the available data are directly used to calculate the emitted masses an their temporal variability.

Transitional operating conditions: The first phase of the study has addressed the current operating conditions, as resulting at the end of year 2013 (a scenario herein referred as "**transitional operating conditions - TOC**"). Consequently, for TOC scenario CEMS data for 2013 have been used. At Marsa, during year 2013, boilers 3 to 8 (stacks M1 and M2) were not used, boilers 7 & 8 (stacks M3 and M4) were still in operation, while the OCGT unit (stack M5) was used only for a very limited time. At Delimara, all units were operational, even if not continuously. Due to technical problems, from Feb 2012 to Jan 2013 the combined cycle gas turbines (CCGT) were switched to the open cycle mode using the bypass stacks (D2 and D3), although for a limited number of operating hours, for efficiency reasons. According to IPPC obligations concentrations of heavy metals are measured at DPS and MPS by analyzing samples periodically collected at the

stacks. For the TOC scenario, measurements made in July-Aug 2013 have been used, modulated for modelling application according to the flow rates recorded by CEMS.

New operating conditions: The second phase of the study has addressed the new operating regime of Delimara Power Station, as the result of closure of Marsa Power Station and the operation of the interconnector. The related scenario ("**new operating conditions – NOC**") relies on the most recent full set of CEMS data, collected during year 2014, and project them on the basis of the operating conditions expected over the whole year as the result of the new configuration: boilers used alternately, combined cycle turbines in standby for most of the year, apart from the summer peak, open cycle ones used for a limited number of hours, and diesels working during different periods over the entire year. Despite the increased use of diesel units, the total pollutants emissions resulting from all DPS units combined are lower for NOC scenario than in TOC one.

Other sources: The model application also includes the emissions from most important sources which may contribute to local air quality: Valletta Harbour ship, Malta Freeport, Malta International Airport, major fuel storage depots (Oil Tanking Malta, San Lucjan Oil Company, 31st March 1979 Fuel storage, Wied Dalam Depot, Marsa Thermal Treatment Facility, road traffic, fishing activities and international shipping routes. There emissions are consistently described using the data of the national emission inventory for 2011 officially reported by MEPA to CLRTAP (Convention on Long-range Transboundary Air Pollution), integrated with additional information: among others, ships statistics and movements in M'Xlokk and Valletta harbours from Port Authority and Malta Freeport, aircraft movements from the International Airport, the amount of fuel stored in the depots, road network features. The emissions from international shipping routes around the Maltese archipelago are assigned from the EMEP database. The contribution from long-range sources is taken into account through a modelling nesting procedure (zooming), allowing to assign proper boundary conditions, ie. background concentrations for chemical species as resulting on an area wider than the target domain of analysis.

Meteorology: The study is carried out using full dynamic and three-dimensional dispersion model, requiring as input three-dimensional meteorological fields on hourly basis over the entire considered period. This means that to correctly drive simulations, simple ground-based meteorological measurements at one or more stations are not sufficient to give a complete view of the atmospheric flow dispersing the emitted pollutants. In particular, a correct simulation of the path of the hot plumes emitted by the elevated stacks of the power plants requires a coherent reconstruction of wind flow, turbulence and temperature fields also at upper atmospheric levels. This is realized through a detailed 3D meteorological modeling over the Maltese Island, starting from the meteorological output fields operationally produced by the QualeAria Air Quality Modeling System, and taking into account Maltese orography and land-use. Data from MEPA continuous monitoring stations have been used for model verification, showing that the reconstructed meteorological scenario can be considered as reliable, also in accounting for the seasonal features. It has to be also noted that the local winds generated by the model from southern sectors exhibit lower speeds, thus allowing to perform a more conservative simulation of the dispersion of pollutants released from DPS.

Results for DPS in transitional operating conditions: The dispersion of pollutants released from DPS stacks, accounting for the interannual meteorological variability (simulated considering three meteorological years) leads to the following results. in the worst conditions the overall maximum across the domain can reach 5.8 μg/m³ of NO_x. As a consequence of the prevailing winds, such

value occurs anyway over the sea SE of the plant. Over land in fact, annual average NO_x values can exceed 2 µg/m^3 inside an area of about 3 km of radius from DPS, and can be above 4 µg/m^3 only for a small area extending up to 500 m SE of the plant. The contribution of DPS alone can be responsible in the worst case of no more than a few exceedances over a year of the NO_2 hourly standard, only over a very small part of the coast at the NE of the power plant. In the case of PM_{10}, the results indicate that over land the annual average contribution from DPS are in the worst conditions below 0.3 µg/m^3. The contribution to $PM_{2.5}$ concentrations does not exceed 0.15 µg/m^3. The values are well below the annual limits for PM_{10} and $PM_{2.5}$. Over all three meteorological years the estimated contribution from DPS to PM_{10} concentrations never exceed the limit value on 24-hour average. The simulation results for heavy metals indicate that in the worst conditions over the whole domain the annual average concentrations of lead and arsenic are below 0.1 ng/m^3, and the ones of cadmium below 0.03 ng/m^3. In the worst conditions, annual average concentrations of nickel can reach the 5-6 ng/m^3 range in the immediate surroundings of DPS over Delimara peninsula, and progressively go down below 2 ng/m^3 at distances of more than 3 km from DPS. So for all these heavy metals, the resulting contribution of DPS annual concentrations is below the limits. As for vanadium, the yearly maxima of 24-hours average computed concentrations indicated that over land the guideline value is likely to be respected.

Results for DPS in new operating conditions: For NOC the contribution to ambient concentrations from DPS emissions scenario has been simulated over the same meteorological years of TOC one, making the two scenarios comparable. For each meteorological year, the resulting shape of the concentrations spatial patterns for NOC is the same of TOC, while lower values of concentration indicators are obtained for NOC, as the result of lower emissions from DPS units, considered as a whole. In the case of NO_x, in the worst conditions the overall maximum concentrations across the domain can reach 4.9 µg/m^3, the area over land experiencing annual average values exceeding 2 µg/m^3 is slightly reduced, and the area where they can exceed 4 µg/m^3 becomes almost negligible. In the worst case, DPS alone is expected be responsible for one to two exceedances a year of the NO_2 hourly standard over a very limited part of the coast NE of DPS. Annual average contribution from DPS to PM_{10} and $PM_{2.5}$ concentrations are well below the annual limits; contributions for heavy metals are also below the limits, and in the case of vanadium the DPS contribution to yearly maxima of 24-hours average concentrations is below the WHO guideline value.

Background contributions: Rural and urban background are estimated through the use of larger scale model simulations, including contributions from all other major Maltese sources, as well long-range transport and natural sources. Rural background for annual average PM_{10} and $PM_{2.5}$ concentrations is estimated from EMEP data as 26.3 and 13.8 µg/m^3, respectively, including also the contribution from the natural sources which are relevant for Malta (sea salt and Saharan dust). According to MEPA, following the method indicated by the European Commission, the contribution from sea salt to PM_{10} is estimated to be 3.1 and 2.7 µg/m^3, at the Msida traffic site and Gharb rural background site, with maximum reaching 14.5 µg/m^3. The Sahara dust contribution to PM_{10} concentrations is reassessed in this study, also using a methodology indicated by the European Commission, based on the identification of Saharan dust outbreak episodes and on the analysis of the time series of PM_{10} concentration measured by regional background stations; the resulting contribution to the PM_{10} yearly average concentration is estimated as in the 3.5-4.5 µg/m^3 range for years 2011 and 2012, with episodes ranging between 1.5 and 191 µg/m^3, and respectively 18 and 11 exceedancees of the PM_{10} daily average concentration limit; a higher number of dust outbreaks

is estimated for year 2010, with an corresponding contribution to yearly average concentration substantially higher. The urban background is estimated through a 3D photochemical model, run over a whole year, fed by hourly meteorology and all the emissions from the Maltese Islands, also modulated at hourly level. Figure 72 shows the maps of the urban background estimated for NO_2, PM_{10} and $PM_{2.5}$ (bottom, right). For NO_2 annual average concentrations the estimated contribution is above 10 μg/m^3 around the Valletta and Sliema agglomeration (where it reaches a maximum of 20 μg/m^3) and the airport area, with minima in the northwestern part of Gozo in the order of 1 μg/m^3. PM_{10} is estimated to be above 3 μg/m^3 (2 μg/m^3 for $PM_{2.5}$) over most of Malta island and the central part of Gozo, and above 5 μg/m^3 (3.5 μg/m^3 for $PM_{2.5}$) over the main urbanized area, where the its maximum reaches 8 μg/m^3 (near 6 μg/m^3 for $PM_{2.5}$); the minimum values in the northwestern part of Gozo are around 1.5 μg/m^3 for $PM_{2.5}$ and 1 μg/m^3 for $PM_{2.5}$.

The modelling analyses assess the likelihood that respect to the ones from other sources, the contribution from DPS in exceeding the limits and targets on ambient concentrations of NO_2 and metals is limited, and very limited in the case of particulate matter, both in its recent transitional configuration as well in the new one resulting from MPS closure and the operation of the interconnector.

CONTENTS

1 Introduction

Enemalta Corporation, the state-owned energy utility responsible for providing electricity to the Maltese Islands, as of 2013 operated two power stations for the production and distribution of electricity: Marsa (MPS) and Delimara (DPS), with a total installed electrical capacity of 720 MW. The generation plant mix is composed of conventional steam units gas turbine driven plant and a new combined cycle diesel engines block.

According to earlier plans and to the LCP Directive, in March 2015 MPS has been shut down and put on cold standby, pending final decommissioning, replaced in stages by:

    i.   the new Diesel engine block at DPS, and

    ii.   a 200 MW submarine interconnection to the European grid, inaugurated in April 2015.

The two installations utilize liquid fossil-fuels, namely 0.7%-sulphur residual (heavy) fuel oil (RFO), and 0.1%-sulphur gas/diesel oil (GDO). Each installation has fuel unloading and storage facilities.

Technical specifications of the main parts of the two plants (fuel tanks, boilers, turbines, diesel engines, stacks) have been given in the background information section of the tender.

Continuous Emissions Monitoring Systems allow to monitor dust, SO2, NOx and CO emissions at each stack of MPS and of combined-cycle gas turbines and diesel engines of DPS; the open-cycle gas turbine stacks of DPS do not have a CEMS.

The revised Delimara IPPC permit requires that the dispersion modelling study made for DPS in 2011 as part of the IPPC obligations is updated to reflect changes in the combustion plants at Delimara, the shutting down of the Marsa installation, and the installation of the cable interconnector with the European grid.

2 Scope of work

The scope of this study is a 2-stage process to update the existing study by re-assessing, using dispersion models, the likelihood of current and future emissions from DPS causing exceedances of the limit and/or target values for NO_2, PM_{10}, $PM_{2.5}$, metals (lead, cadmium, arsenic, nickel) in the Ambient Air Quality Regulations of 2010 (Legal Notice 478, 2010), and to assess the likelihood of such emissions causing exceedances of any applicable guideline values for vanadium, especially but not limited to the most sensitive receptor(s) in the prevailing wind direction within a 15 km radius.

This study consists of two stages:

- the **first stage** includes an assessment of the impact from the operation of the diesel engines and the partial closure of MPS at the end of year 2013; this scenario is referred in the following as "**transitional operating conditions (TOC)**";

- the second stage (mid of year 2015) includes an assessment of the impact of the new operating regime of Delimara Power Station, as the result of closure of Marsa Power Station and operation of the interconnector; this scenario is referred in the following as "**new operating conditions (NOC)**".

Moreover the study includes as well an assessment of the combined influence on background concentration levels of the main sources also present in the area: ship movements at Valletta harbour, Malta freeport and international airport, and fuel storage depots.

3 Site description

3.1 *Domains of analysis*

Figures 1 and 2 show aerial photos of Delimara and Marsa power plants and the position of their main stacks, while Tables 1 and 2 contain data about each stack: fuel used by the corresponding power unit, height from the ground, diameter at the emission point, flue gas temperature at maximum load, its nominal flow rate and the corresponding exit speed. Where continuous emission monitoring system are available, the speed has then be recalculated on a hourly basis from measured flow rates, to better describe real operating conditions.

Figure 1. Stacks of Marsa plant.

Table 1. Summary of stack characteristics for Marsa power plant.

Unit	Fuel	Stacks	Stack height (m)	Stack diameter (m)	Stack temperature at max load (°C)	Nominal flue gas flow rate (Nm³/h)	Exit speed at nominal flow rate (m/s)
Boilers 3 & 4	RFO	M1	52	3.81	200	234 000	9.88
Boilers 5 & 6	RFO	M2	52	3.81	200	286 000	12.07
Boiler 7	RFO	M3	75	4.2	200	260 000	9.03
Boiler 8	RFO	M4	75	4.2	200	234 000	8.13
OCGT	GDO	M5	30	3.7	560	495 000	39.02

Figure 2. Stacks of Delimara plant.

Table 2. Summary of stack characteristics for Delimara power plant.

Unit	Fuel	Stacks	Stack height (m)	Stack diameter (m)	Stack temperature at max load (°C)	Nominal flue gas flow rate (Nm³/h)	Exit speed at nominal flow rate (m/s)
Boilers 1 & 2	RFO	D1A	154	2.9	165	234 000	15.79
		D1B	154	2.9	165	234 000	15.79
OCGT		D2	16	3.5	560	495 000	43.61
		D3	16	3.5	560	495 000	43.61
CCGT Bypass	GDO	D4A	66	3.1	560	495 000	55.59
CCGT		D4B		3.2	170	495 000	27.74
CCGT Bypass		D5A	66	3.1	560	495 000	55.59
CCGT		D5B		3.2	170	495 000	27.74
Diesel	RFO/GDO	D6A/B/C/D	65	2	170	234 000	33.57

The contribution of the emissions from Enemalta power plants to local air quality levels must be assessed also in relationship with the effect from all the other potentially polluting sources, either located in Malta or outside. This can be realized through the consistent and combined use of a dispersion model at a high resolution, to reconstruct in detail the contribution of the sources of main interest (DPS and MPS) and a dispersion model at a relatively lower resolution to describe the effects of all the other sources determining background pollution levels, including also long-range contributions. In this study, a Lagrangian Particle Dispersion Model (LPDM) is used to derive the local direct impact of the power plants, while a Eulerian Chemical Transport Model (CTM) is used to compute the background levels. The two models are described later in the report.

The LPDM is applied on a "local domain", chosen in order to describe, with an high level of details, the local impact of DPS and MPS on the air quality. The domain cover the southeastern part of Malta island, centered around the tow power plants, and it is 16 x 16 km² wide. Three-dimensional

meteorological fields driving dispersion simulations and the resulting pollutants concentrations are computed on a grid at the horizontal resolution of 200 m, depicted in Figure 3, having the following characteristics:

- number of cells in x-y direction: 80x80
- horizontal resolution: 200 m
- coordinates (expressed in m) of the South-West point in UTM33 (WGS84) projection: (448500, 3959500)
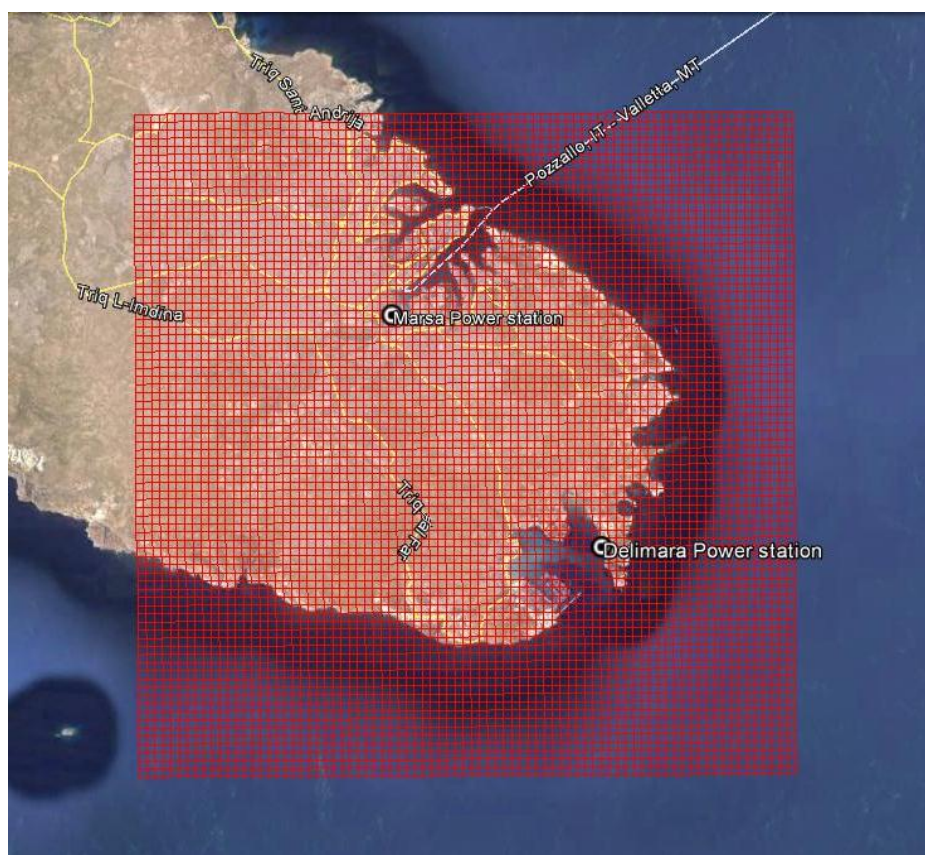- horizontal dimensions: 16000 x 16000 m^2

Figure 3. Domain used to describe in detail the local impact of DPS and MPS with the LPDM model, with a grid of 200 m horizontal resolution.

The CTM is applied on a 50 x 50 km^2 outer domain, chosen to describe at a proper level of detail the background air quality levels, to be added to DPS and MPS effects. This "background domain" cover all Maltese Islands, with a grid of 50x50 cells grid at the horizontal resolution of 1000 m. (Figure 4, also showing the position of the inner local domain). The main characteristics of the computational grid as follow:

- number of cells in x-y direction: 50x50
- horizontal resolution: 1000 m
- coordinates (expressed in m) of the South West point in UTM33 (WGS84) projection: (420500, 3951500)
- horizontal dimensions: 50000 x 50000 m^2

Figure 4. Computational grid used to describe the background concentrations through the CTM model, covering the entire Maltese Islands with horizontal resolution of 1 km. The inner red square represents the localization of the LPDM local domain.

4   Methodology

The following paragraphs illustrate in detail how the main components of the modelling study have been set up: emission sources, local meteorology and pollutants dispersion. The data sets collected for the different activities are also summarized in the Appendix B.

4.1 *Emission sources*

4.1.1   Power plants – Transitional operating conditions (TOC)

The main goal of this study is evaluate the contribution of Enemalta power plants emissions to ambient concentrations, so the information with the maximum level of detail on the characteristics of their operating units and the flue gas emitted concentrations has been collected from Enemalta and employed for the model application. On most stacks, continuous emission monitoring systems (CEMS) are installed to measure hourly concentrations of flue gases, and the available data were used to calculate the emitted masses an their temporal variability. For those stacks where CEMS are not installed, because of the low height of the stack which would cause false readings due to turbulence (Delimara open cycle gas turbines – OCGT), Enemalta calculates the loads through emission factors depending on the quantity of burnt fuel, assuming that the operation is the same as the gas turbine at Marsa, which is very similar. Most of the installed EMS measure the hourly flow rate of the emitted gases, from which the actual exit speed can be determined. The CEMS for Delimara's diesel units do not measure the flows, so the authorized flow was used to calculate the speed.

In accordance with the purpose of the first part of the study, addressing current operating conditions at the end of year 2013 (in this report referred as "transitional operating conditions (TOC)"), CEMS data for 2013 have been used. The working conditions of each unit are summarized in Tables 3 and 4. At Marsa, during year 2013, boilers 3 to 8 (stacks M1 and M2) were not used, boilers 7 & 8 (stacks M3 and M4) were still in operation, while the OCGT unit (stack M5) was used only for a very limited time. At Delimara, during 2013, all units were operational, even if not continuously. Due to technical problems, from Feb 2012 to Jan 2013 the combined cycle gas turbines (CCGT) have been switched to the open cycle mode using the bypass stacks (D2 and D3). The OCGT mode is much less efficient than the CCGT mode, so the number of operating hours is small.

At the time of the first stage of the study (Nov 2013), only CEMS data until the previous month (Oct 2013) were available. In order to complete the remaining period, the same working conditions have been assumed, so data from the last available month have been replicated to fill the end of the year. For most stacks the missing months were November and December, while the boilers in Delimara lacked October data as well. For Delimara OCGT units, only the monthly total number of operation hours was available: for a conservative impact evaluation the total emissions from those units have been arbitrarily modulated in time, assuming the units working for a few hours each Monday morning, preserving the total emitted mass.

The resulting total mass emitted from each stack over year 2013 is also summarized in Tables 3 and 4.

In line with a conservative impact assessment, during model calculations all the emitted dust has been considered as PM_{10}. According with what reported by the national emission inventory for the public power sector (MEPA, 2013), $PM_{2.5}$ emissions have been estimated on hourly basis as 60% of PM_{10} ones.

Table 3. Summary of emission data for Delimara power plant, "transitional operating conditions (TOC)" scenario.

Unit	Stack	Conditions during 2013	NO$_x$ (t/yr)	CO (t/yr)	SO$_2$ (t/yr)	Dust (t/yr)	Avg. flow (Nm³/h)	Data origin
Boiler	D1A	Worked continuously	635	2.35	1737	59.2	195619	CEMS
Boiler	D1B	Worked continuously, Feb&Mar reduced use	473	1.48	1324	42.8	174896	CEMS
OCGT	D2	Worked only 82 hours	9.96		0.75	0.01		Amount of fuel burnt
OCGT	D3	Worked only 68 hours	6.95		0.53	0.008		Amount of fuel burnt
CCGT	D4B	Worked continuously, except Jan&May (stop), Feb&Mar (reduced use)	204.6	1.26	17.84	0.849	246547	CEMS
CCGT	D5B	Worked from Apr (except May)	76.9	1.72	13.11	0.045	247449	CEMS
Diesel	D6A		108.8	76.46	70.09	5.709	117000	CEMS, except flow rate
Diesel	D6B	Worked alternatively, over the whole year	136.6	83.26	72.27	6.874	117000	CEMS, except flow rate
Diesel	D6C		111.1	78.8	61.52	5.636	117000	CEMS, except flow rate
Diesel	D6D		117.3	92.26	64.15	5.942	117000	CEMS, except flow rate

Table 4. Summary of emission data for Marsa power plant, "transitional operating conditions (TOC)" scenario.

Unit	Stack	Conditions during 2013	NO$_x$ (t/yr)	CO (t/yr)	SO$_2$ (t/yr)	Dust (t/yr)	Avg. flow (Nm³/h)	Data origin
Boiler	M1	Decommissioned						
Boiler	M2	Decommissioned						
Boiler	M3	Worked from Jan to Apr, then Aug to Sep	520	1.68	1140	37.5	242433	CEMS
Boiler	M4	Worked since April	533	2.41	1589	77.4	240456	CEMS
OCGT	M5	Worked for about 50 hrs	14	0.38	2.8	0.05	784000	CEMS

According to the environmental obligations as stipulated in the IPPC permits for the operation of the Marsa and Delimara power plants, concentrations of heavy metals are measured by analyzing samples periodically collected at the stacks. For the "transitional operating conditions" scenario, the most recent available measurements (July-Aug 2013) have been used (Ecoserv and Cada, 2013), summarized in Table 5.

Table 5. Summary of results of analysis for heavy metals from discontinuous stack emissions monitoring (ND = Not Detected, levels below the detection limit of 0.001 mg/Nm^3).

Plant	Unit	Stack	Emission rates [mg/Nm^3]				
			Pb	**Cd**	**As**	**Ni**	**V**
Marsa	Boiler	M4	0.004	ND	ND	0.1	0.17
Delimara	Boilers	1A	0.01	ND	0.01	0.9	0.56
		1B	0.01	ND	0.004	0.74	0.46
	Diesel	6A	ND	ND	ND	0.01	0.004
		6B	ND	ND	ND	0.01	0.01
		6C	ND	ND	ND	0.01	0.002
		6D	ND	ND	ND	0.01	0.003

These emission rates have then been used as input for the model simulations, modulated on a hourly basis according to the dust measurements recorded by CEMS, adjusted in proportion of the ratio between the flow rate recorded during sampling and the hourly flow rates recorded by the CEMS. For a conservative impact assessment, values below the detection limit (0.001 mg/Nm^3), have been set equal to detection limit. The resulting figures for yearly emissions are summarized in Table 6.

Table 6. Summary of heavy metals yearly emissions (kg) from DPS and MPS.

Plant	Unit	Stack	Pb	Cd	As	Ni	V
Marsa	Boiler	M4	6.18	1.55	1.55	154.53	262.69
Delimara	Boilers	1A	25.16	2.52	25.16	2264.26	1408.87
		1B	20.02	2.00	8.01	1481.41	920.87
	Diesel	6A	1.22	1.22	1.22	12.20	4.88
		6B	1.14	1.14	1.14	11.41	11.41
		6C	1.29	1.29	1.29	12.90	2.58
		6D	1.39	1.39	1.39	13.87	4.16

4.1.2 Power plants – New operating conditions (NOC)

The purpose of the second stage of the study addresses the impact of the new operating regime of Delimara Power Station, as the result of closure of Marsa Power Station and the operation of the interconnector. The related scenario - "new operating conditions (NOC)" – has been set up on the basis of the information available at the time of the study (mid of year 2015), summarized for DPS in Table 7:

- the operating conditions expected over the whole year as the result of the new configuration have been communicated by Enemalta;

- those conditions have been translated into assumptions (last column of Table 7) to be applied to the latest set of emissions resulting from CEMS data (year 2014), taken as a starting reference.

The resulting total mass emitted from each stack for NOC scenario is summarized in Table 8 and 9. The other stack parameters, including the average flow, have been kept as in the TOC scenario.

As with TOC scenario, all the emitted dust has been considered as PM$_{10}$, and PM$_{2.5}$ emissions have been assumed as 60% of PM$_{10}$ ones.

Table 7. Assumptions related to "new operating conditions (NOC)" scenario for Delimara power plant.

Units	Stacks	Expected operating conditions	2014 conditions (CEMS data)	Assumptions on NOC scenario emissions
Boilers	D1A + D1B	One unit is to be kept in service, the other is to be kept on standby; alternated every 2 months.	Both units worked continuously, except a couple of months each one	NEC emissions as 2014 ones, for the corresponding active months
OCGTs	D2 + D3	Operations in summer very limited, will be put in service only for emergency circumstances or when there are high unexpected peaks	One unit worked intermittently; the other one worked Jul to early Nov	NEC emissions as 2014 ones
CCGTs	D4B + D5B	Standby for most of the time during the year, apart from the summer peak when the half block combined cycle will be put in service	Each unit worked for 6÷7 months	NEC emissions as 2014 ones only for summer months (one unit only); no emissions during the rest of the year
Diesels	D6A + D6B + D6C + D6D	Working during different periods over the entire year	Worked during different periods over the entire year	NEC emissions as 2014 ones

Table 8. Summary of emission data for Delimara power plant, "new operating conditions (NOC)" scenario.

Unit	Stack	NO$_x$ (t/yr)	SO$_2$ (t/yr)	Dust (t/yr)
Boiler	D1A	337	740	28
Boiler	D1B	337	740	28
OCGT	D2	12.38	1.95	0.01
OCGT	D3	12.38	1.95	0.01
CCGT	D4B	40.8	107.3	0.13
CCGT	D5B	40.8	107.3	0.13
Diesel	D6A	165.4	118.1	7.83
Diesel	D6B	165.4	118.1	7.83
Diesel	D6C	165.4	118.1	7.83
Diesel	D6D	165.4	118.1	7.83

Table 9. Summary of heavy metals yearly emissions (kg) from DPS, "new operating conditions (NOC)" scenario.

Plant	Unit	Stack	Pb	Cd	As	Ni	V
Delimara	Boilers	1A	25.16	2.52	25.16	2264.26	1408.87
		1B	20.02	2.00	8.01	1481.41	920.87
	Diesel	6A	1.22	1.22	1.22	12.20	4.88
		6B	1.14	1.14	1.14	11.41	11.41
		6C	1.29	1.29	1.29	12.90	2.58
		6D	1.39	1.39	1.39	13.87	4.16

4.1.3   Other sources

To properly assess the actual impact of concentrations produced by the emissions from the power plants under study, it is appropriate to consider also the presence of the main other important sources and their contribution to local air quality.

Emission inventories can be developed in different ways, according to the availability of data. On one side there is the "bottom-up approach", needing detailed information on each individual sector and source and requiring a great effort, and on the other there is the "top-down approach", using generalized indicators (like population, energy used, total manufacturing jobs) to estimate the emissions. The product of emission factors with relevant parameters representing the activity levels provides an estimate of the total emissions that can then be allocated on the territory using some proxy data. The two approaches are often used together: emissions from specific well-defined sources for which the necessary information is available and/or are of particular interest can be estimated using a bottom-up approach, while all other emissions can be estimated using a top-down approach.

In this study both approaches have been used, as described in the following.

The most important sources considered for their contribution to local air quality are:

- Valletta Harbour ship;
- Malta Freeport;
- Malta International Airport;
- fuel storage depots located near DPS: Oil Tanking Malta, San Lucjan Oil Company, 31st March 1979 Fuel storage (ENEMALTA), Wied Dalam Depot;
- Marsa Thermal Treatment Facility;
- road transport on Malta and Gozo network;
- fishing activities;
- international shipping routes.

Emission produced by ships movements in **M'Xlokk and Valletta harbours** can represent an important contribution to local pollutant concentrations, also for their continuity during the year.

The emissions produced by navigation are a consequence of combusting the fuel in an internal combustion (marine) engine. Consequently, the main pollutants are those from internal combustion engines. These are CO, VOC, NOx and PM derived from soot which mainly have to do with engine technology, and others, like SOx, CO2, heavy metals or further PM (mainly sulphate-derived) which originate from the fuel speciation (EMEP/EEA - Air Pollutant Emission Inventory Guidebook 2013).

To compute emissions in detail, it is necessary to know the total number of ships, their engine types, gross tonnage (GT), type of fuel employed, the duration of hotelling and maneuvering phases at the port.

The emission for the two ports in question have been estimated on the basis the summary statistics about shipping movements provided by Port Authority (extract in Table 10). Shipping movements during the whole year 2012 subdivided in categories have been considered, and then combined with statistics about ships types (derived from individual ships identified from the information available from the official website of Malta Freeport) and literature data.

Table 10. Example of data provided by Port Authority.

		Shipping Movements				
	Calls	*Valletta* GRT	NRT	Calls	*M'Xlokk* GRT	NRT
Cargo Operations						
Container Operations	11	81,348	45,048	1,484	51,874,005	26,679,275
Dry Bulk Operations	19	172,737	96,163	7	32,133	14,508
Unitised Operations	355	9,501,893	2,951,150	60	1,673,423	569,812
Liquid Bulk Operations	26	466,647	200,299	474	8,221,243	3,625,504
General Cargo Operations	237	636,223	298,304	79	1,459,037	678,468
Passenger Operations						
Cruise Liners	320	21,584,775	14,276,676	0	0	0
Ferry	0	0	0	0	0	0
Passenger Catamaran Ferry	410	3,182,921	955,079	0	0	0

Applying to those types of ships the emission factors of the EEA methodology, it has then been possible to estimate emissions for the different phases of ship movements. The results are summarized in Table 11.

Table 11. Harbour emissions (t/year or kg/year for heavy metals).

	CO	NMVOC	NH3	NOX	TSP	SO2	Pb	Cd	Hg	As	Cr	Cu	Ni	Se	Zn
Valletta waterfront	451	18	0	402	27	2	16	2	3	37	39	109	1689	16	123
M'Xlokk	45	3	0	57	5	0	2	0	0	4	5	13	194	2	14

In the subsequent modelling phase, harbour emissions have then been assigned to the areas shown in blue in Figure 5, and distributed along the vertical dimension allocating 70% of the mass in the layer below 20 m over ground, and the remaining 30% in the layer above, in order to account for emissions from high chimneys.

Figure 5. Valletta and Marsaxlokk ports areas.

Time modulations for these emissions have been derived from data received from Valletta Port Authority and available at the Valletta Cruise Port website (http://www.vallettawaterfront.com). Figures 6 and 7 show the resulting yearly and daily modulations, while weekly modulations are kept constant, except for ferries, that are active on Sundays only.
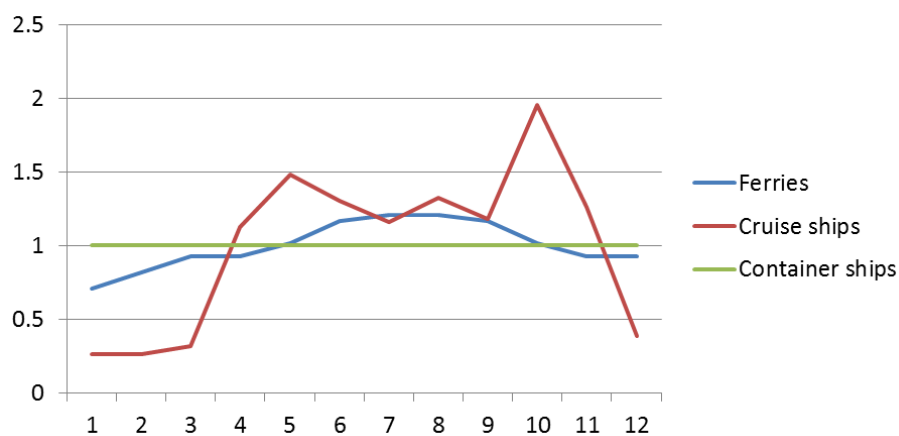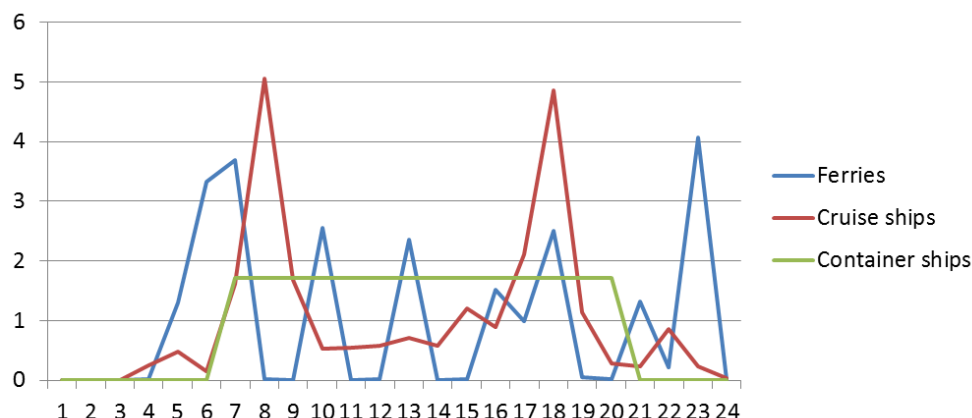

Figure 6. Yearly modulation for emissions from ships.

Figure 7. Daily modulation for emissions from ships.

The emissions produced by **aviation** come from the use of jet fuel (jet kerosene and jet gasoline) and aviation gasoline (used to fuel small piston engine aircraft only) that are used as fuel for the aircraft. Consequently, the principal pollutants are those common to other combustion activities, i.e. CO_2, CO, hydrocarbons and oxides of nitrogen, with SO_2 emissions being dependent of the level of sulphur in the fuel. Other important species, emitted at relatively low concentrations include PM, N_2O and CH_4 (EMEP/EEA - Air Pollutant Emission Inventory Guidebook 2013).

For the estimation of the emissions that can affect air quality, the most important phases are the landing and take-off cycles, that includes all activities near the airport that take place below a height of 3000 ft (914 m). This therefore includes taxi-in and -out, take-off, climb-out and approach-landing.

To compute emissions related to Malta International Airport, the starting point has been the number of passages registered during year 2012 (Table 12).

Table 12. Malta International Airport: extract from Annual Statistical Summary (2012).

Monthly Summary of Passengers, Aircrafts & Cargo

Passenger Movements	Jan	Feb	Mar	Apr	May	Jun	Jul	Aug	Sep	Oct	Nov	Dec
Arrivals	82,120	86,867	114,544	154,989	175,610	191,965	228,829	220,991	204,210	168,407	99,745	95,785
Departures	83,849	82,822	107,498	149,209	168,716	183,329	216,543	240,926	203,817	180,304	111,793	97,070
Total [Scheduled & Non-Scheduled]	165,969	169,689	222,042	304,198	344,326	375,294	445,372	461,917	408,027	348,711	211,538	192,855
Transit [counted only on departure]	39	570	843	256	617	293	44	685	214	436	26	322
Total International	166,008	170,259	222,885	304,454	344,943	375,587	445,416	462,602	408,241	349,147	211,564	193,177
General Aviation	292	217	280	384	421	442	702	351	634	497	294	206
Passenger Total	166,269	170,476	223,165	304,838	345,364	376,029	446,118	462,953	408,875	349,644	211,858	193,383

Aircraft Movements	Jan	Feb	Mar	Apr	May	Jun	Jul	Aug	Sep	Oct	Nov	Dec
Arrivals	798	767	952	1,205	1,372	1,414	1,567	1,606	1,433	1,299	837	847
Departures	802	768	951	1,208	1,369	1,420	1,568	1,605	1,433	1,297	838	841
Total [Scheduled & Non-Scheduled]	1,600	1,535	1,903	2,413	2,741	2,834	3,135	3,211	2,866	2,596	1,675	1,688
General Aviation	292	300	303	326	415	400	449	360	362	359	290	233
Aircraft Total	1,892	1,835	2,206	2,739	3,156	3,234	3,584	3,571	3,228	2,955	1,965	1,921

Cargo Movements	Jan	Feb	Mar	Apr	May	Jun	Jul	Aug	Sep	Oct	Nov	Dec
Import	457,439	730,845	600,608	741,174	712,886	870,138	507,813	564,739	552,249	425,656	510,079	397,901
Export	589,045	635,552	667,952	676,995	770,093	709,066	781,958	571,816	590,185	669,721	781,331	589,513
Total	1,046,484	1,366,397	1,268,560	1,418,169	1,482,979	1,579,204	1,289,771	1,136,555	1,142,434	1,095,377	1,291,410	987,414
Mail	109,210	110,765	115,595	113,783	116,713	109,614	104,281	105,386	109,457	124,672	130,453	133,082
Cargo Total [in Kilos]	1,155,694	1,477,162	1,384,155	1,531,952	1,599,692	1,688,818	1,394,052	1,241,941	1,251,891	1,220,049	1,421,863	1,120,496

Basing on the total number of LTO cycles, the total fuel used has been estimated, multiplying the number of LTOs by the fuel use factors for one representative aircraft suggested in the methodology and then by the relevant emission factors, to obtain the total emissions. Results are reported in Table 13.

Table 13. Aviation emissions (t/year).

	CO	NMVOC	NH3	NOX	PM10	SO2
Malta International Airport	330.7	14.011	0	232.6	1.962	22.42

For subsequent model simulation, emissions from the airport have then been allocated to the area shown in grey in Figure 8, and distributed in time according to the monthly data reported by Malta International Airport traffic statistics (Table 12).

Figure 8. Malta International Airport area.

Another important emission source in the considered domain is represented by some **fuel storage depots**. For this kind of activity the most important emission is methane, but small quantities of NMVOC are emitted as well (Table 14). Emissions have been estimated starting from the total amount of fuel, applying an average emission factor that takes into account different fuels and different phases of the storage.

Table 14. Fuel storages emissions (t/year).

	Oil Tanking Malta	San Lucian Oil Company	31st March 1979 Fuel storage	Wied Dalam Depot
NMVOC	14.84	1.19	7.62	0.42

Emissions from fuel depots have then been allocated to the areas shown in orange in Figure 9.
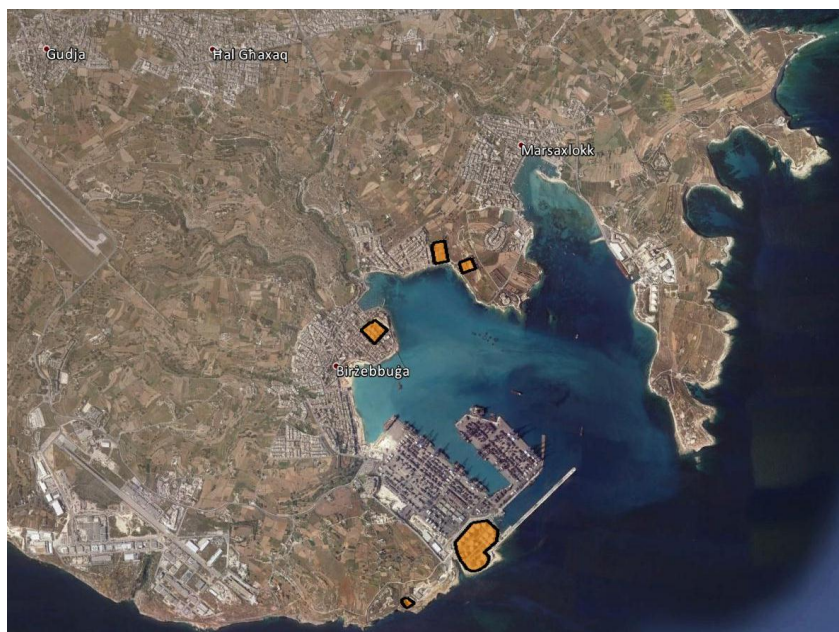
Figure 9. Marsaxlokk fuel depots.

Atmospheric emissions from **vehicular traffic** have been assigned over the whole road network through a "top-down" approach, starting consistently from aggregated data at country level and then disaggregated in space and time.

The total emissions from on-road transport (Table 15) are included in the national emission inventory for 2011 officially reported by MEPA to CLRTAP, the Convention on Long-range Transboundary Air Pollution (MEPA, 2013).

Table 15. Total emissions from on-road transport (t/year).

Sector	NFR Code	NO$_X$	SO$_X$	PM$_{10}$	CO	Pb	Cd	As	Ni
Passenger cars	1 A 3 b i	734.15	1.07	26.18	9728.75				
Light duty vehicles	1 A 3 b ii	423.76	0.51	100.02	507.43				
Heavy duty vehicles	1 A 3 b iii	1330.01	0.50	43.47	289.79				
Mopeds & motorcycles	1 A 3 b iv	6.70	0.01	2.67	484.15				
Tyre and brake wear	1 A 3 b vi			402.15		3.28	0.01	0.04	0.19
Road abrasion	1 A 3 b vii			399.81					
Total		*2494.62*	*2.09*	*974.30*	*11010.11*	*3.28*	*0.01*	*0.04*	*0.19*

Since there is still a high level of uncertainty in its estimation, particulate emissions do not take into account the contribution of resuspension, ie. the ambient material deposited on the road which can be lifted again in the air by the passage of vehicles. The relevance of those emission grows during wind calms and dry meteorological conditions, and can be an important aspect to be considered in the estimation of PM concentrations in urban area or near major roads.

Road traffic emissions have then been disaggregated in space on the basis of the road network layout, extracted from the Open Street Map project. Basing on the road classification hierarchy, a subset of links has been selected, considering only trunk, primary and secondary roads (Figure 10), and then associating them different weights. This coefficient reflects the road relevance in traffic distribution and consequently in the production of atmospheric pollutants emissions.
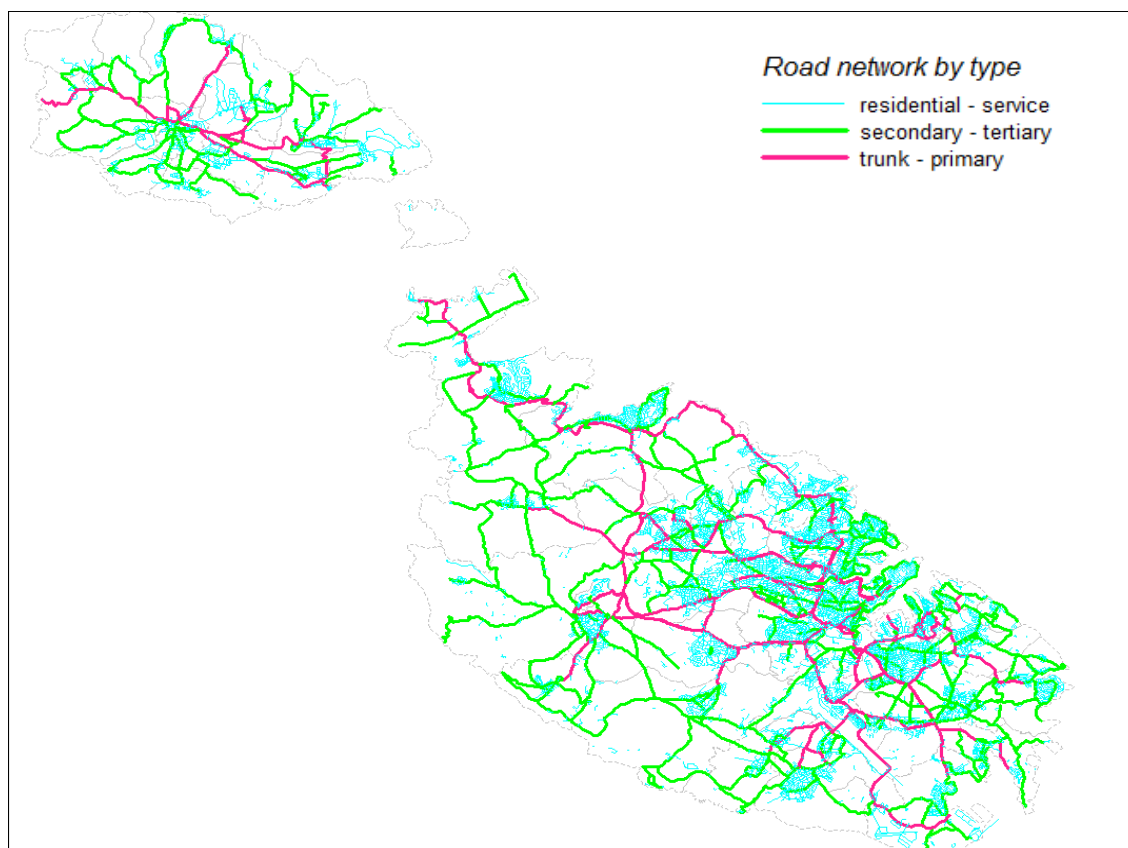
Figure 10. Road sources considered for the spatial distribution of traffic emissions.

The time modulation used for the temporal disaggregation of traffic fluxes throughout the day has been extracted from the National Travel Survey (Transport Malta, 2010) and reflects the analysis carried out during 2010, while for weekly distribution different coefficients (derived from other case studies) have been applied to working days, Saturday and Sunday. The graphs in Figure 11 show the modulation profiles used to distribute the trips during the day and the week. The trend of road traffic emissions is assumed to be constant throughout the year.
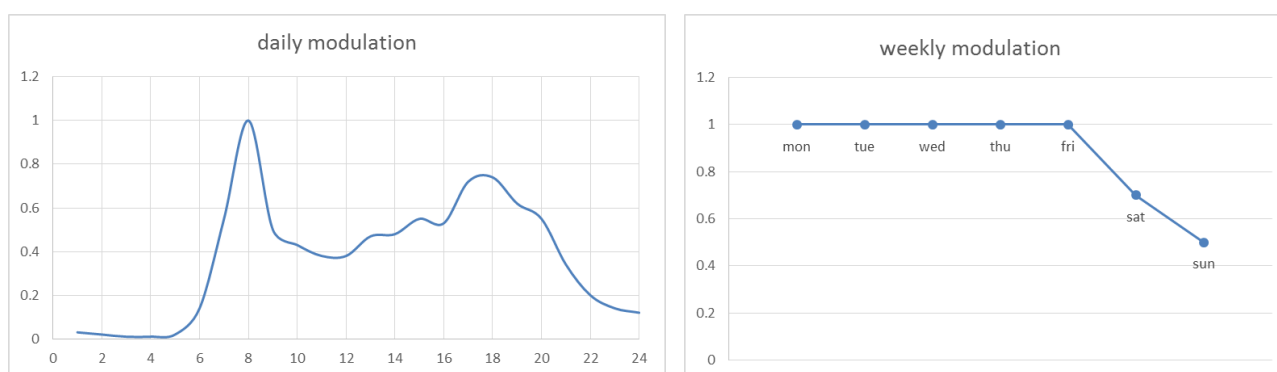
Figure 11. Daily and weekly modulations considered for the time modulation of road traffic emissions.

Emissions from sea activities have been included from two sources: fishing and international shipping. Data for **fishing** has been obtained from Malta national emission inventory, contained in the Annex IV sent yearly from MEPA to UNECE/EMEP, updated to the year 2011 (see Table 16). The emissions have been allocated to a buffer area 10 km wide around the Maltese archipelago.

Table 16. Emissions from fishing activities (t/year).

	NOx	NMVOC	SOx	PM2.5	PM10	CO
Fishing activities	203.87	18.26	0.13	3.71	3.98	19.63

Emissions from **international shipping routes** have been obtained by the EMEP database, which provides emissions allocated on 50x50 km^2 cells. The emitted mass associated to the intersection between the EMEP cells and the modelling domain (see Table 17) was allocated outside a buffer area at least 2.5 km wide around the Maltese archipelago, with the exception of two areas of approach to Valletta and Marsaxlokk ports, added to account for the stopovers.

Table 17. Emissions from international shipping routes (t/year).

	NOx	NMVOC	SOx	PM2.5	PM10	CO
International ships	4453	178	3310	363	383	514

Emissions from the **Marsa Thermal Treatment Facility** have been determined from aggregated data retrieved from WasteServ Ltd website (http://statistics.wasteservmalta.com/scadamonthly.aspx), as data from the plant's CEMS were not readily usable (see Table 18). The time modulation was kept constant throughout the year.

Table 18. Emissions from Malta's incinerator at Marsa (t/year).

	VOC	NOx	Dust	CO	Hg	As	Pb	Cr	Ni
WasteServ Thermal Treatment Facility	0.669	7.383	0.186	3.227	0.00042	0.00054	0.00504	0.00142	0.00188
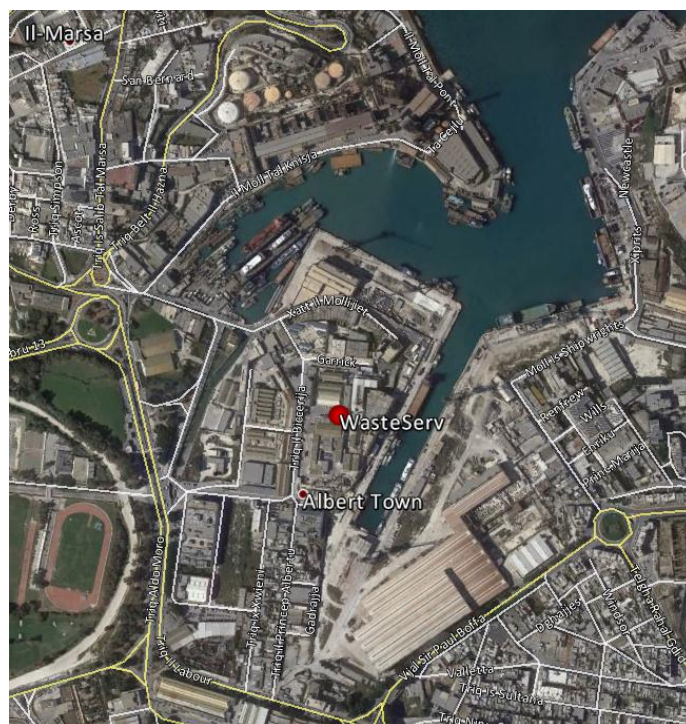
Figure 12. WasteServ Marsa Thermal Treatment Facility.

Table 19. Stack data of Marsa Thermal Treatment Facility.

UTM 33 x coord.	UTM 33 y coord.	Height (m)	Diameter (m)	Temperature (°C)	Exit speed (m/s)
454760	3970490	18	0.632	165	7.45

Finally, all **remaining areal sources** have been taken from Malta national emission inventory, as contained in the Annex IV sent yearly by MEPA to CLRTAP, updated to the year 2011 (MEPA, 2013). The data by pollutant and sector as summarized in Table 20.

The total masses have been allocated in space using land-use proxies from the CORINE Land Cover 2006 database (see Table 20 and Figure 13) and distributed in time using literature modulation profiles.

Table 20. Emissions from other area sources (t/year).

Activity	Spatial proxy	NOx	NMVOC	SO2	NH3	PM10	CO
Manufacturing industries and construction	Industrial areas	89.07	8.91	92.02	0	19.15	35.63
Commercial - Institutional	Builtup areas	30.36	7.59	16.28	0	17.90	0
Residential	Urban fabric areas	40.01	31.82	12.38	0	1.89	158.30
Agriculture Forestry Fishing	Agricultural land	187.81	24.92	7.70	0	1.89	3.51
Road paving with asphalt	Builtup areas	0	31.49	0	0	0	0
Food and drink industry	Industrial areas	0	163.55	0	0	0	0
Solvents use	Industrial areas	0	1781.11	0	0	0	0
Livestock	Agricultural land	0	0	0	1489.65	94.28	0
Synthetic N-fertilizers	Agricultural land	0	0	0	7.74	0	0
Field burning of agricultural wastes	Agricultural land	0	0	0	0.02	0	0
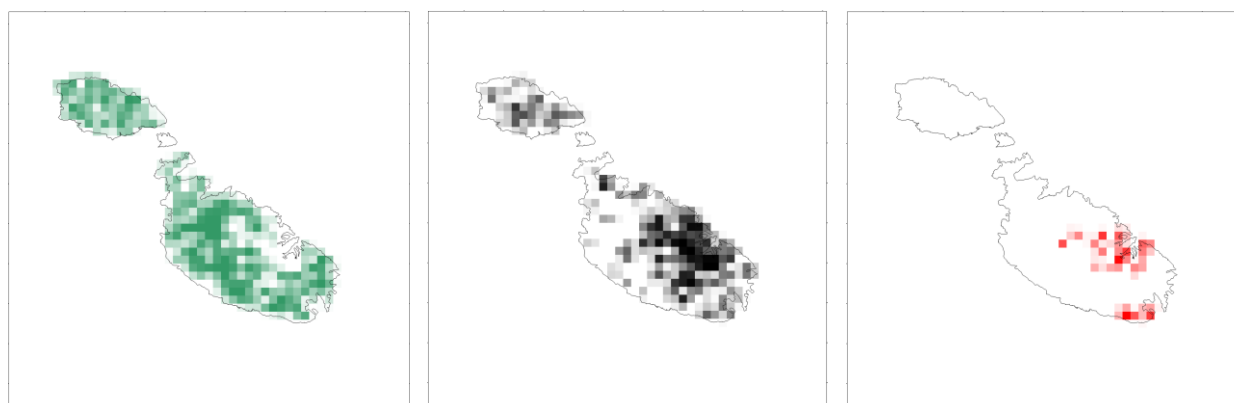
Figure 13. CORINE land cover: 1x1 km relative weight tiles for agricultural land, builtup areas, industrial sites.

4.2 *Meteorology*

Both pollutants dispersion models chosen for this study are full dynamic and three-dimensional: to correctly drive simulations they requires as input three-dimensional meteorological fields on hourly basis over the entire considered period. This means that simple ground-based meteorological measurements at one or more stations are not sufficient to give a general view of the atmospheric

flow dispersing the emitted pollutants. In particular, a correct simulation of the path of the hot plumes emitted by the elevated stacks of the power plants requires a coherent reconstruction of wind flow, turbulence and temperature fields also at upper atmospheric levels. This can be realized through three-dimensional meteorological modeling over the area of interest, that when made for a long enough period, can provide a statistically significant sequences of the needed 3D fields.

To reach this goal, the meteorological output fields operationally produced by the Air Quality Modeling System (AQMS) QualeAria (http://www.aria-net.eu/QualeAria/index_en.html) are used to feed a downscaling procedure on the Maltese area. The modeling system has the main aim to simulate regional scale air pollution over the Italian peninsula starting from national and European emission inventories, synoptic scale weather analysis and global scale air quality levels. It has been developed within the research project FUMAPEX, funded by the European Commission within the 5th Framework Programme, and the COST Action ES0602 collaboration framework. QualeAria implements state-of-the-art techniques to describe physical and chemical processes involving pollutants in the atmosphere (e.g. emissions, transport, dispersion, deposition and chemical reactions). From the meteorological point of view, QualeAria employs RAMS (Cotton et al., 2003) prognostic meteorological model for synoptic weather downscaling and description of local scale atmospheric flows, and FARM CTM for pollutants dispersion and transformations. It stems also from the experience of MINNI national modelling system, realized by ENEA (National Agency for New Technologies, Energy and Sustainable Economic Development) and ARIANET on behalf the Italian Ministry of the Environment, to support integrated assessment over the whole country, which is based on the same combination of models.

In QualeAria, the models are applied simultaneously to a background domain including a large fraction of continental Europe and the Mediterranean basin and to an inner target area, including the whole Italian peninsula and, in his southern part, also the Maltese Islands. The two nested domains are depicted in Figure 14. The inner domain is covered with a grid of 12 km horizontal resolution.
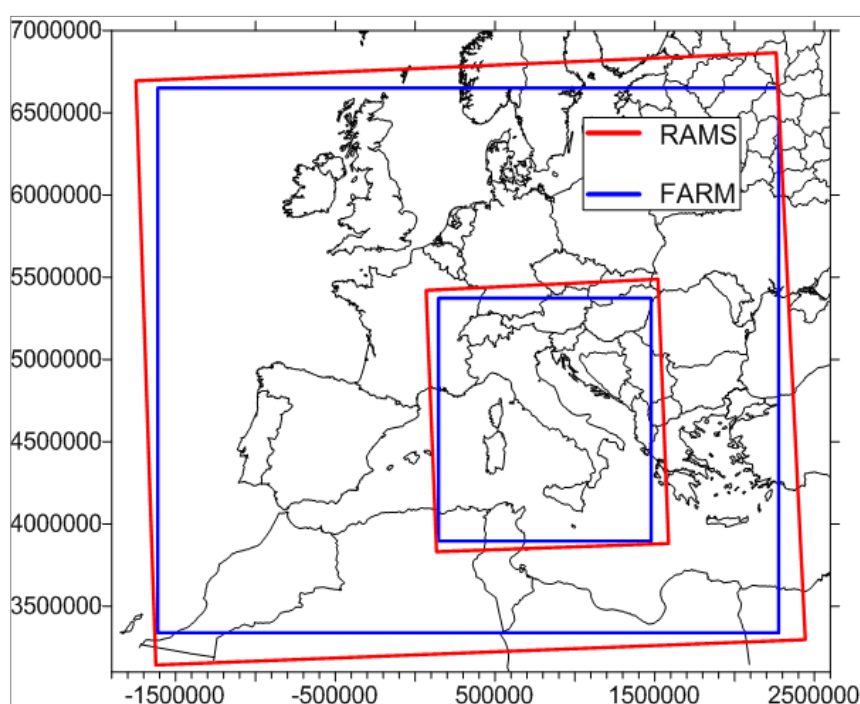
Figure 14. Computational domains of the QualeAria AQMS.

For this study, 3D meteorological and air quality fields produced by QualeAria on hourly basis over years 2010-2011-2012 are used. Fields coming from the meteorological prognostic model are coherent between lower level and higher level layers, being produced by the same physics, and are available for a sufficiently long period to drive pollutants dispersion simulation whose results can be compared to local regulatory air quality limits. Moreover, data provided by meteorological models are continuous, so no problems arise to cover possible gaps often present in experimental databases.

Figure 15 shows the grid points at 12 km horizontal resolution from which data produced by QualeAria simulations are extracted and the used to drive the simulation on the background and the local domains considered in this study, including also a number of points located in an external frame.
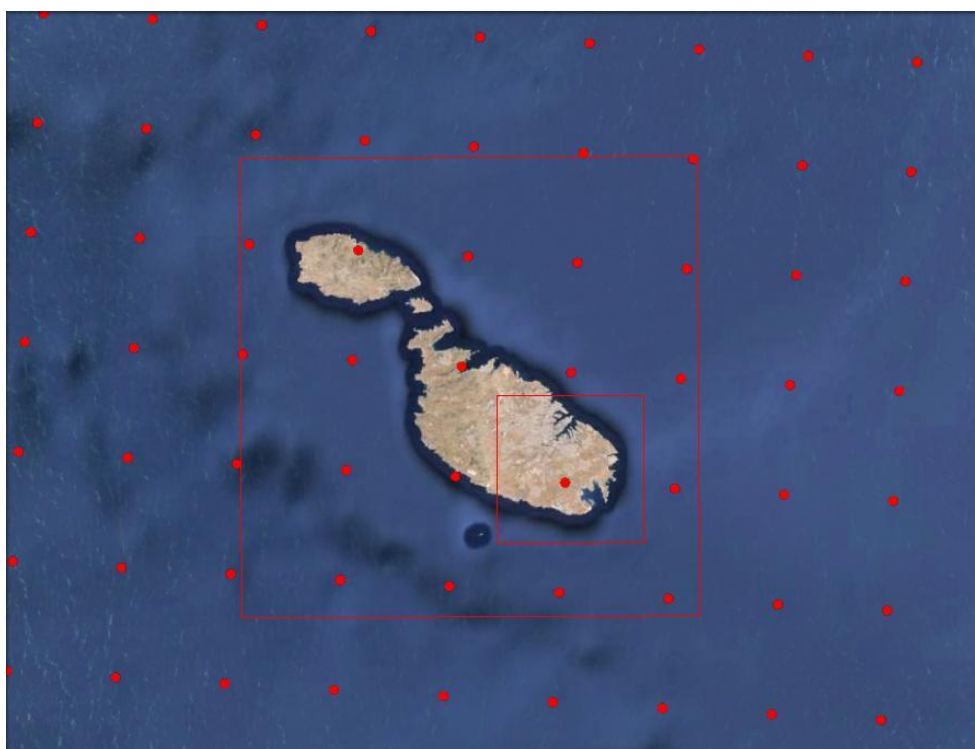
Figure 15. Layout of the meteorological points available from the QualeAria AQMS inside the LPDM detailed area (inner square) and CTM background area (outer square).

The meteorology (mean wind ant turbulence fields) is downscaled on the background domain using the GAP/SURFPro diagnostic system (Kukkonen et al., 2012) and on the local domain using SWIFT/MINERVE and SURFPro zero-divergence diagnostic models. The models are able to take into account horizontal variations induced on meteorological fields by the local inhomogeneities generated by surface topography, roughness and land-use characteristics at the different considered scales. The adopted approach allows to produce internally consistent 3D meteorological fields that reflect both synoptic framework as well terrain morphology, avoiding possible hour-by-hour discrepancies that may arise from the direct insertion of ground-based stations measurements, often affected by very local features related to scales well below the model resolution, or inconsistencies between lower and upper layer features generating local artifacts. The resulting meteorological fields are suitable for use with dispersion models, providing that at stations locations they exhibit statistical properties that are comparable to the ones of against observational data. To be reliable, it is in fact necessary that the information given by the

meteorological models define a scenario which is similar to the one captured by measurements; this is particularly important for the wind flow, which is the main responsible of the transport of the plumes emitted by the different sources considered, especially power plants stacks.

The meteorological reconstruction on both domain also makes use of CORINE Land Cover (EEA Data Service, http://dataservice.eea.europa.eu/dataservice). Those data are used to define a cell-by-cell surface roughness and the response of the ground to the incoming solar radiation, driving both the boundary layer growth and the behaviour of the other scaling variables through the parameterization schemes implemented in SURFPro. The CORINE land cover on the two domains at 1 km and 200 m horizontal resolution are shown in Figure 16, with the corresponding classification table listed in Table 21. The builtup areas are clearly depicted.
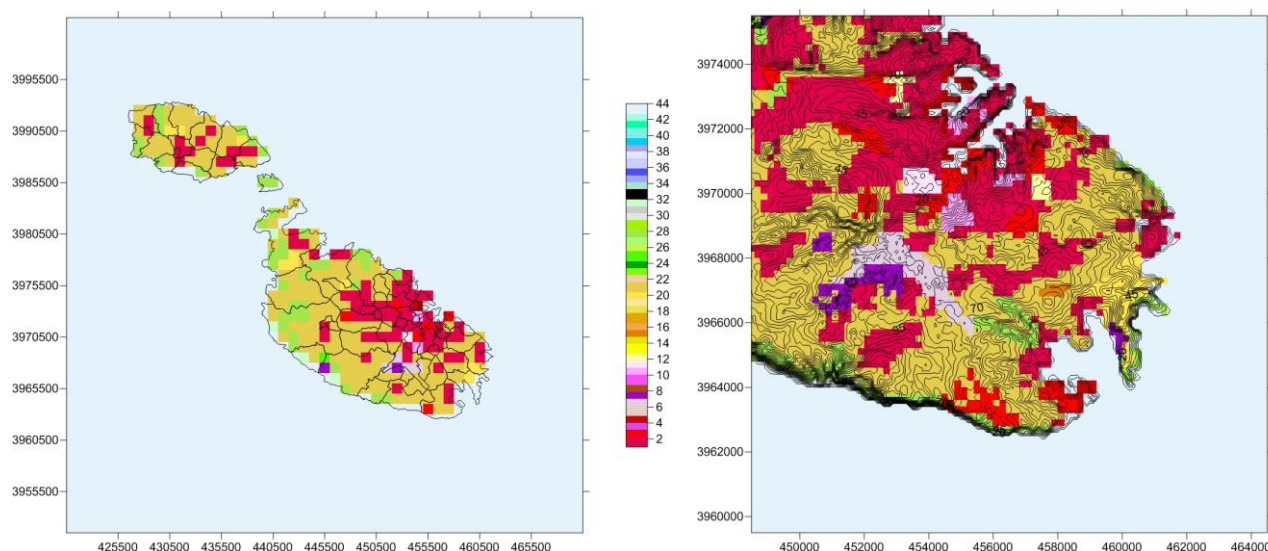
Figure 16. CORINE Land Cover for the background domain at 1 km horizontal resolution (left) and detailed domain at 200 m horizontal resolution (right); land cover types corresponding to classes codes are reported in Table 21.

Table 21. CORINE Land Cover classification.

1	Continuous urban fabric	23	Broad-leaved forest
2	Discontinuous urban fabric	24	Coniferous forest
3	Industrial or commercial units	25	Mixed forest
4	Road and rail networks and associated land	26	Natural grasslands
5	Port areas	27	Moors and heathland
6	Airports	28	Sclerophyllous vegetation
7	Mineral extraction sites	29	Transitional woodland-shrub
8	Dump sites	30	Beaches, dunes, sands
9	Construction sites	31	Bare rocks
10	Green urban areas	32	Sparsely vegetated areas
11	Sport and leisure facilities	33	Burnt areas
12	Non-irrigated arable land	34	Glaciers and perpetual snow
13	Permanently irrigated land	35	Inland marshes
14	Rice fields	36	Peat bogs
15	Vineyards	37	Salt marshes
16	Fruit trees and berry plantations	38	Salines
17	Olive groves	39	Intertidal flats
18	Pastures	40	Water courses
19	Annual crops associated with permanent crops	41	Water bodies
20	Complex cultivation patterns	42	Coastal lagoons
21	Land principally occupied by agriculture	43	Estuaries
22	Agro-forestry areas	44	Sea and ocean

4.2.1 Mesoscale modelling

Data from MEPA continuous monitoring stations have been used for models verification. Those stations collect both meteorological and air quality parameters and are located as depicted in Figures 17 and 18. Table 22 reports also the classification of the stations from the point of view of air quality.

Table 22. Location and type of meteorological / air quality continuous monitoring stations.

Point	X-UTM33 (m)	Y-UTM33 (m)	Type
Zejtun	458369	3967661	Urban background
Gharb	427705	3991681	Rural background
Msida	459963	3972519	Traffic
Kordin	455871	3970810	Industrial

Figure 17. Location of continuous monitoring stations on Maltese Islands.
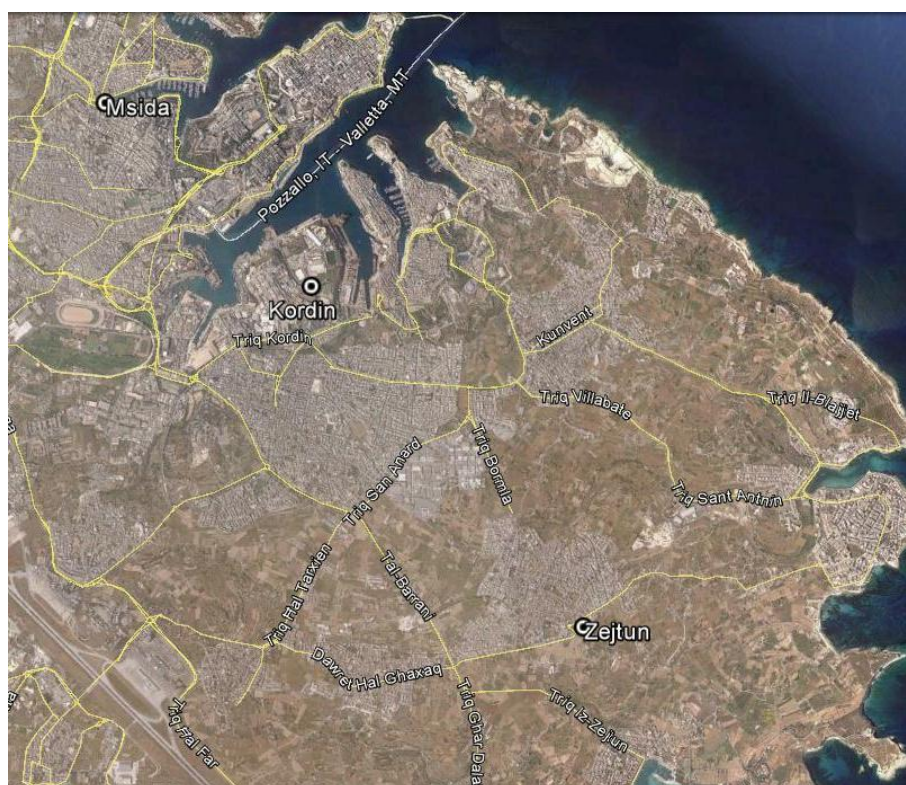
Figure 18. Detail of the position of Zejtun, Kordin and Msida monitoring stations.

Looking at the position of the different stations, some preliminary considerations can be made. The Gharb station, sited in a rural site far from industrial or urban environments on the Gozo island, represents the background flow impacting on the Maltese Islands. Msida and Kordin stations are located in two positions that can be easily affected by urban (Msida) or industrial (Kordin) structures, not directly resolved at the scale adopted by the modeling system. Measurements at the Zejtun station, even if probably not directly affected by local structures, can experience the effect of the roughness due to the corresponding built-up area located just North-West of the monitoring point, that could generate local decelerations of the low-level wind when the flow is coming from northern sectors. Table 23 summarizes the data availability from the stations anemometers over the three considered years: 2010, 2011 and 2012. The number of available data for Kordin station is too low, so it is excluded from the comparison.

Table 23. Local wind data availability at different monitoring stations, as % over each year.

Station	Year 2009	Year 2010	Year 2011
Zejtun	95.8	99.4	96.9
Gharb	96.8	98.8	71.5
Msida	96.5	94.2	94.9
Kordin	16.3	N/A	20.0

The following figures present the comparison between the wind roses for years 2010 and 2011 derived from data measured at Gharb, Zejtun and Msida stations and the ones modeled by QualeAria system at the same locations.

Figure 19 and 20 show the comparison between annual measured and modeled wind roses at Gharb, respectively for year 2010 and 2011. The comparison evidences very similar behaviors

both in terms of speed and direction, with the main flow coming from North-West and a substantial absence of directions coming from North to North-East. Looking also at the interannual variability, both measurement and model results show winds with generally decreasing speeds in 2011, with a smaller number of high speed episodes with respect to 2010. In this respect the QualeAria system seems to correctly describe the wind at Gharb, which represents the synoptic flow scarcely influenced by the local circulation.
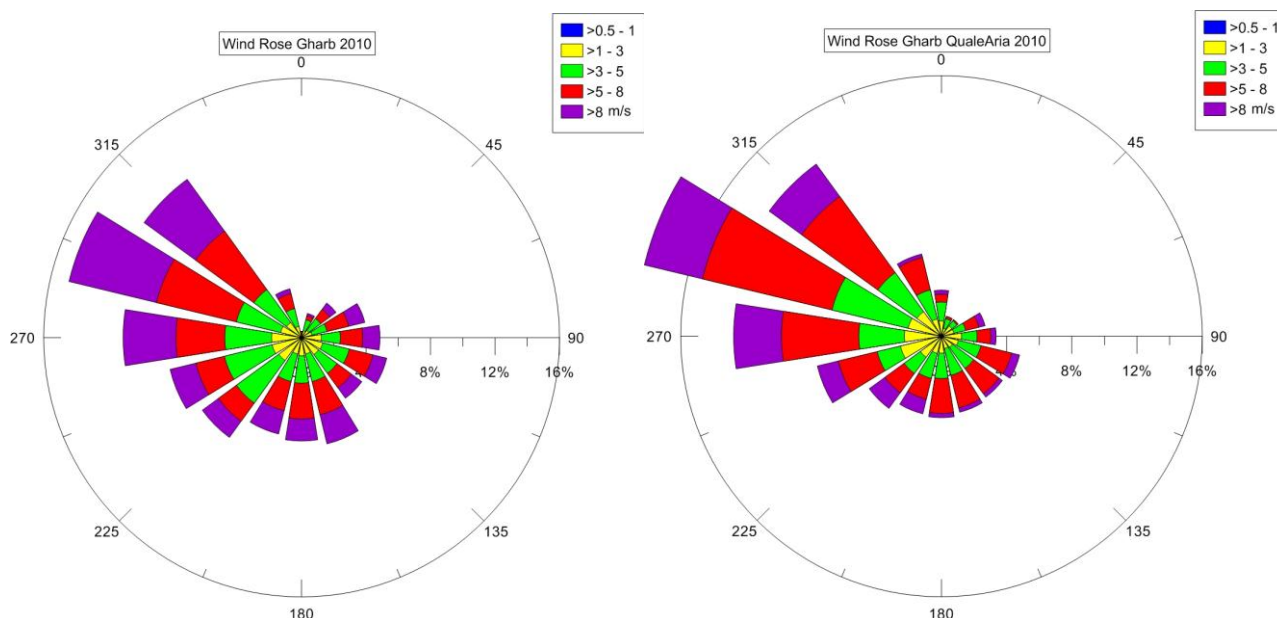
Figure 19. Annual wind rose at Gharb, year 2010: from measured data (left) and from QualeAria mesoscale modelling (right).
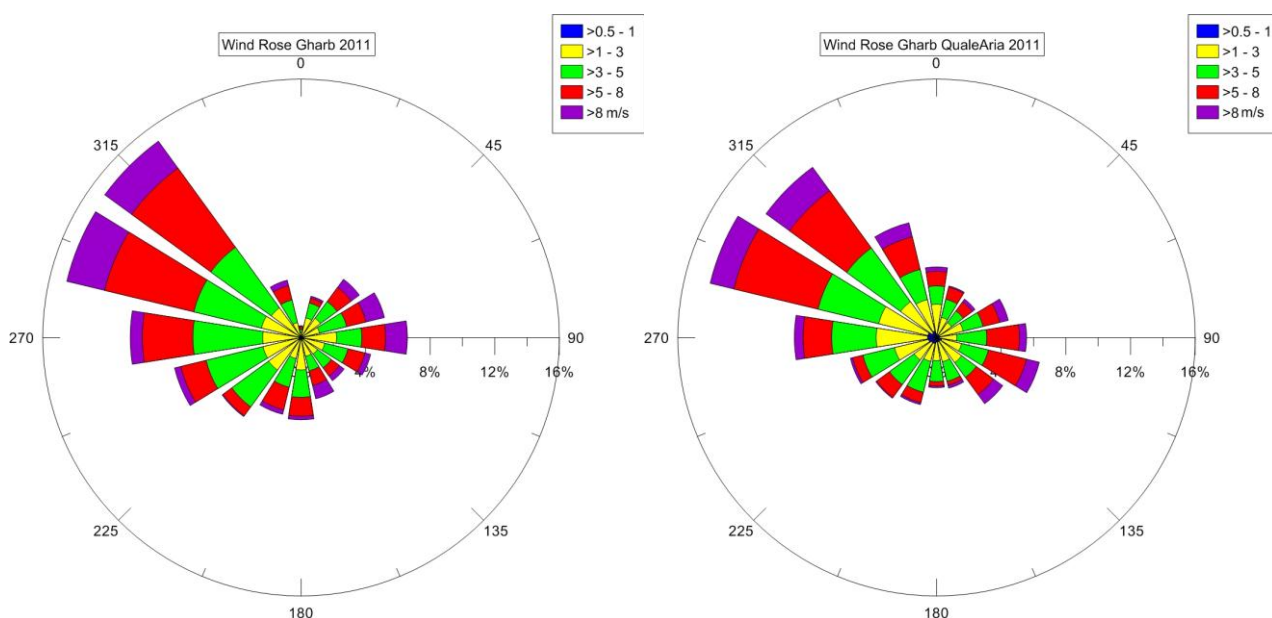
Figure 20. Annual wind rose at Gharb, year 2011: from measured data (left) and from QualeAria mesoscale modelling (right).

Figure 21 and 22 show the comparison between annual measured and modeled wind roses respectively for year 2010 and 2011 at Zejtun, the station closest to the DPS. In this case the measurement are more influenced by the local roughness, particularly for directions coming from

Nort-West, and shows lower speeds. Also for this station, the QualeAria system correctly captures the main structure of the flow, and in fact it is also able to model winds which are lower compared to the ones in Gharb. Despite that general coherence, its relatively coarse horizontal resolution (12 km) does not allow to fully describe the same deceleration process probably induced by local roughness patterns, being a subgrid feature for the meteorological model.
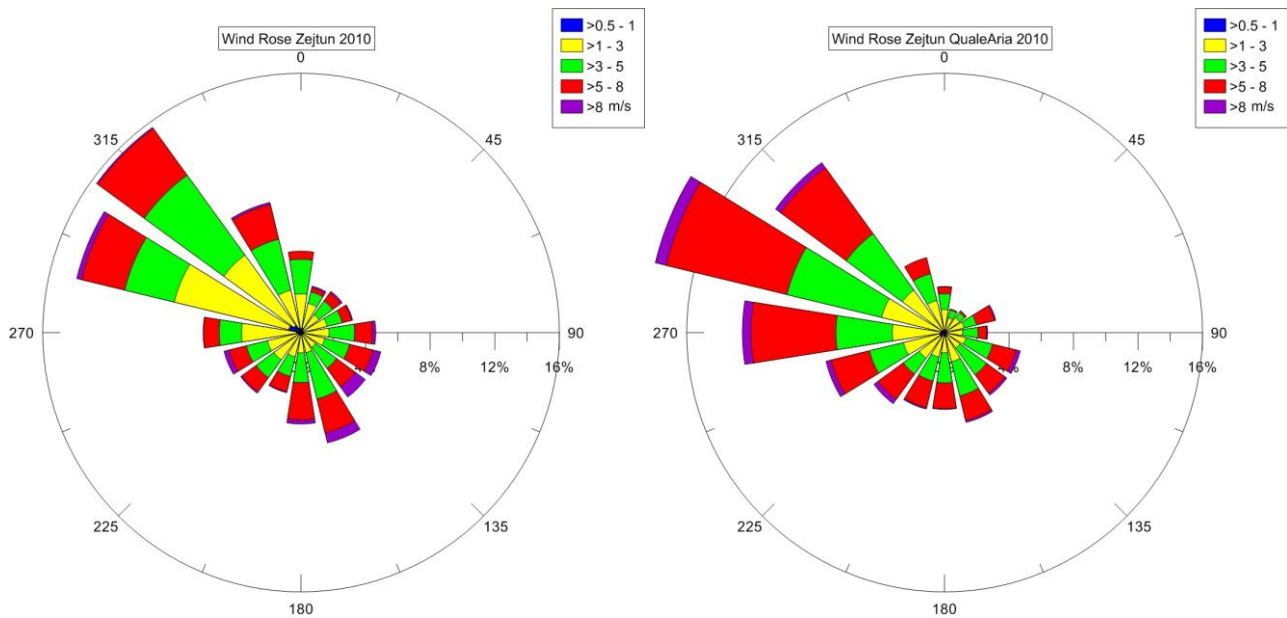
Figure 21. Annual wind rose at Zejtun, year 2010: from measured data (left) and from QualeAria mesoscale modelling (right).
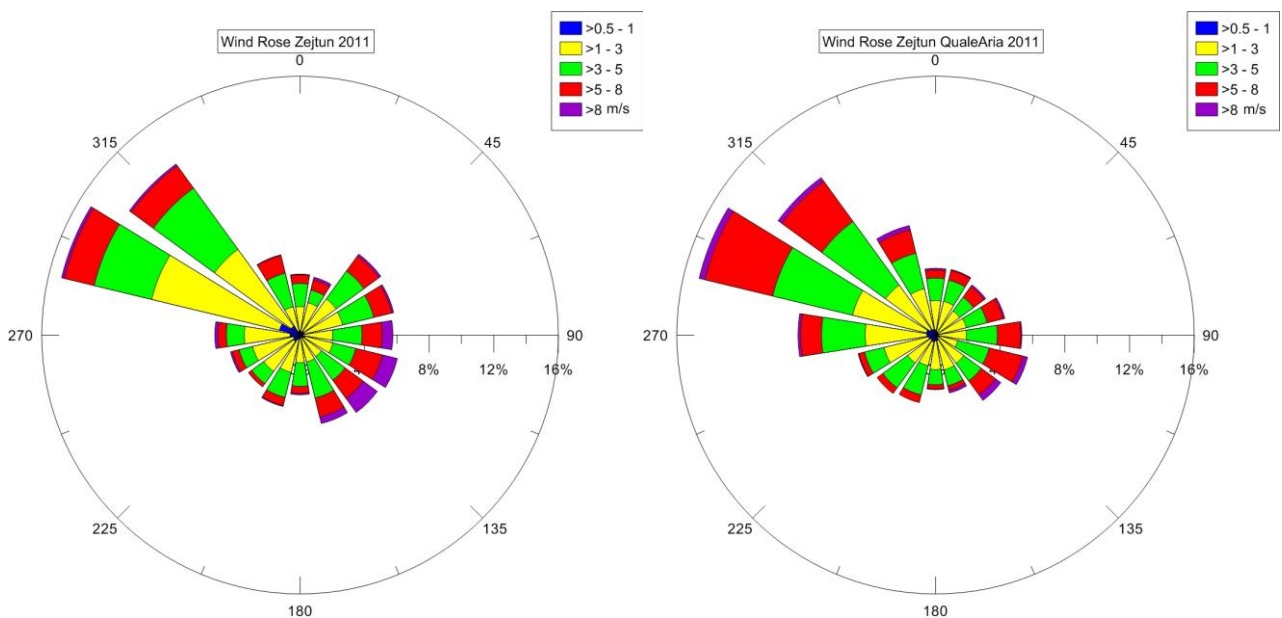
Figure 22. Annual wind rose at Zejtun, year 2011, measured data (left) and from QualeAria mesoscale modelling (right).

Finally, Figures 27 and 27 show the comparison between annual measured and modeled wind roses respectively for year 2010 and 2011 at Msida, the urban station located in a high traffic area.
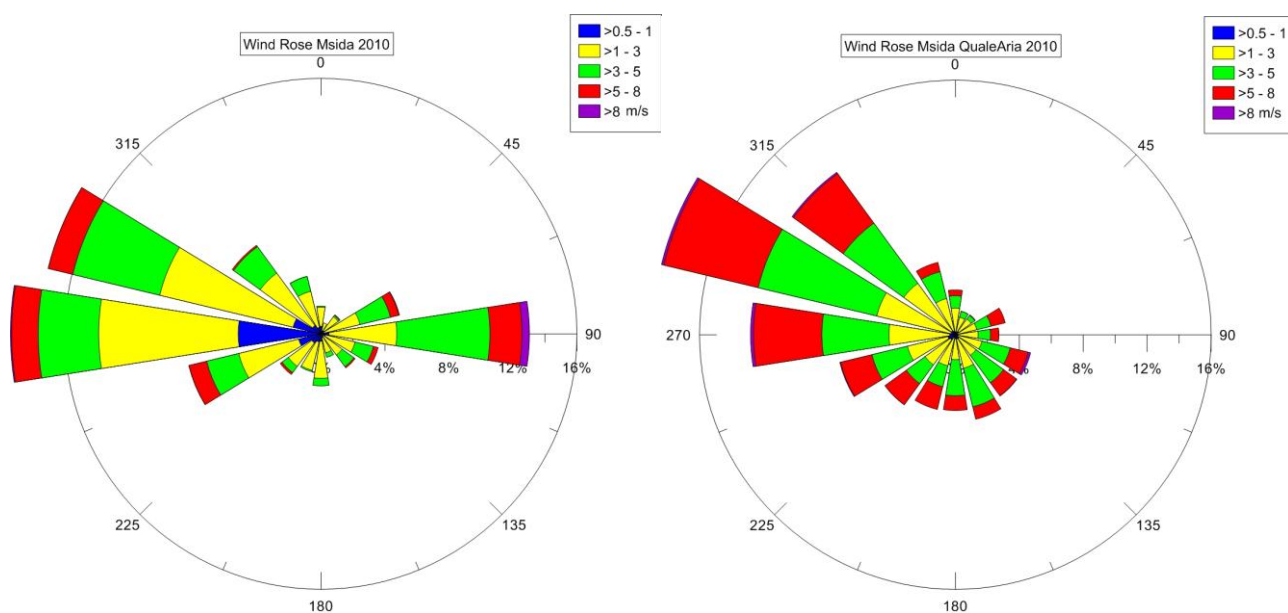
Figure 23. Annual wind rose at Msida, year 2010: measured data (left) and from QualeAria mesoscale modelling (right).
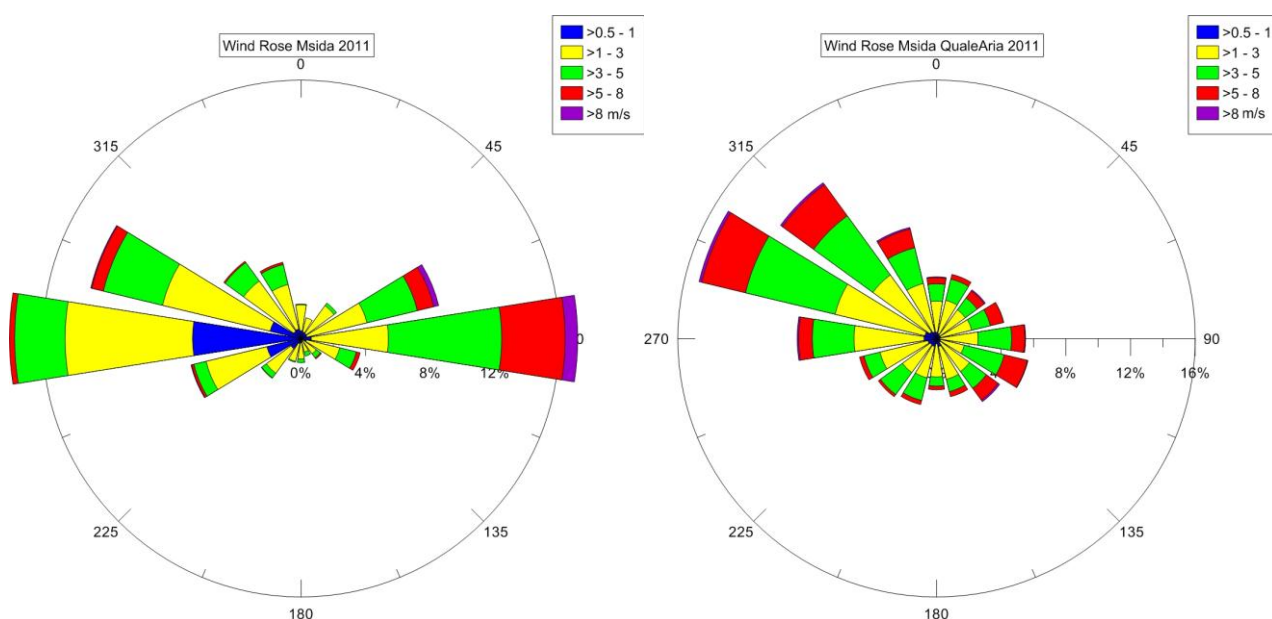
Figure 24. Annual wind rose at Msida, year 2011: measured data (left) and from QualeAria mesoscale modelling (right).

Data measured at this station show evident local channeling effects, probably due to masking processes generated by the obstacles present in the proximity of the station. These effects represent a very particular aspect, closely related to the local features of the of the measurement site.

The comparison evidences that from the point of view of the wind flow, the data provided by the QualeAria system describe a correct scenario on a statistical basis, comparable with measurements at Gharb and Zejtun stations. Some features such as the flow structure at the urban site of Msida cannot be reproduced by the modeling system but, representing very local characteristics, they should not be represented inside the models at the target scale used in this work.

4.2.2 Modelling on target domains

The following figures illustrate some examples of the meteorological fields generated through GAP and SWIFT/MINERVE on the background and local domains, then used by pollutants dispersion models.

Figure 25 shows the wind field close to the ground generated at 1 km and at 200 m horizontal resolutions in a winter nocturnal case, when the wind blows from the most recurrent direction. The high resolution model shows local wind variations over the Maltese Islands due to horizontal inhomogeneities of orography and surface roughness, that tend to reduce the speed particularly over the urbanized areas.

Figure 26 shows the wind field close to the ground generated at both resolutions in a winter diurnal case, showing a more persistent and homogeneous flow blowing from North-West, with higher speeds, partially reduced over the urbanized area.

Finally, Figures 27 and 28 respectively show a nocturnal and diurnal cases during spring. In the first case again the persistent flow from North-West is present but with smaller speeds, while in the second one the flow is completely reversed showing directions mainly from South-West, a sector that, as indicated by the wind rose in Figure 31, exhibit a relatively large occurrence of higher speeds.
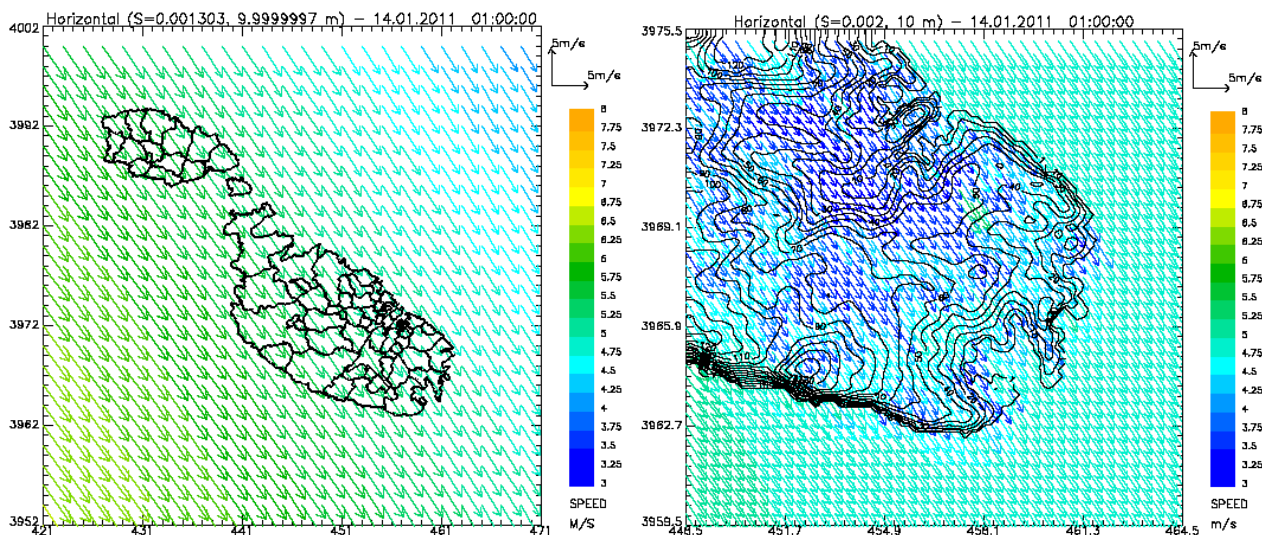
Figure 25. Wind fields at 10 m reconstructed on the background (left) and local (right) domains at 14/1/2011 01:00 (local time); wind vectors are colored according to the color scale for speed reported on the right (m/s).
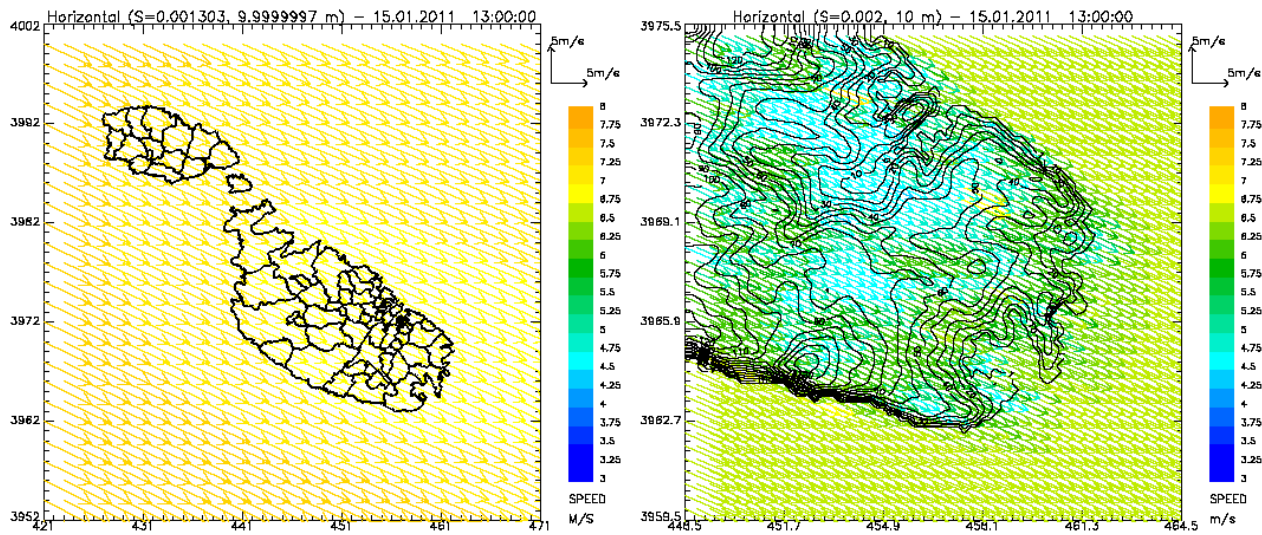
Figure 26. Wind fields at 10 m reconstructed on the background (left) and local (right) domains at 15/1/2011 13:00 (local time).
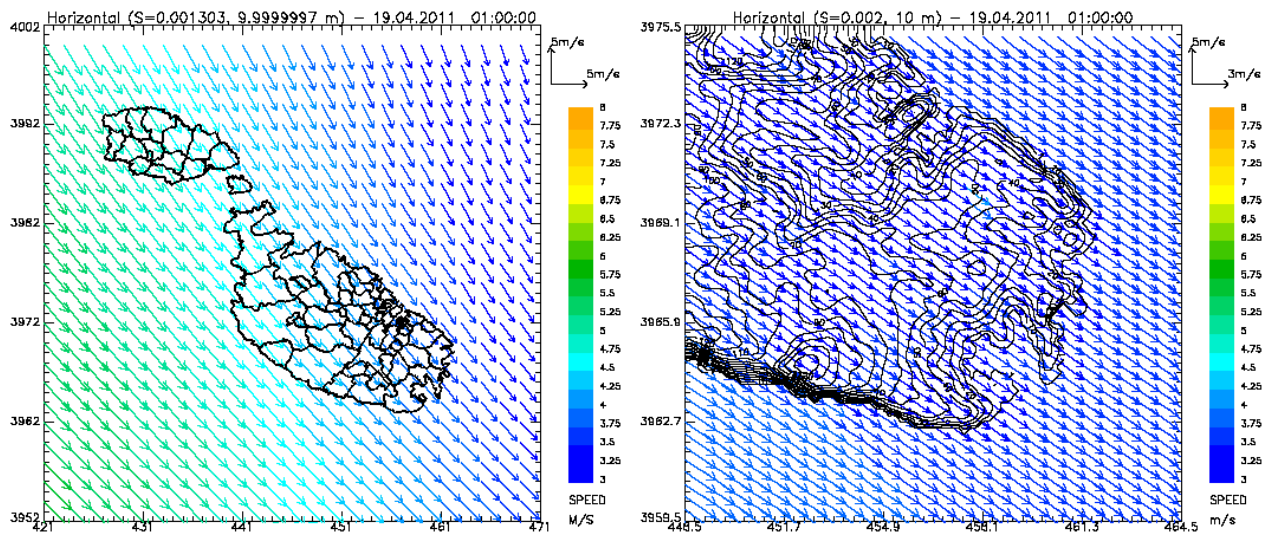
Figure 27. Wind fields at 10 m reconstructed on the background (left) and local (right) domains at 19/4/2011 01:00 (local time).
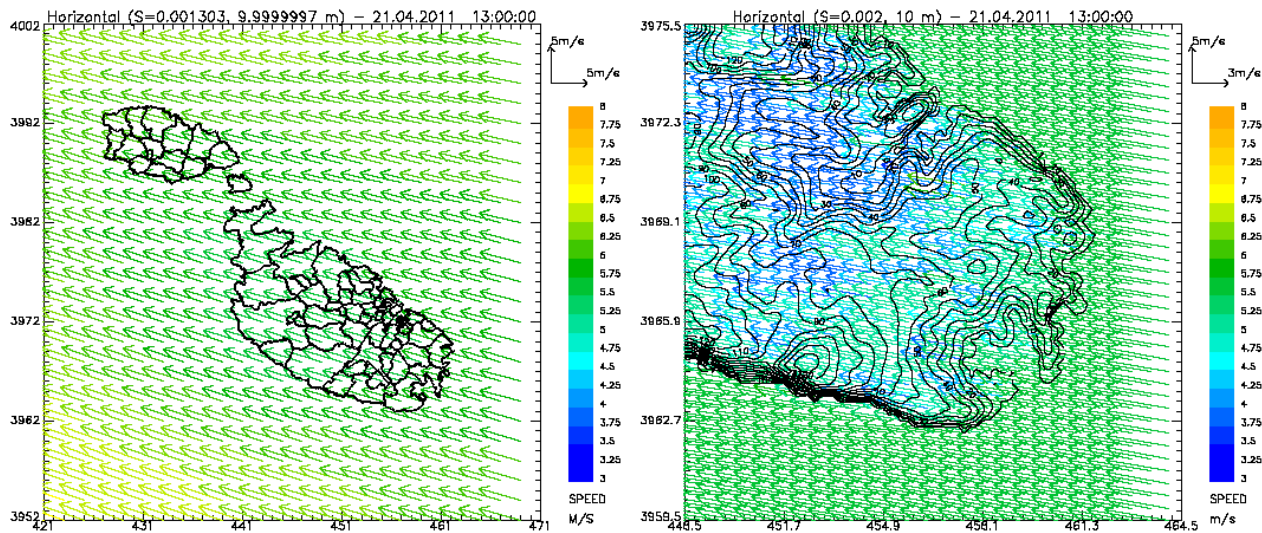
Figure 28. Wind fields at 10 m reconstructed on the background (left) and local (right) domains at 21/4/2011 13:00 (local time).

Figure 29 shows an example of the air temperature fields close to the ground for the two domains. Results at finer resolution contain more details, mainly related to the topographical structure of the island, which can be better represented than in the background domain.
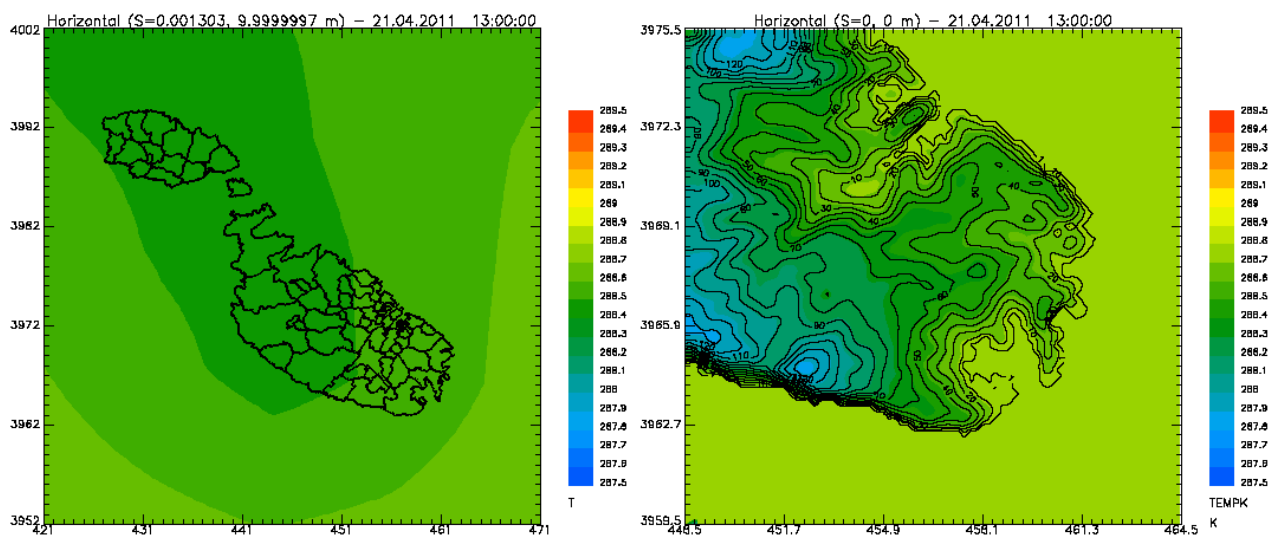
Figure 29. Air temperature field close to the ground reconstructed on the background (left) and local (right) domains at 21/4/2011 13:00 (local time).

The following figures illustrate the comparison between the data measured by the anemometer of the Zejtun station (the one closest to DPS, most significant for pollutants dispersion) and the data at the same location extracted from the wind fields reconstructed on the local domain.

Figure 30 shows the comparison between the measured wind rose and the one reconstructed by SWIFT model: the behavior is quite similar to the one of QualeAria system (Figure 22).

Further insights can be obtained examining the comparison by season for year 2011: Figures 31, 32, 33 and 34 show wind roses respectively for spring (Mar-Apr-May), summer (Jun-Jul-Aug), autumn (Sep-Oct-Nov) and winter (Dec-Jan-Feb). The behaviors of experimental and modeled winds are very similar. During spring, both of them show the dominance of wind sectors from

North-West, as well as non-negligible contributions from East and especially South-East. The local winds generated by the model from southern sectors exhibit lower speeds, thus allowing to perform a more conservative simulation of the dispersion of pollutants released from DPS. In summer, the southeastern component is still present but is less important, and speeds are slower. In autumn, southeastern flow becomes more pronounced than northeastern one, and is also characterized by higher speeds. Finally, during winter the component from South-East totally disappears, in measurements as well in simulations.

The seasonal analysis reinforce the fact that the reconstructed meteorological scenario can be considered as reliable.
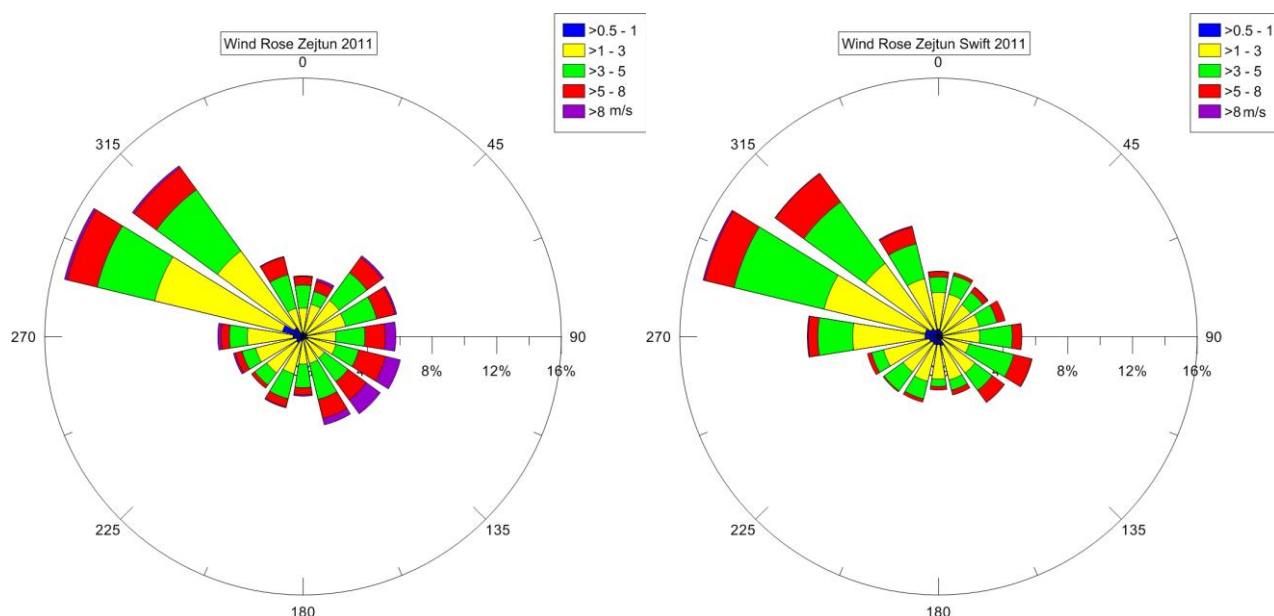
Figure 30. Annual wind rose at Zejtun, year 2011: from measured data (left) and modeled by SWIFT (right).
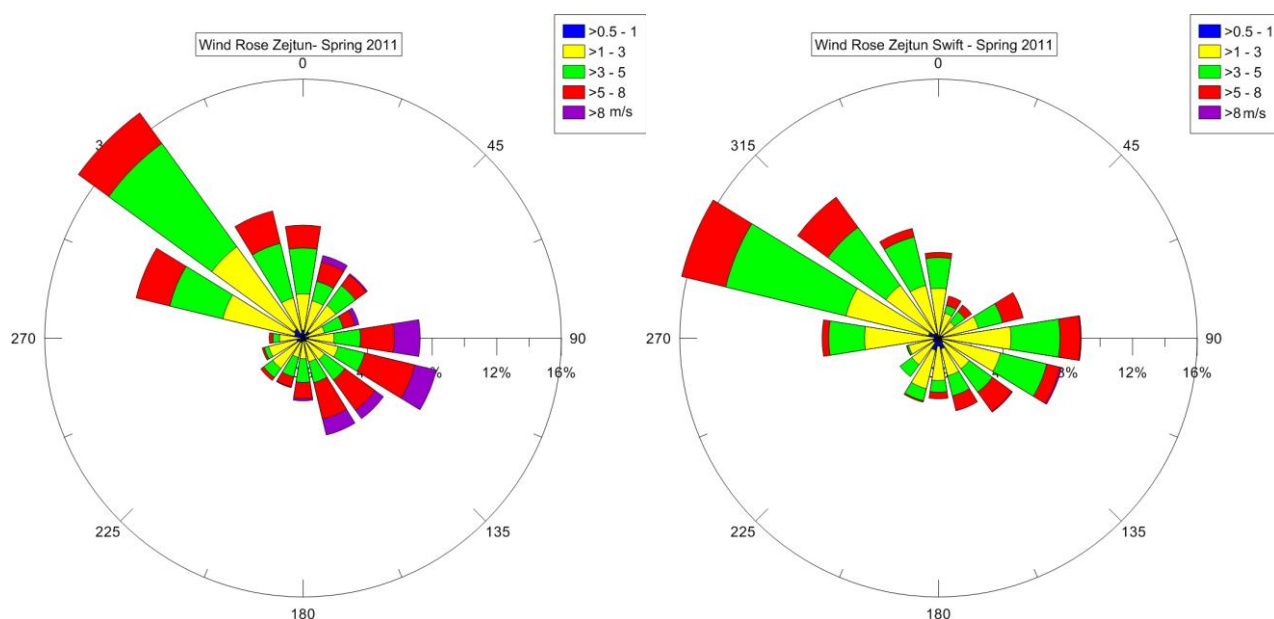
Figure 31. Wind rose at Zejtun, spring 2011: from measured data (left) and modeled by SWIFT (right).
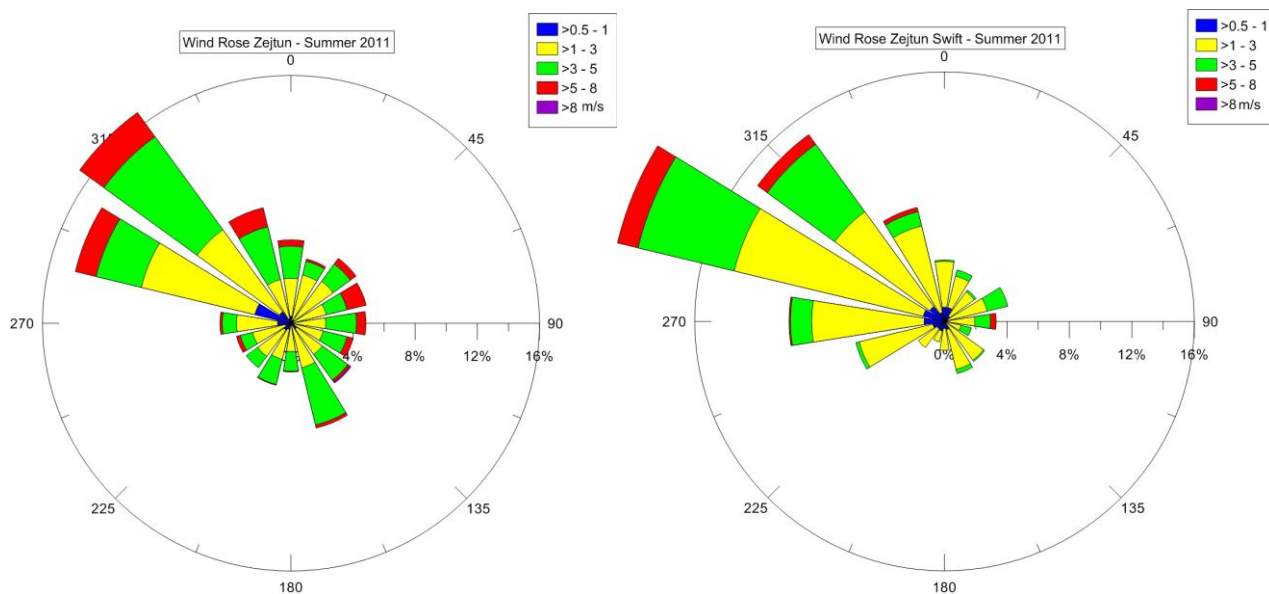
Figure 32. Wind rose at Zejtun, summer 2011: from measured data (left) and modeled by SWIFT (right).
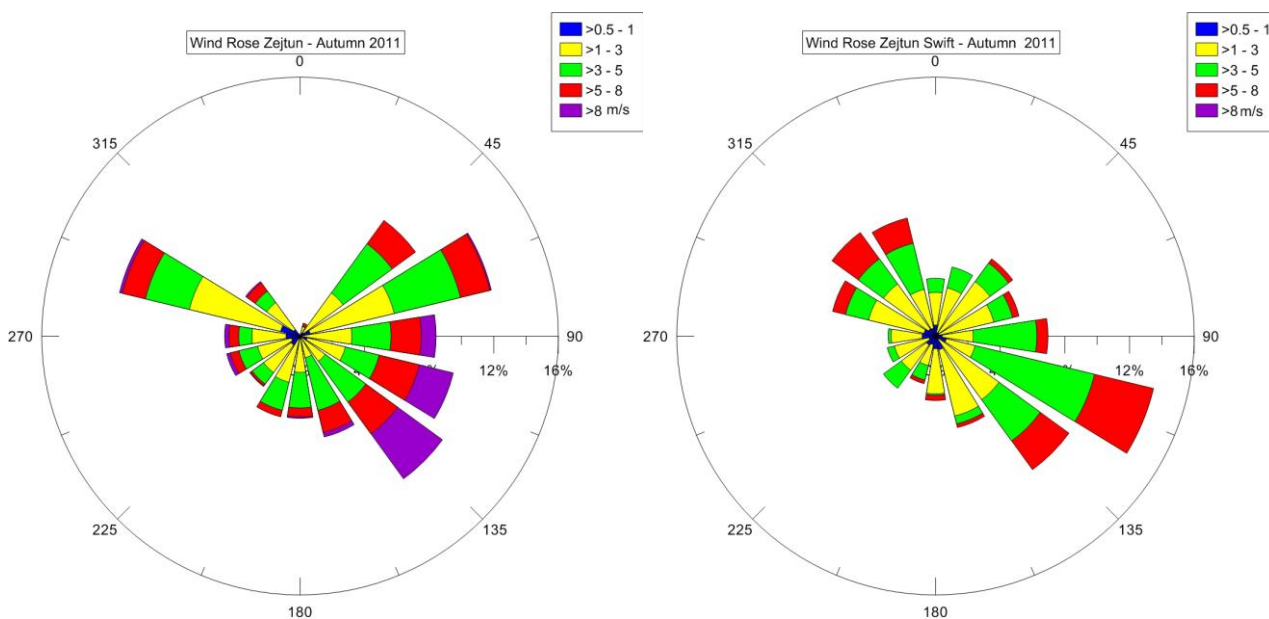
Figure 33. Wind rose at Zejtun, autumn 2011: from measured data (left) and modeled by SWIFT (right).
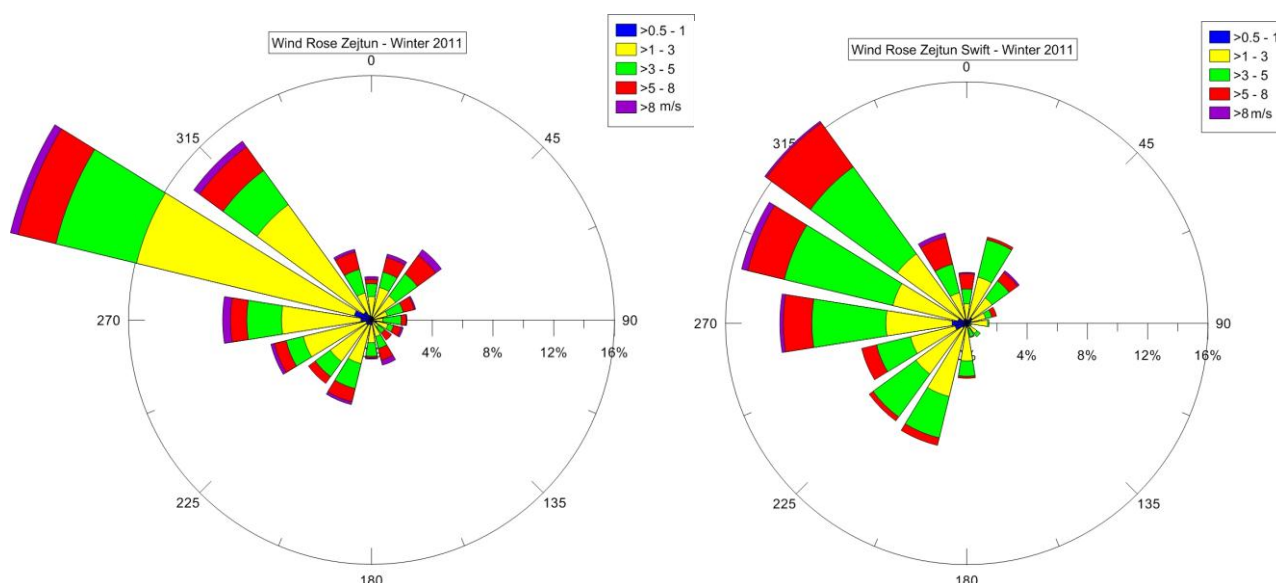
Figure 34. Wind rose at Zejtun, winter 2011: from measured data (left) and modeled by SWIFT (right).

Hourly wind and temperature 3D fields over complex terrain generated by GAP and SWIFT models are then passed to the SURFPro, to produce corresponding 2D inhomogeneous hourly fields of turbulence scale parameters of the surface and planetary boundary layers, to be used by dispersion models to describe the atmospheric diffusivity. SURFPro generates hourly 2D fields of the friction velocity u_*, Monin-Obukhov length L, mixing height H_{mix}, convective velocity scale w_*, surface roughness z_0 starting from:

- wind close to ground
- vertical temperature profiles
- total cloud cover available from the QualeAria system simulations
- CORINE Land Cover over the target domain

To give an example of the fields of turbulence variables generated by SURFPro, Figures 35, 36, 37 and 38 shows 2D fields over both domains of u_*, L, H_{mix}, and w_* respectively, relative to 21/4/2011 13:00. Variables on the maps describe the situation of a spring sunny day, with unstable convective conditions over the ground and the growth of a relatively high PBL internal to the coast. Larger values of u* are present mainly over the urban regions of the islands, where also the maximum of the PBL levels are developed. The local domain shows the presence of more details as a consequence of the finer resolution adopted.
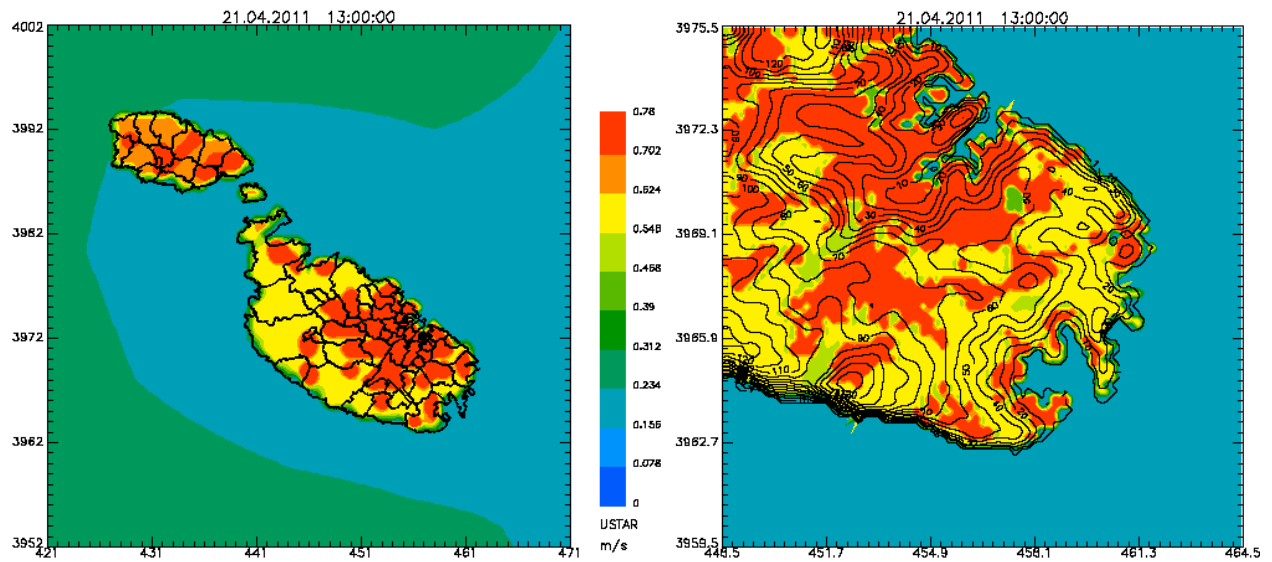
Figure 35. Example of u∗ fields at 21/4/2011 13:00 (local time): on background domain at 1 km horizontal resolution (left), and local domain at 200 m horizontal resolution (right).
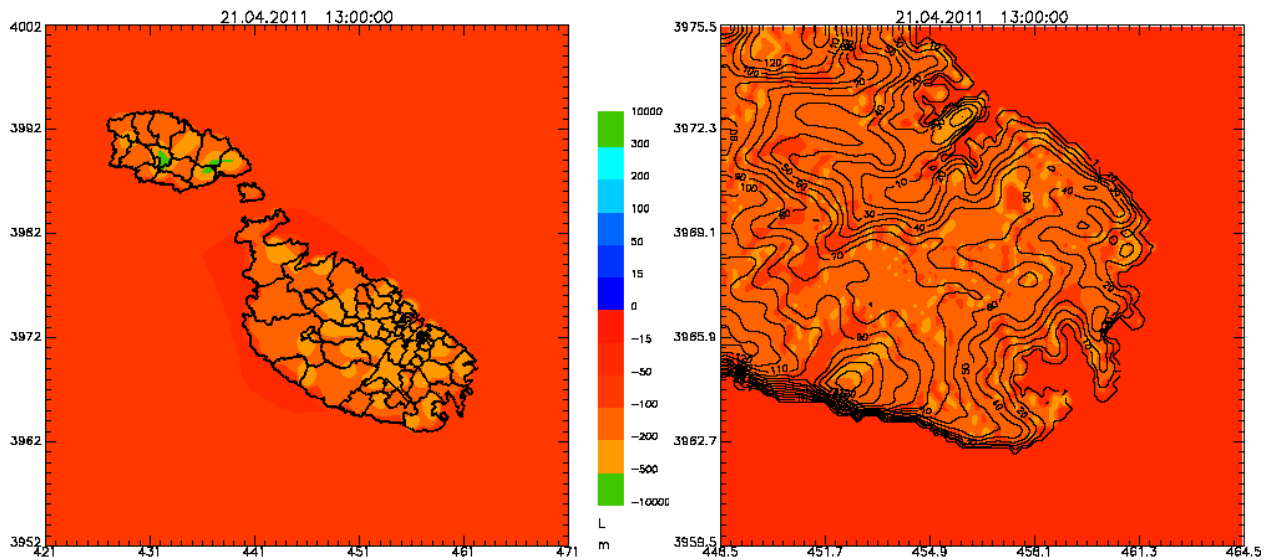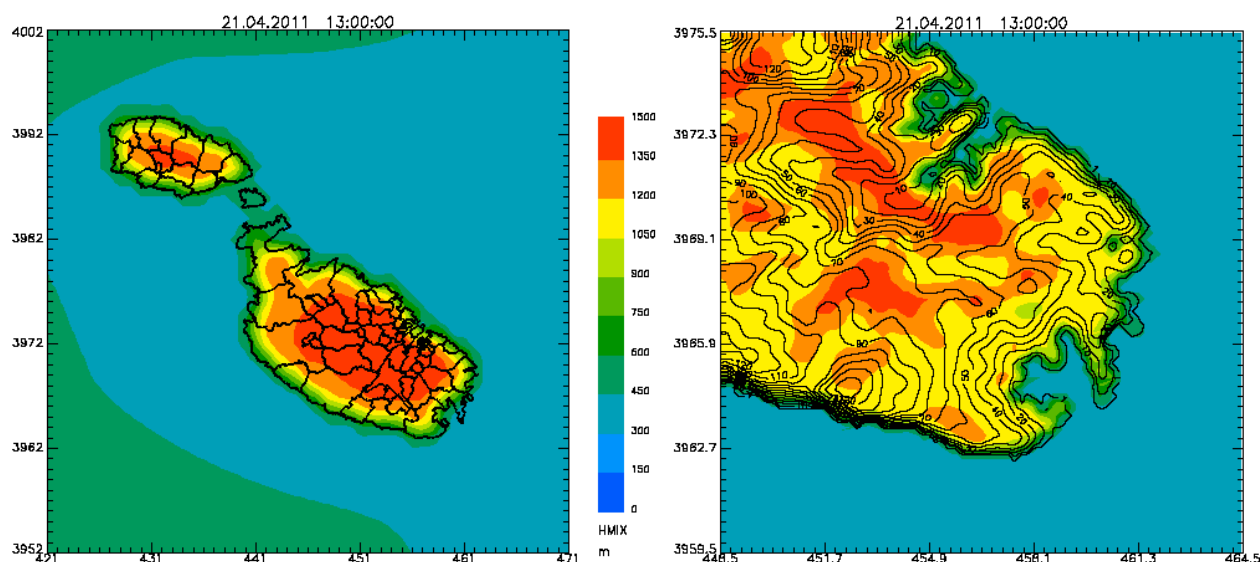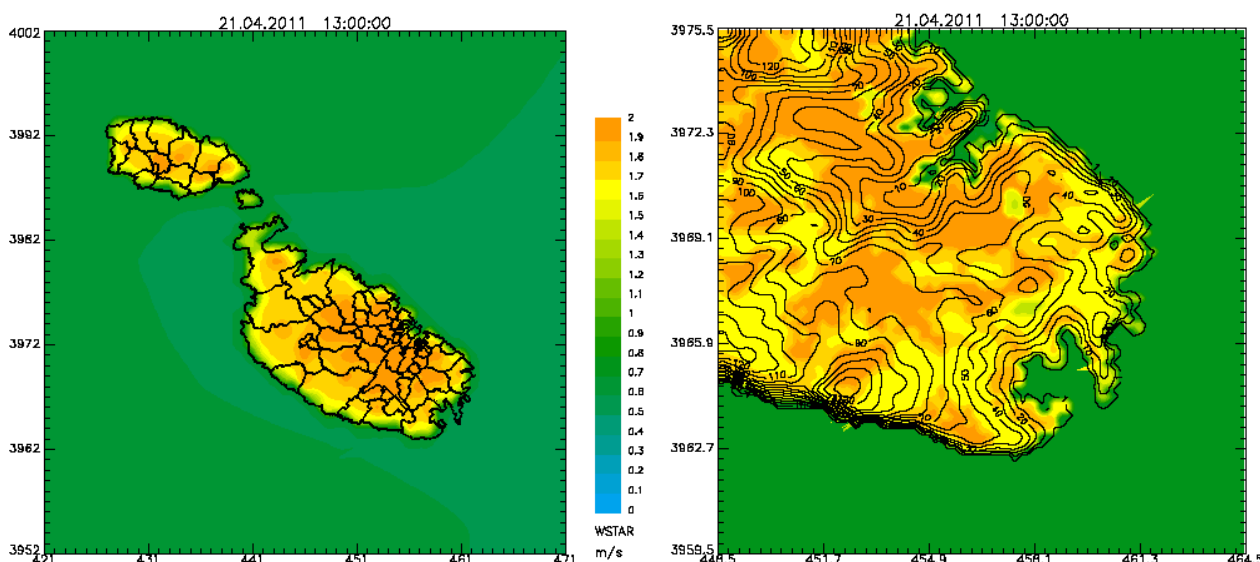

Figure 36. Example of L fields at 21/4/2011 13:00 (local time): on background domain at 1 km horizontal resolution (left), and local domain at 200 m horizontal resolution (right).

Figure 37. Example of H$_{mix}$ fields at 21/4/2011 13:00 (local time): on background domain at 1 km horizontal resolution (left), and local domain at 200 m horizontal resolution (right).

Figure 38. Example of w* fields at 21/4/2011 13:00 (local time): on background domain at 1 km horizontal resolution (left), and local domain at 200 m horizontal resolution (right).

Hourly meteorological fields have been produced on the background domain for the entire year 2011, while on the local domain they have been generated over the three full years (2010-2011-2012) to properly take into account the effect of inter-annual variability on dispersion of pollutants released from the power plants.

4.3 Dispersion modelling

Pollutants dispersion modelling has been carried out through ARIA Industry and ARIA Regional, two integrated software suites for atmospheric dispersion modelling. The embedded dispersion models are able to cater, among other things, all the requirements given for this study:

- simple, intermediate and complex terrain, including over stretches of sea;

- the ability to use real-time meteorological data and ambient (background) pollutant concentrations for prediction of emissions;
- continuous release modelling (depending on inputting of stack height, plume parameters, temperature, etc.);
- screening of continuous or single releases in simple or complex terrain;
- industrial source complex modelling;
- graphics system for illustration of modelling results.

The dispersion modeling related to **DPS and MPS** have been carried out with **SPRAY**, a 3D dynamic Lagrangian particle-based dispersion model.

SPRAY is in fact designed to simulate the dispersion of airborne gaseous or particle pollutant released, either continuously or intermittently, from by point, line, area or volume sources, taking into account the spatial and temporal inhomogeneities of both the mean flow and turbulence.

The behavior of the airborne pollutants is simulated through "virtual particles" whose mean movement is defined by the local wind, while the dispersion is determined by velocities obtained as solution of Lagrangian stochastic differential equations, able to reproduce the statistical characteristics of the turbulent flow. Different portions of the emitted plumes can therefore experience different atmospheric conditions, allowing more realistic reproductions of complex phenomena (low wind speed conditions, strong temperature inversions, flow over topography, presence of terrain discontinuities such as land-sea or urban-rural), hard to simulate with more traditional approaches like the steady-state Gaussian one (traditional / hybrid straight-plume models or puff models).

Being able to fully model dynamic emission and pollutants dispersion, in the application to DPS and MPS SPRAY has been directly fed with the hourly data recorded by the continuous emission monitoring systems (CEMS) that are in place. This add another degree of realism, allowing to directly consider transients in plants operating conditions and extreme events.

The **background concentrations**, including long-range transboundary sources, have been computed with **FARM**, a three-dimensional Eulerian model that accounts for the transport, chemical conversion and deposition of atmospheric pollutants, considering the contribution from all sources in a given geographic domain and, through pollutants boundary conditions, from the a wider area. FARM can be used for impact assessment studies, operational forecasting, yearly air quality evaluations and policy scenarios assessment respect to EU legislation.

The **Appendix** includes a description of both models, with full list of scientific references.

5   Dispersion models results

5.1 *Delimara Power Station*

To proper consider the effect of interannual meteorological variability in assessing the contribution from DPS to ambient concentrations, dispersion of pollutants released from DPS stacks has been simulated considering three meteorological years, 2010, 2011 and 2012. This has been repeated for both scenarios of DPS emissions: TOC and NOC.

- In the following, for each scenario the maps of the concentration indicators which are relevant for the limit and target values are reported:NO_x annual average concentrations;

- number of exceedances of the hourly standard for NO_2 concentrations (200 µg/m3) over a whole year;
- PM_{10} and $PM_{2.5}$ annual average concentrations;
- annual average concentrations for lead, arsenic, cadmium, nickel;
- yearly maxima of 24-hours average concentrations of vanadium.

For a given indicator are reported the individual maps for each meteorological year considered.

5.1.1 TOC scenario

Figures 40-48 show the maps of the concentration indicators resulting from DPS emissions in the transitional operating conditions.

For a rather conservative assessment, NO_x concentrations can be compared against the NO_2 annual limit value for the protection of human health (40 µg/m^3). The results over the three meteorological years (Figure 40) indicate that in the worst conditions the overall maximum across the domain can reach 5.8 µg/m^3 of NO_x. As a consequence of the prevailing winds, such value occurs anyway over the sea SE of the plant. Over land in fact, annual average NO_x values can exceed 2 µg/m^3 inside an area of about 3 km of radius from DPS, and can be above 4 µg/m^3 only for a small area extending up to 500 m SE of the plant.

Using NO_x hourly concentrations to compare against the NO_2 hourly standard (200 µg/m^3, not to be exceeded more than 18 times in any calendar year) usually gives unrealistic results, so NO_2 are also estimated. The percentage of NO and NO_2 in the NO_X mixture in atmosphere varies according to, among the others, the site, the meteorology and the distance from the main sources. Besides, NO continuously transforms into NO_2 due to solar radiation and the presence of ozone and the inverse transformation is performed as well in a dynamic equilibrium state. For a given area, time series of experimental data of the two components can be used to calculate the coefficients of an interpolating curve (Derwent and Middleton, 1996; Dixon et al., 2000; FAIRMODE document, http://acm.eionet.europa.eu/reports/ETCACM_TP_2011_15_FAIRMODE_guide_modelling_NO2), expressing the hourly average values of NO_2 as a function of the known values of the NO_x concentrations. In this study the relationship between these two pollutants is derived from the analysis of the hourly measured values of NO_2 and NO_x for the years 2010-2011 at the Msida monitoring station. Figure 39 shows the experimental values of NO_x and NO_2 (blue symbols) collected at Msida and the estimated curve interpolating them. This function is used to estimate the NO_2 concentration starting from NO_x calculated values.
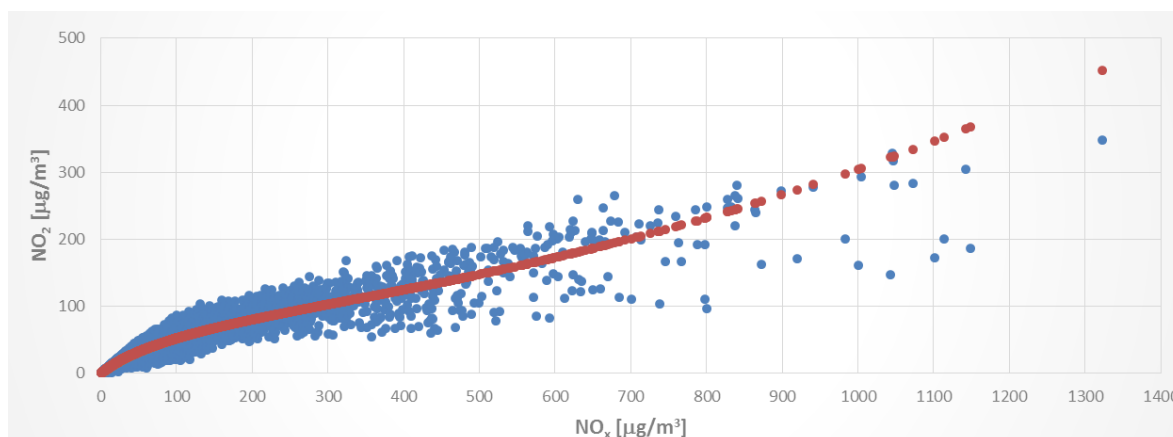
Figure 39. NO₂ vs. NOₓ hourly concentration values measured at Msida monitoring station during years 2010-11 and the function interpolating them.

The maps (Figure 41) of the resulting number of exceedances of the hourly standard over each meteorological year indicate that the contribution of DPS alone can be responsible in the worst case of no more than a few exceedances over a year only over a very small part of the coast at the NE of the power plant.

In the case of PM_{10}, the results over the three meteorological years (Figure 42) indicate that over land the annual average contribution from DPS in the worst conditions are below 0.3 µg/m³. The contribution to $PM_{2.5}$ concentrations does not exceed 0.15 µg/m³ (Figure 43). The values are well below the annual limits for PM_{10} and $PM_{2.5}$ (40 and 24 µg/m³, respectively).

Over all three meteorological years the estimated contribution from DPS to PM_{10} concentrations never exceed the limit value on 24-hour average (50 µg/m³, not to be exceeded more than 35 times in any calendar year).

The simulation results for heavy metals indicate that in the worst conditions over the whole domain the annual average concentrations of lead and arsenic are below 0.1 ng/m³, and the ones of cadmium below 0.03 ng/m³. In the worst conditions, annual average concentrations of nickel can reach the 5-6 ng/m³ range in the immediate surroundings of DPS over Delimara peninsula, and progressively go down below 2 ng/m³ at distances of more than 3 km from DPS. So for all these heavy metals, the resulting contribution of DPS annual concentrations is below the limits (0.5 µg/m³ for lead, and respectively 6, 5 and 20 ng/m³ for arsenic, cadmium and nickel).

No limit or target values are currently in force for vanadium, so the yearly maxima of 24-hours average concentrations have been computed (Figure 48), to be compared against the guideline value indicated by WHO for that averaging period (1 µg/m³). In the worst conditions, the yearly maxima of 24-hours average concentrations computed over land are slightly above 1 µg/m³ over a small area in the surroundings of DPS, so below the guideline value.
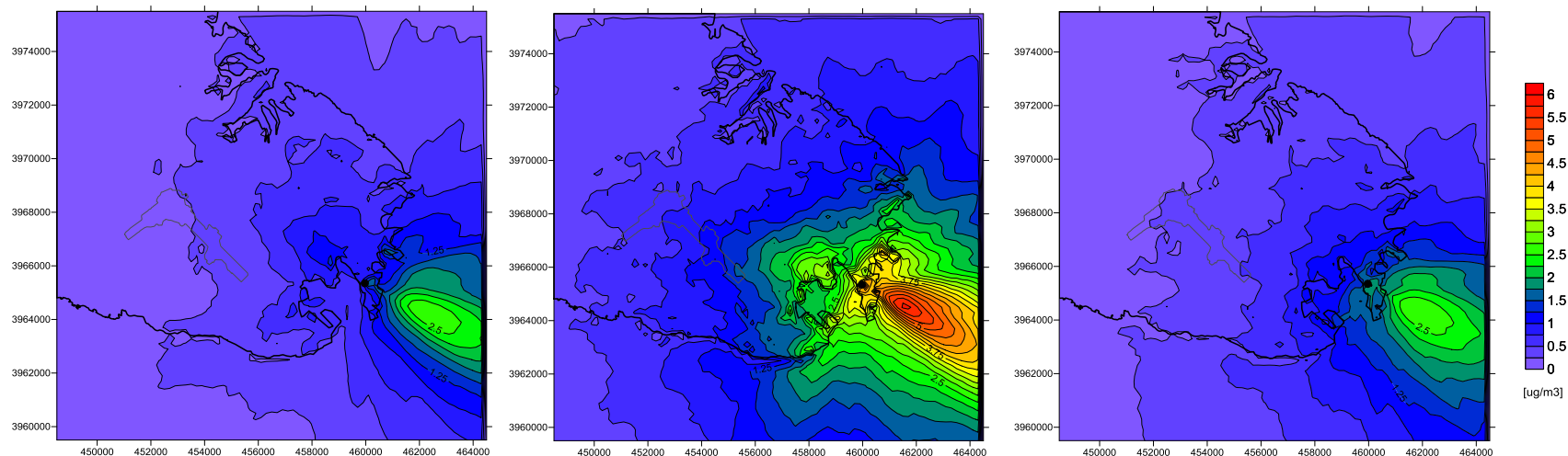
Figure 40. Annual average NOx concentrations from DPS in transitional operating conditions, according to meteorology of year 2010, 2011, 2012 (left, centre, right).
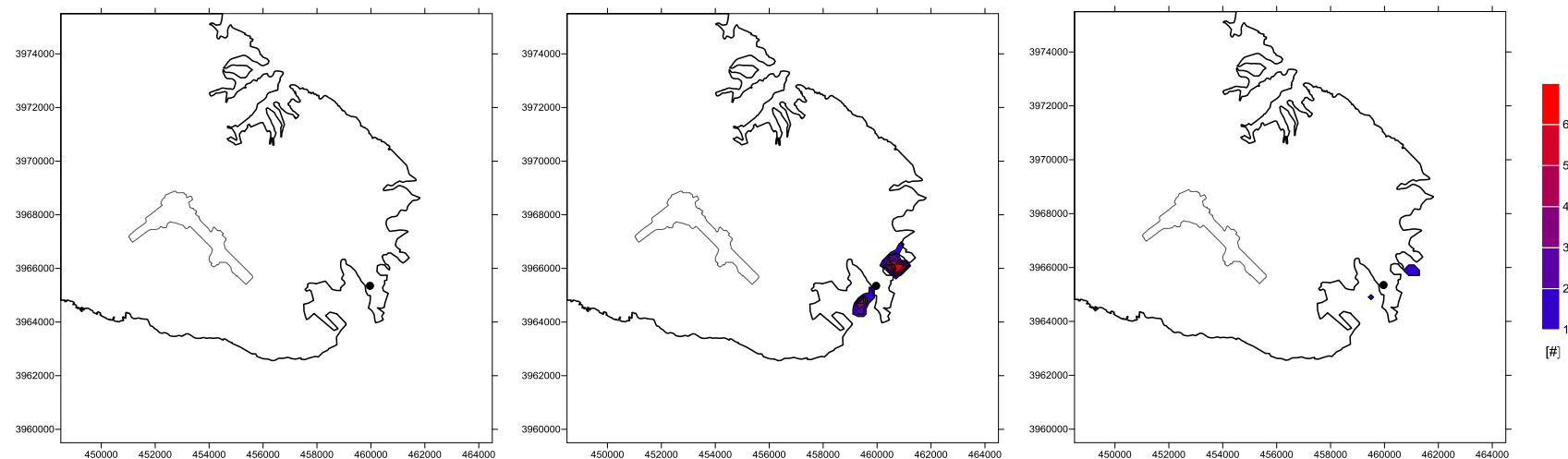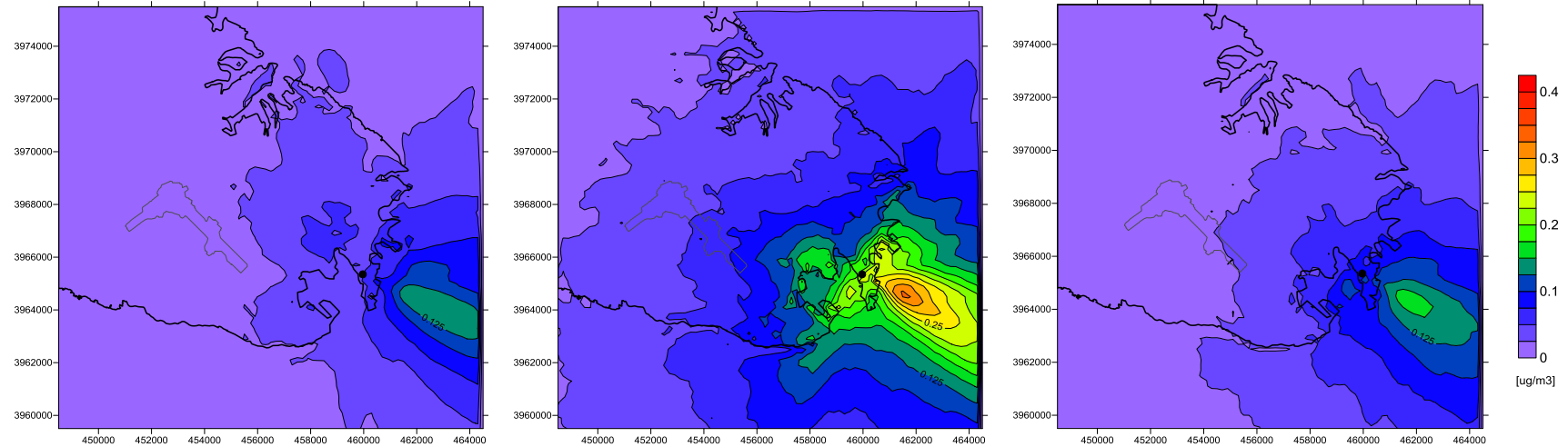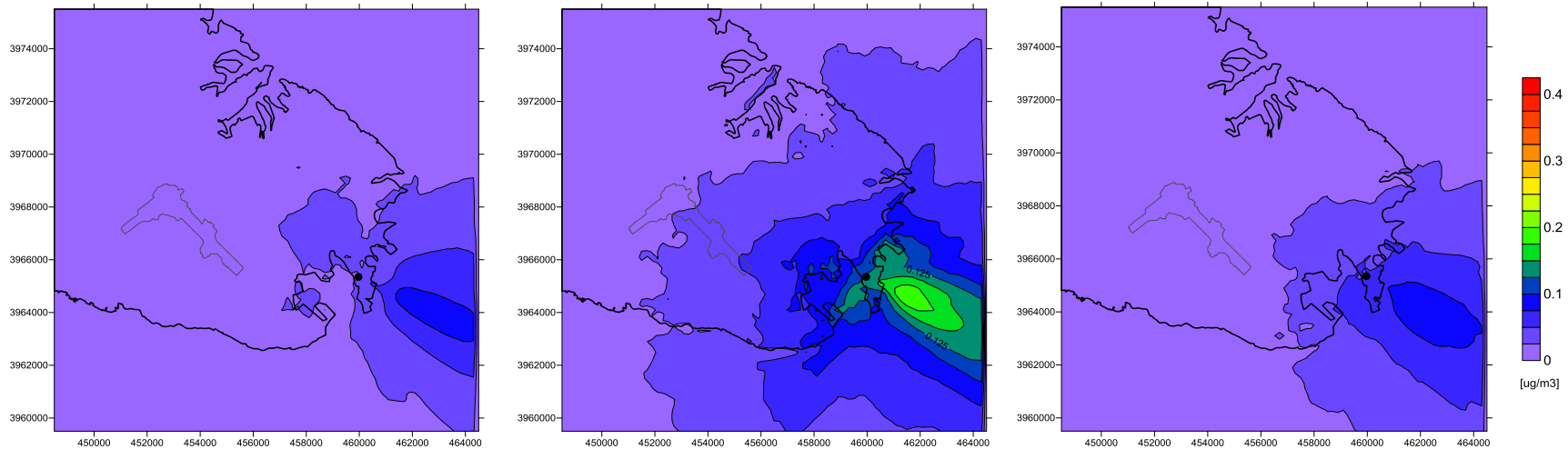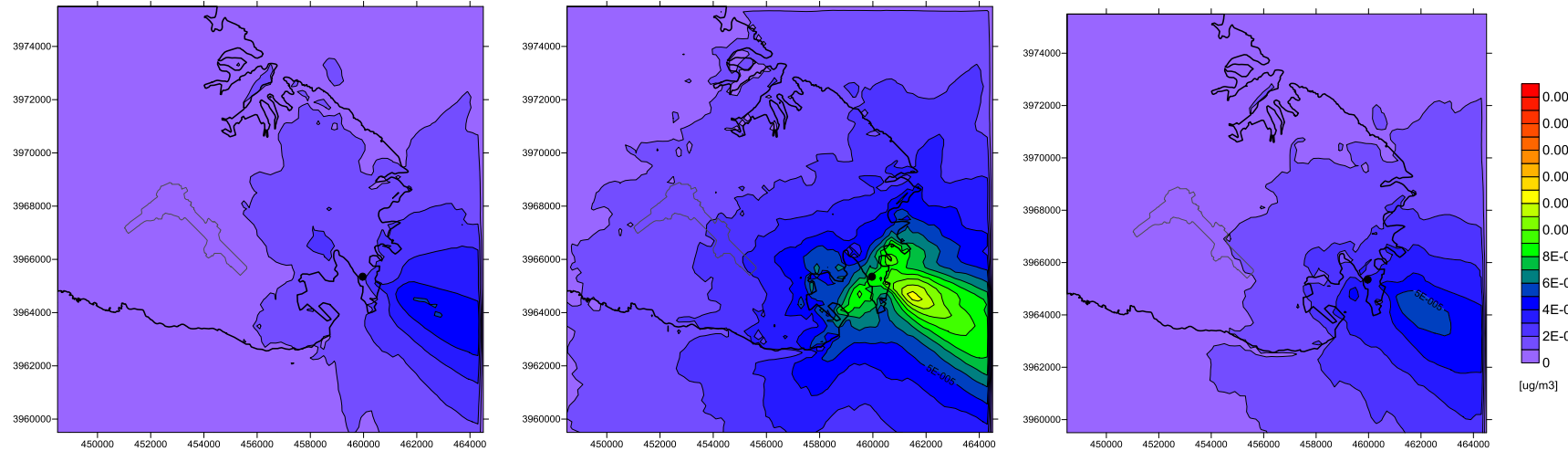

Figure 41. NO$_2$ concentrations from DPS in transitional operating conditions: number of exceedances of the hourly standard (200 μg/m^3) over a whole year, according to meteorology of year 2010, 2011, 2012 (left, centre, right).

Figure 42. Annual average PM₁₀ concentrations from DPS in transitional operating conditions, according to meteorology of year 2010, 2011, 2012 (left, centre, right).

Figure 43. Annual average PM₂.₅ concentrations from DPS in transitional operating conditions, according to meteorology of year 2010, 2011, 2012 (left, centre, right).

Figure 44. Annual average concentrations of lead from DPS in transitional operating conditions, according to meteorology of year 2010, 2011, 2012 (left, centre, right).
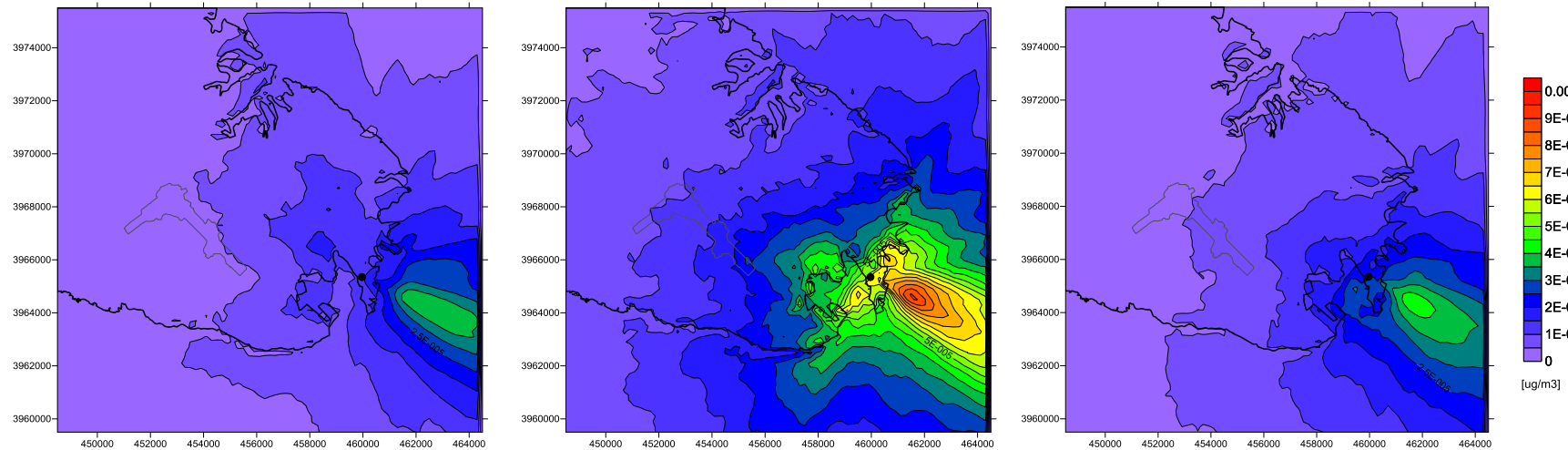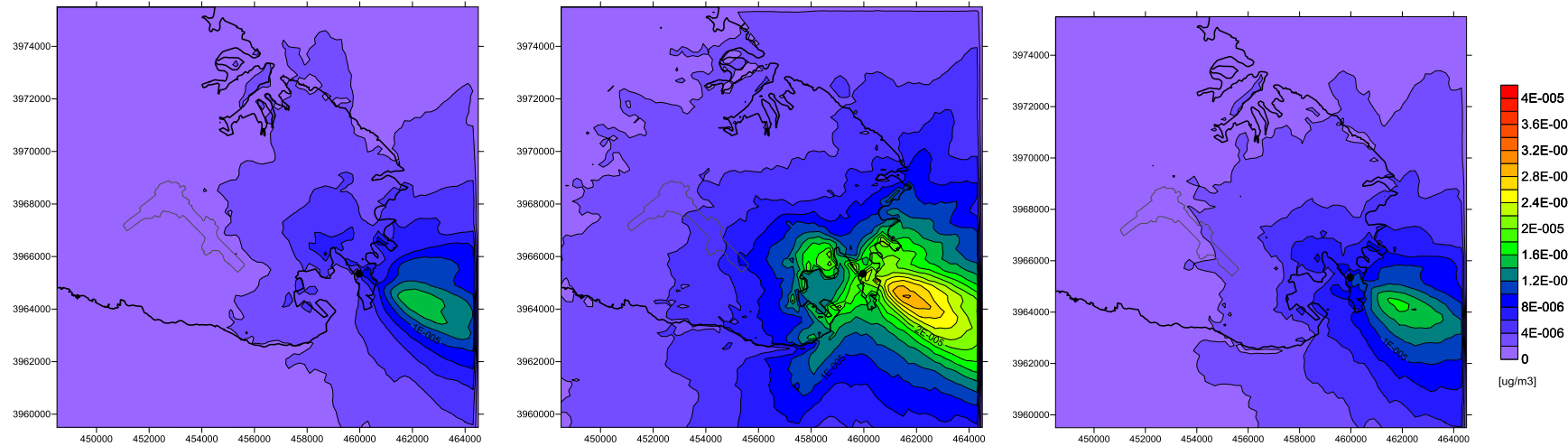

Figure 45. Annual average concentrations of arsenic from DPS in transitional operating conditions, according to meteorology of year 2010, 2011, 2012 (left, centre, right).

Figure 46. Annual average concentrations of cadmium from DPS in transitional operating conditions, according to meteorology of year 2010, 2011, 2012 (left, centre, right).
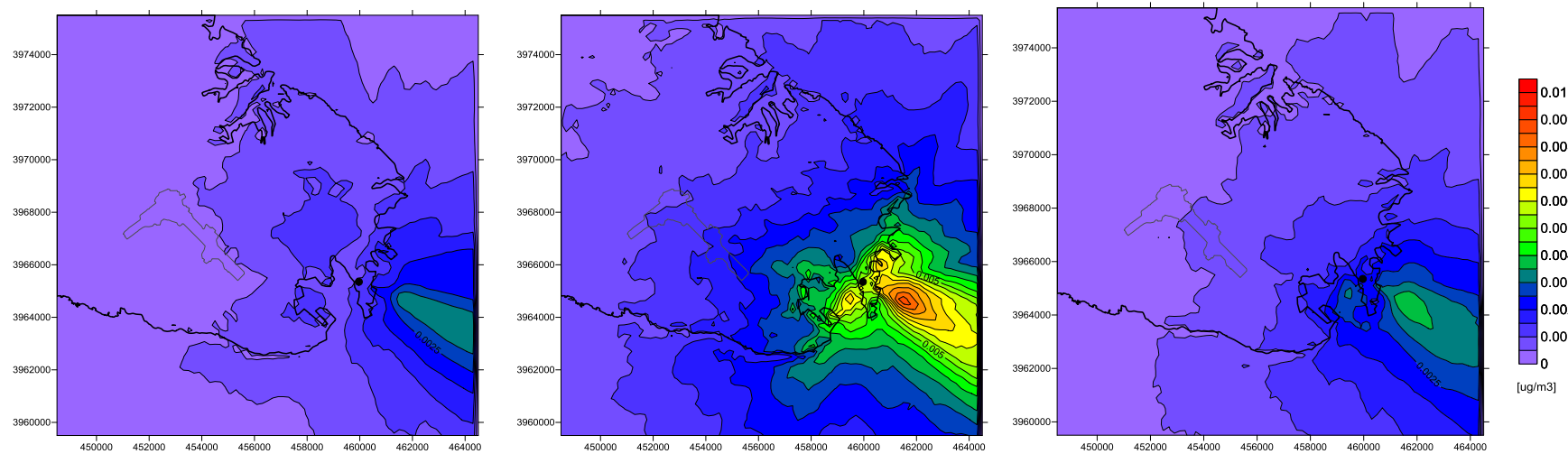

Figure 47. Annual average concentrations of nickel from DPS in transitional operating conditions, according to meteorology of year 2010, 2011, 2012 (left, centre, right).
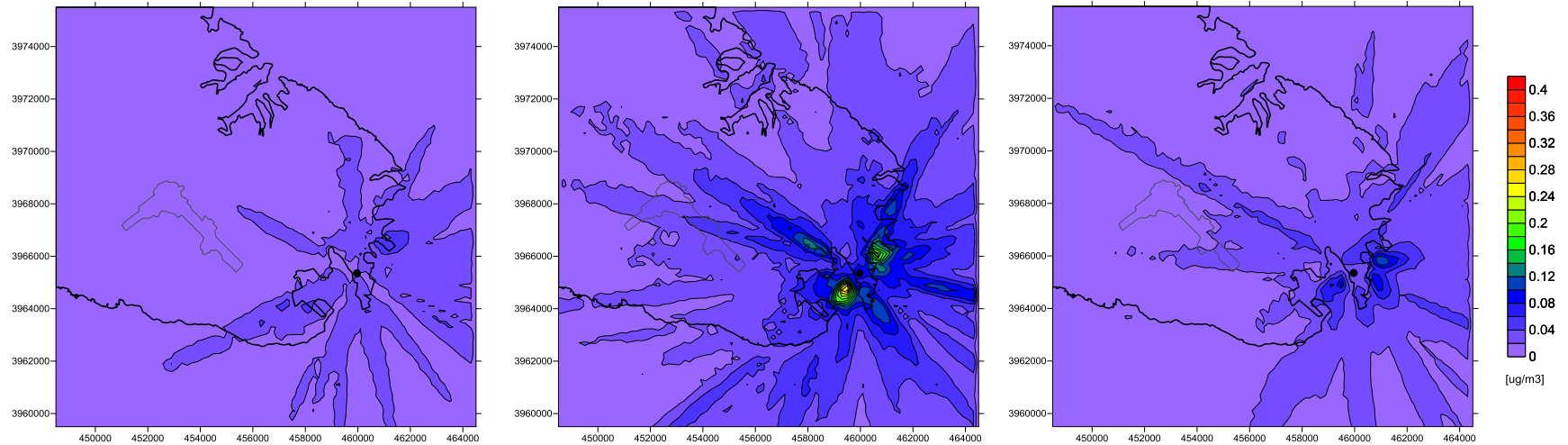
Figure 48. Yearly maxima of 24-hours average concentrations of vanadium from DPS in transitional operating conditions, according to meteorology of year 2010, 2011, 2012 (left, centre, right).

5.1.2 NOC scenario

Figures 49-57 show the maps of the concentration indicators resulting from DPS emissions in the new operating conditions (NOC), following the same approach used for TOC scenario. For each meteorological year, the resulting shape of the concentrations spatial patterns for NOC is the same of TOC, since the underlying meteorology is the same. On the other side as a general result, the lower emissions of NOC scenario, compared with TOC scenario ones, are reflected in lower values of concentration indicators.

The results over the three meteorological years indicate that in the worst conditions the overall maximum of NO_x concentrations across the domain can reach 4.9 μg/m^3 of NO_x (Figure 49). Over land, the area experiencing annual average NO_x values exceeding 2 μg/m^3 is slightly reduced, while the area where they can exceed 4 μg/m^3 becomes almost negligible.

Hourly NO_2 concentrations have been estimated from the corresponding simulated NOx values using the same methodology employed for TOC scenario. The resulting maps (Figure 50) indicate that in the worst case the NO_2 hourly standard (200 μg/m^3, not to be exceeded more than 18 times in any calendar year) is exceeded one or two times a year over a very limited part of the coast NE of DPS.

Also in the case of NOC scenario, the annual average contribution from DPS to PM_{10} and $PM_{2.5}$ concentrations are well below the annual limits, with values over land in the worst conditions respectively below 0.25 μg/m^3 and 0.14 μg/m^3. (Figures 51-52), and DPS contribution to PM_{10} 24-hour average concentrations over all three meteorological years never exceed the limit value (35 times in any calendar year).

As for heavy metals, annual average concentrations of lead and arsenic in the worst conditions are respectively below 0.08 ng/m^3 and 0.024 ng/m^3 over the whole domain (Figures 54-55), while the area in the immediate surroundings of DPS over Delimara peninsula where annual average concentrations of nickel can reach the 5-6 ng/m^3 range (Figure 56) is slightly reduced, respect to TOC scenario. So also for NOC scenario, the resulting contribution of DPS to annual concentrations of arsenic, cadmium and nickel is below the limits.

The DPS contribution to yearly maxima of 24-hours average concentrations of vanadium (Figure 57) even in the worst conditions is below the WHO guideline value for that averaging period (1 μg/m^3).

Figure 49. Annual average NOx concentrations from DPS in new operating conditions, according to meteorology of year 2010, 2011, 2012 (left, centre, right).

Figure 50. NO$_2$ concentrations from DPS in transitional operating conditions: number of exceedances of the hourly standard (200 µg/m^3) over a whole year, according to meteorology of year 2010, 2011, 2012 (left, centre, right).
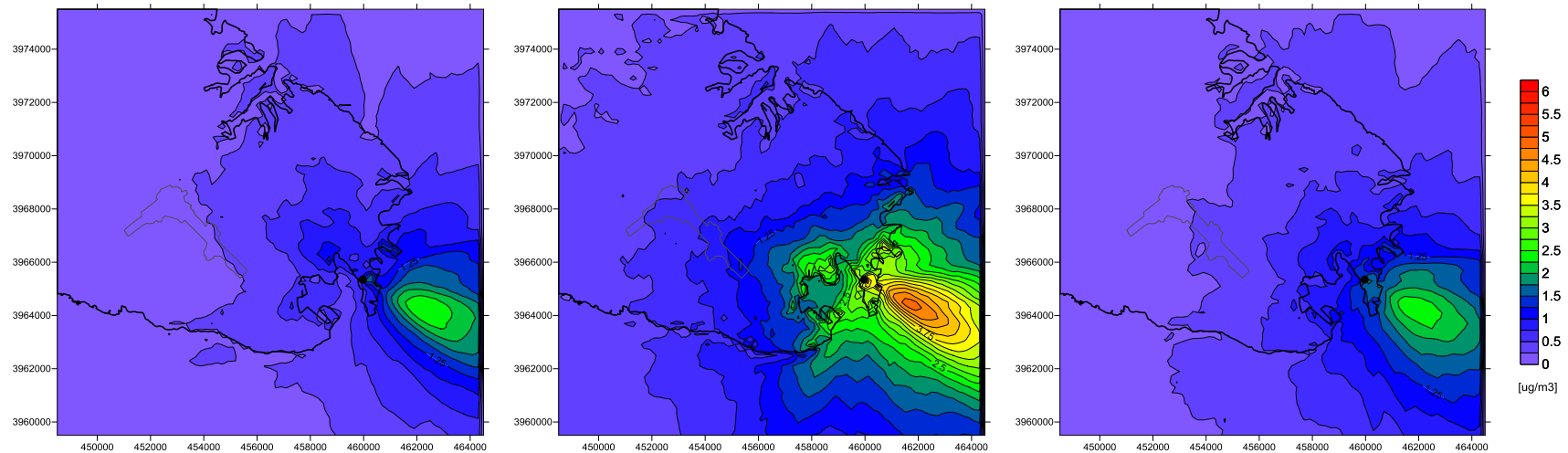
Figure 51. Annual average PM₁₀ concentrations from DPS in new operating conditions, according to meteorology of year 2010, 2011, 2012 (left, centre, right).

Figure 52. Annual average PM₂.₅ concentrations from DPS in new operating conditions, according to meteorology of year 2010, 2011, 2012 (left, centre, right).
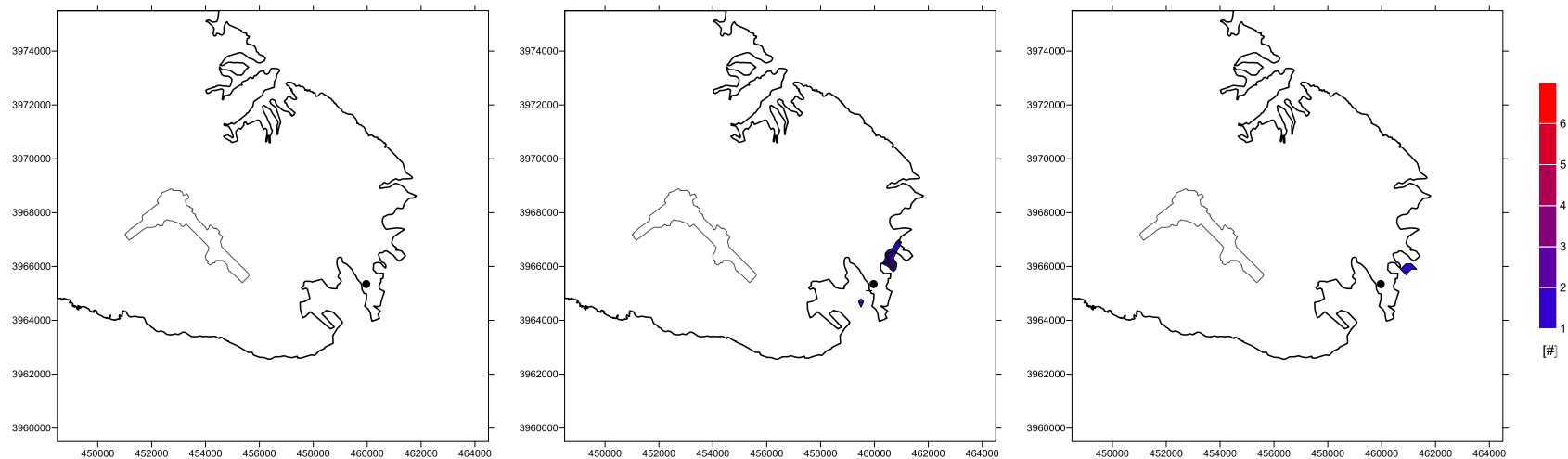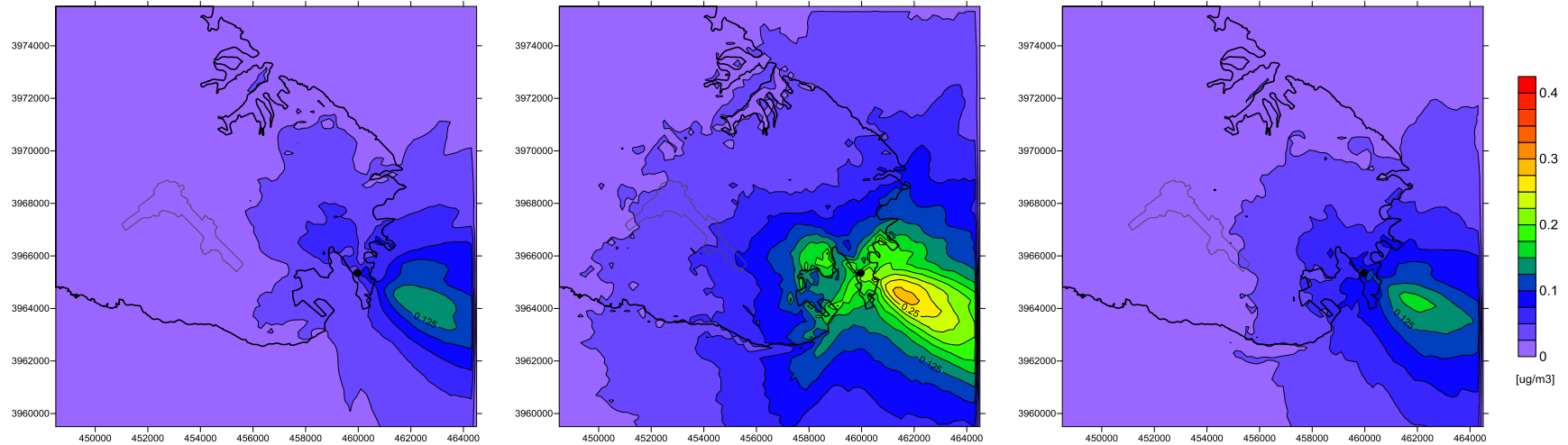
Figure 53. Annual average concentrations of lead from DPS in new operating conditions, according to meteorology of year 2010, 2011, 2012 (left, centre, right).

Figure 54. Annual average concentrations of arsenic from DPS in new operating conditions, according to meteorology of year 2010, 2011, 2012 (left, centre, right).

Figure 55. Annual average concentrations of cadmium from DPS in new operating conditions, according to meteorology of year 2010, 2011, 2012 (left, centre, right).

Figure 56. Annual average concentrations of nickel from DPS in new operating conditions, according to meteorology of year 2010, 2011, 2012 (left, centre, right).
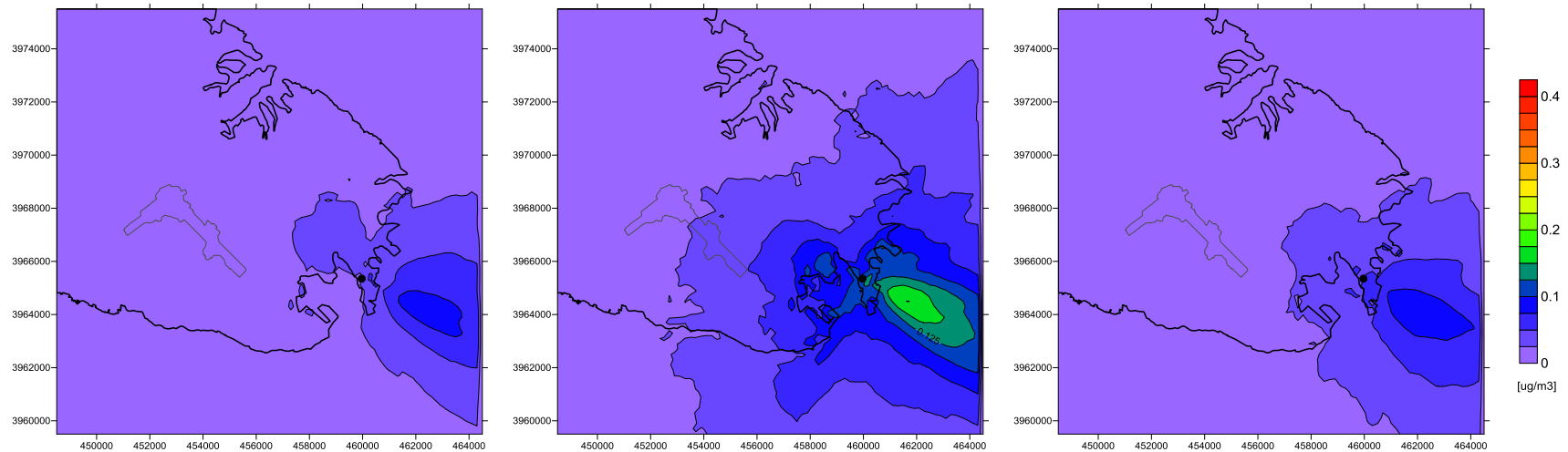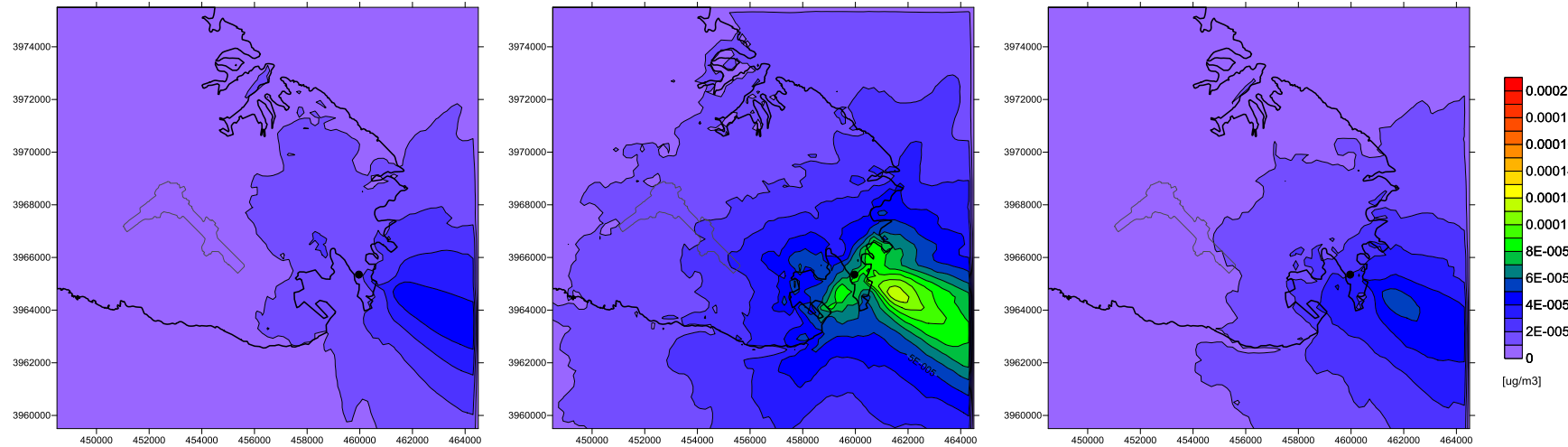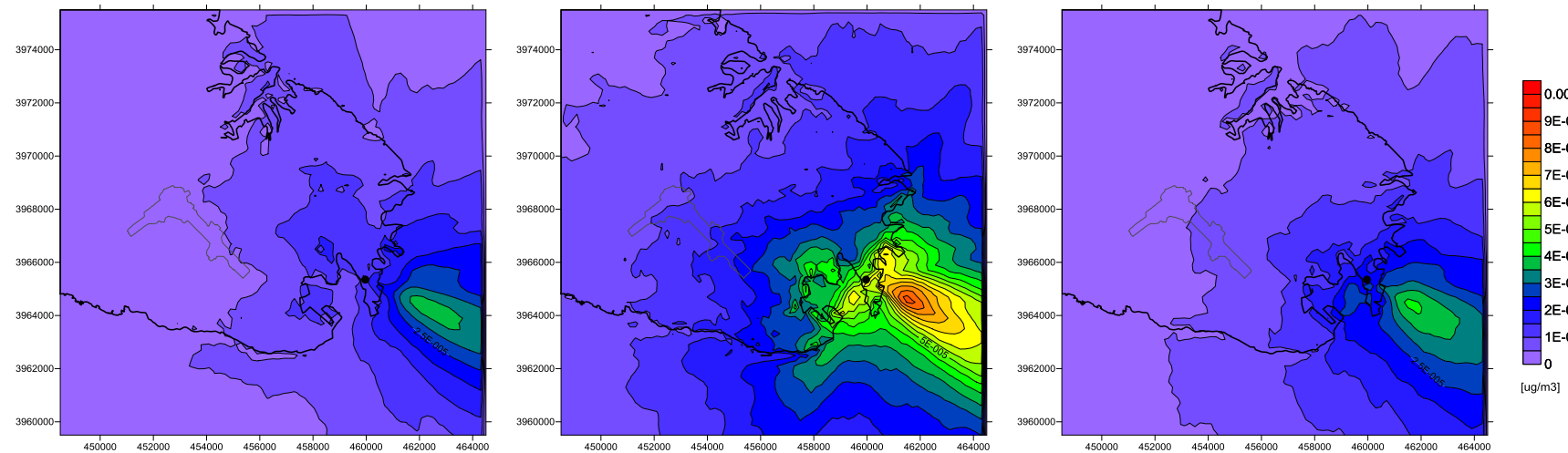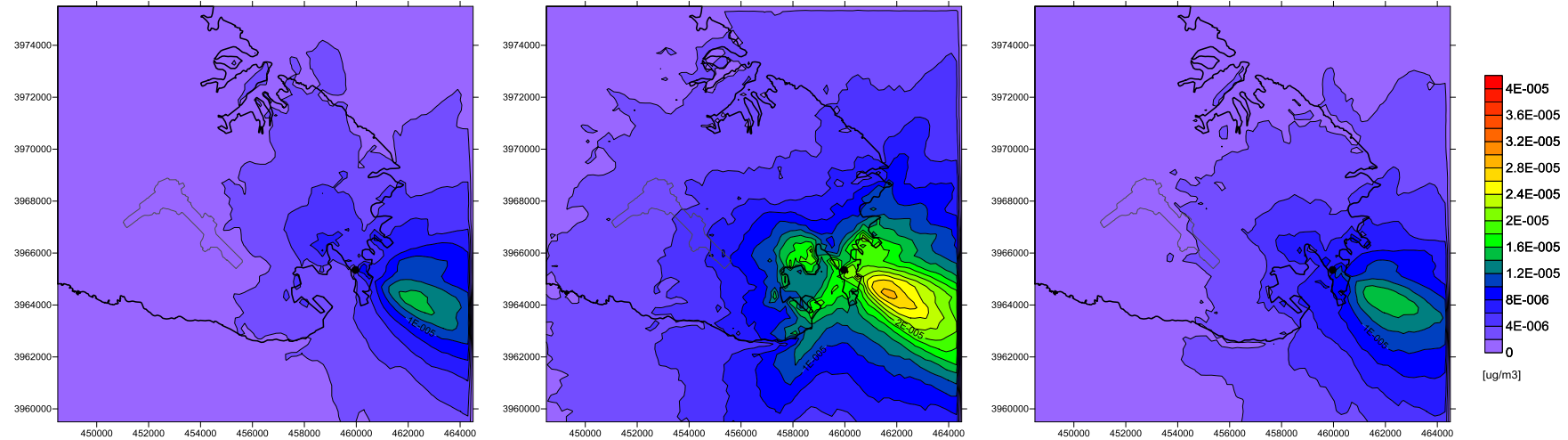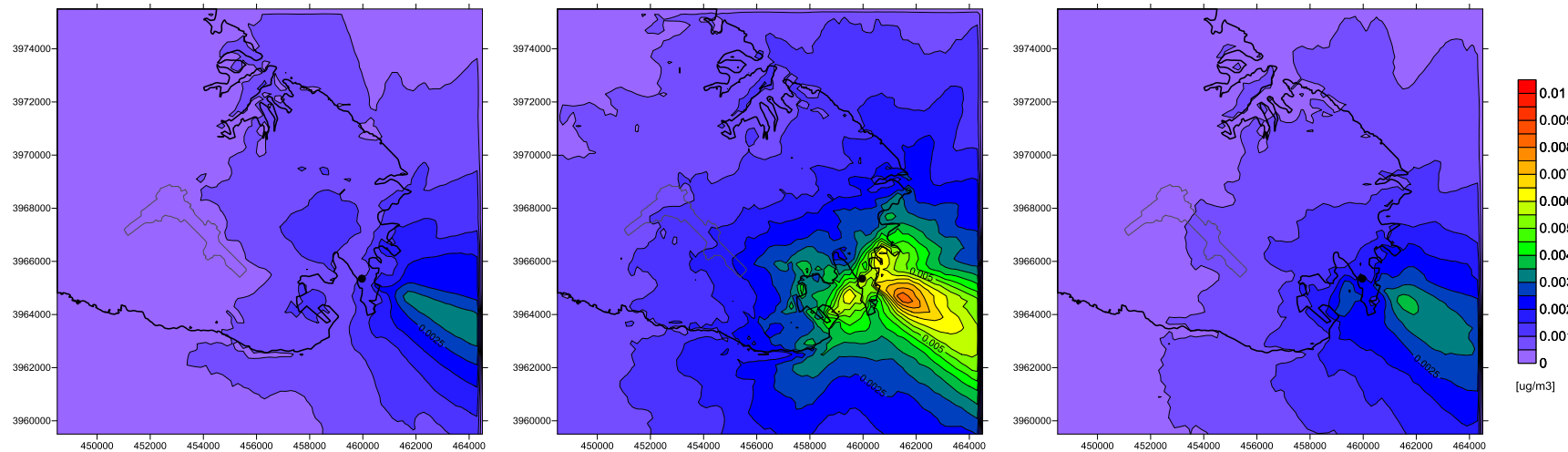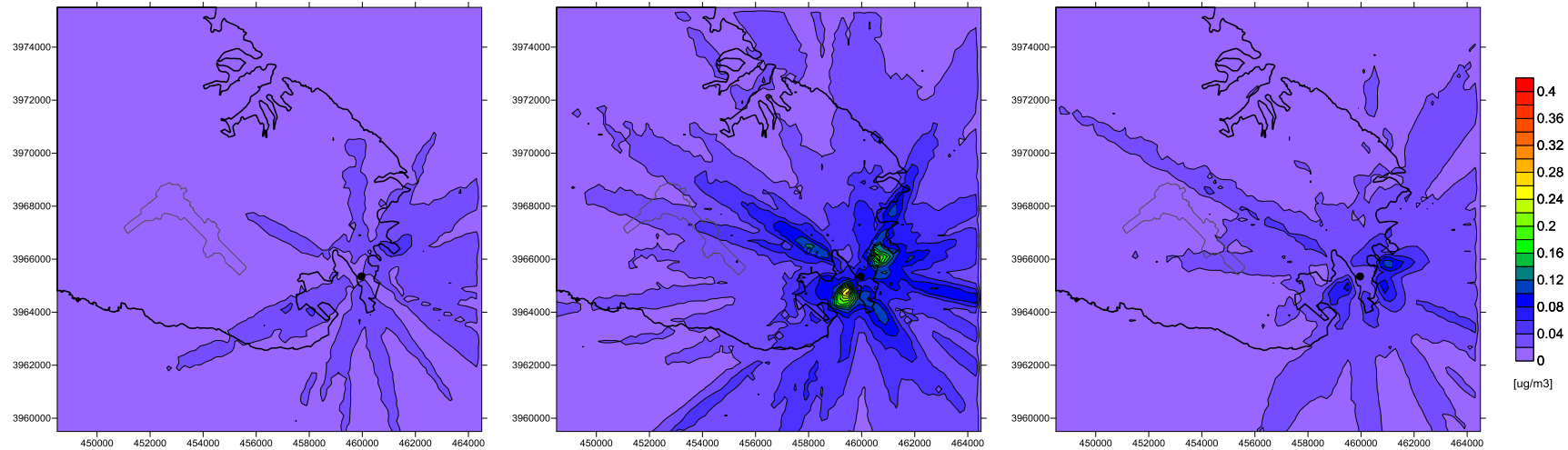
Figure 57. Yearly maxima of 24-hours average concentrations of vanadium from DPS in new operating conditions, according to meteorology of year 2010, 2011, 2012 (left, centre, right).

5.2 Background contributions

5.2.1 Rural background

NO2 rural background is evaluated through QualeAria modelling system, ran over whole year 2011 at 12 km resolution. The annual average concentrations are depicted in Figure 58. Calculated values are in the 7-8 µg/m^3 range in the northeastern part of Malta island and in the 5-6 µg/m^3 range in its southwestern part.
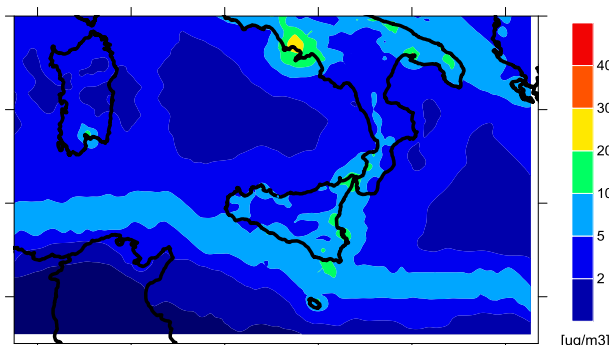
Figure 58. Annual average NO$_2$ concentrations for year 2011 simulated by QualeAria.

For PM rural background, the data from EMEP model at 50 km resolution are used, that include also the contribution from the natural sources which are relevant for Malta (sea salt and Saharan dust). Figure 59 shows the annual average PM$_{10}$ and PM$_{2.5}$ concentrations computed for year 2011; over Malta the calculated values are respectively 26.3 and 13.8 µg/m^3 (http://www.emep.int/mscw/index_mscw.html).
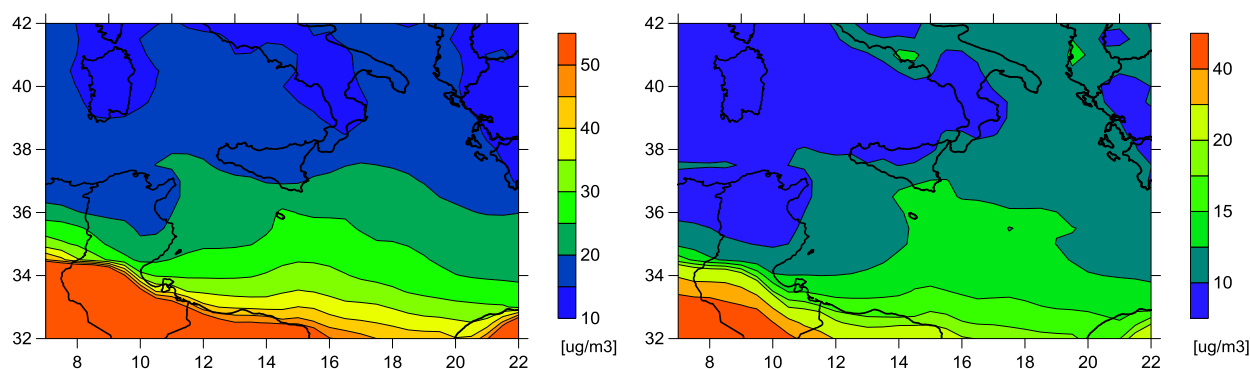
Figure 59. Annual average PM$_{10}$ (left) and PM$_{2.5}$ (right) concentrations for year 2011 (data source: EMEP/MSC-W).

EMEP model data contributions of PM in Malta (Figure 60) indicate that over 85% of rural background concentrations comes from sources outside Malta, with the largest fraction coming from emissions related to international navigation in the Mediterranean.
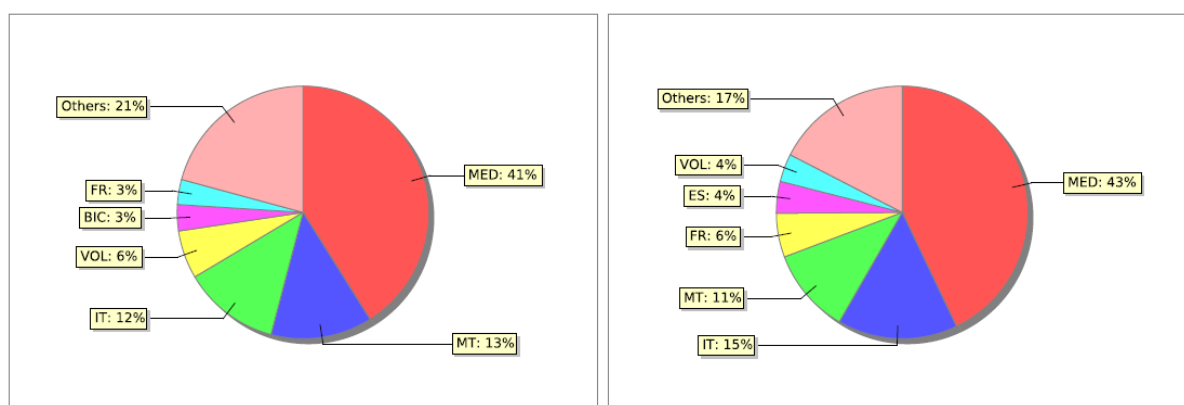
Figure 60. Main contributors to background concentrations of PM$_{2.5}$ (left) and PM$_{coarse}$ in Malta (EMEP, 2012).

5.2.2 Natural sources

Due to its geographic position in central Mediterranean, Malta is frequently exposed to dust transported by air masses advected from the African continent, as well as from particles originating from sea spray.

According to source apportionment analyses of the PM$_{10}$ fraction conducted by MEPA on data collected since 2007 from a rural background site, not affected or minimally affected by anthropogenic contributions from the agglomeration, a minimum of 8% of the PM$_{10}$ fraction is generated by mineral dust events, while another 8% is generated from sea salt (MEPA, 2010).

With this respect, the current European legislation (Directive 2008/50/EC) gives to Member States the possibility to subtract the contribution of natural sources from the measured PM$_{10}$ concentrations. The guidelines to demonstrate and subtract the natural contribution to local air quality measurements have been later published by European Commission (European Commission, 2011).

Following the method indicated by the guidance (European Commission, 2009) the contribution from sea salt has been estimated from chloride and sodium concentrations measured during year 2008 from a total of 38 low-volume PM$_{10}$ sampler filters collected at the Msida traffic site and Gharb rural background site. The resulting average sea salt concentrations at Msida and Gharb are 3.1 and 2.7 µg/m^3, respectively, with maximum reaching 14.5 µg/m^3 (MEPA, 2010b).

The Sahara dust contribution to PM$_{10}$ concentrations has been reassessed in this study. The methodology outlined to evaluate desert dust contribution to the PM concentrations is based on the subjective identification of Saharan dust outbreak episodes and on the analysis of the time series of PM$_{10}$ concentration measured by regional background stations, as originally proposed by Escudero et al. (2007).

The Sahara dust contribution has been calculated for all the three meteorological years that were used in the model simulations. Monitoring data available for year 2011 have been analyzed during the first stage of the study, while during the second stage the calculation has been extended to year 2010 and 2012.

Figure 61, 62 and 63 show the PM_{10} measurements from continuous monitoring stations available at Malta for years 2010, 2011 and 2012, as time series of daily average concentrations. Gharb, Kordin, Zeijtun and Msida stations are classified respectively as "rural background", "suburban background", "urban industrial" and "urban traffic". Their classification is also confirmed by the comparison of PM_{10} measured concentrations values, showing the lowest values in Gharb and the highest ones in Msida. Gharb measurements show higher PM concentration during summer months, as it is common for stations exposed mainly to regional background concentrations in the southern Mediterranean basin and receiving a relevant contribution from natural aerosol sources. Otherwise, the urban station of Msida shows a different PM concentration seasonal trend, with higher values during winter, of possible local anthropogenic origin, and concentrations slightly higher than Gharb background values during summer. This behavior of PM concentrations is clearly observable during years 2011 and 2012, while it is masked by the frequent short-term high concentration episodes recorded in 2010. The yearly average PM_{10} concentrations ranged between 25 and 45 µg/m^3 (with the only value larger than 40 µg/m^3 recorded at the Msida station in 2010), while short-term episodes occur at all stations, causing high concentrations exceeding the air quality limit for PM_{10} daily average. It can be observed that the episodes giving rise to the highest concentrations occur often simultaneously at all the monitoring stations, suggesting a possible common cause, as e.g. the long-range transport of aerosol of natural or anthropogenic origin. Kordin and Zeijtun stations have a percentage of valid data respectively of about 11% and 88% for year 2010, 50% and 60% for year 2011 and 50% and 34% for year 2012, therefore they have not been used for desert dust impact analysis.

To identify the desert dust outbreak episodes occurred during years 2010, 2011 and 2012, the following sources of information have been analyzed:

- synoptic meteorological reanalyzes charts (http://www.wetterzentrale.de/);
- back-trajectories of the daily air masses at 12 h, as provided by the HYSPLIT model (http://ready.arl.noaa.gov/HYSPLIT_traj.php);
- maps of aerosol index of Ozone Monitoring Instrument (OMI) and maps of the Aerosol Optical Depth (AOD) from Moderate Resolution Imaging Spectroradiometer (MODIS), obtained at https://ozoneaq.gsfc.nasa.gov/data/aerosols/ and http://giovanni.gsfc.nasa.gov/giovanni/);
- concentration maps produced by desert dust transport models SKIRON from the University of Athens (http://forecast.uoa.gr) and BSC-DREAM from the Barcelona Supercomputing Center (http://www.bsc.es/earth-sciences/mineral-dust-forecast-system/bsc-dream8b-forecast);
- $PM_{2.5}$ and PM_{10} concentrations measured at the rural background station of Gharb.
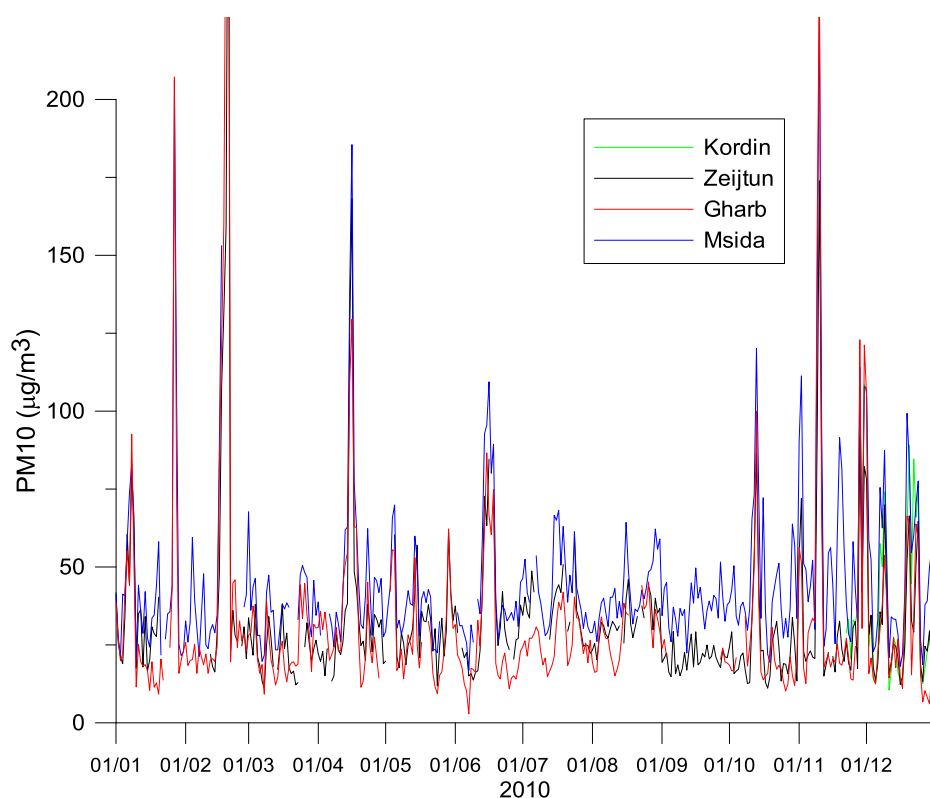
Figure 61. PM$_{10}$ daily average concentrations measured by Malta air quality network stations during year 2010 (the maximum of the vertical axis, as also in the following figures, is limited to 200 µg/m^3 for readability).
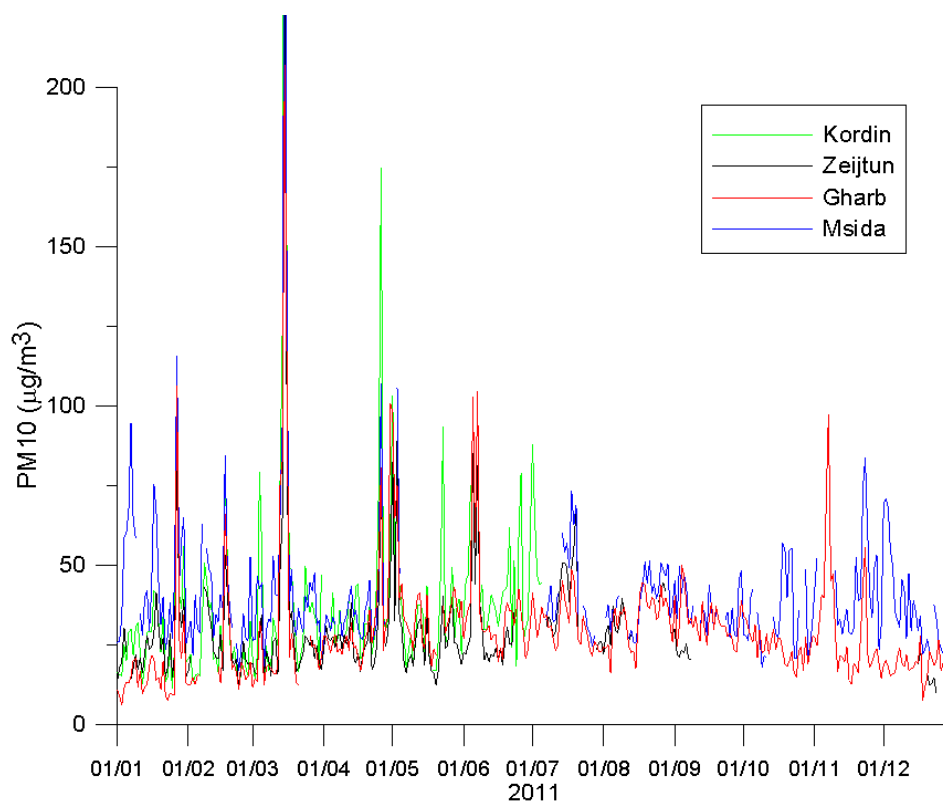

Figure 62. PM$_{10}$ daily average concentrations measured by Malta air quality network stations during year 2011.
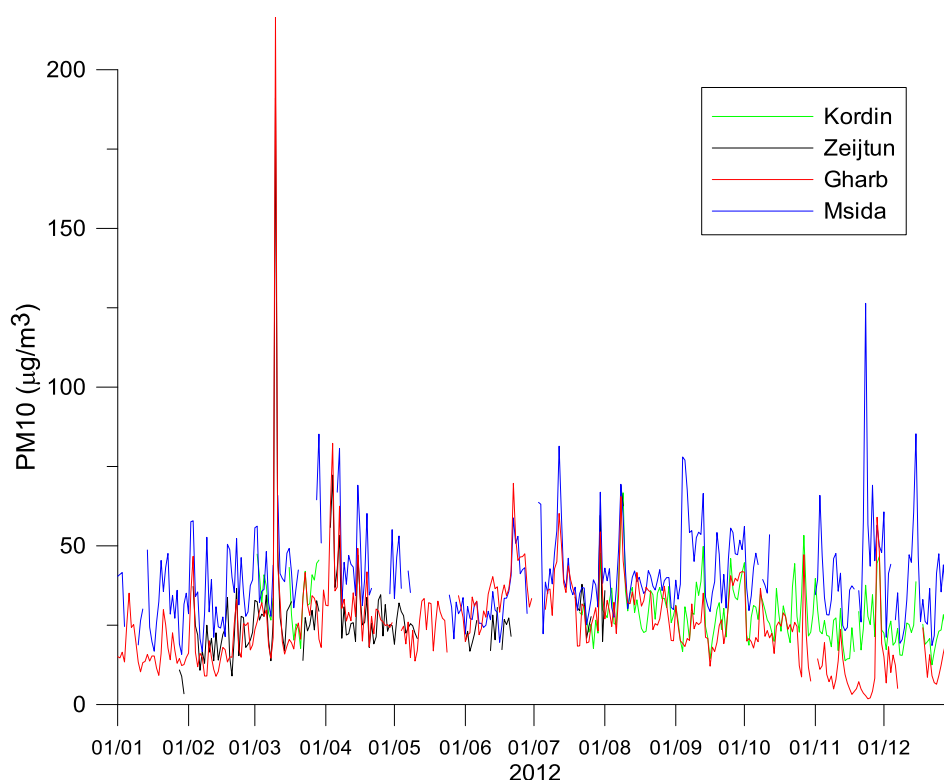
Figure 63. PM$_{10}$ daily average concentrations measured by Malta air quality network stations during year 2012.

The Saharan dust outbreak episodes identified for years 2010, 2011 and 2012 are marked in Figures 64, 65 and 66 by the periods covered by gray bars. Their analysis shows that all the elevated concentration episodes recorded during the considered years occurred under atmospheric circulation conditions causing desert dust advection. Furthermore, the PM$_{2.5}$/PM$_{10}$ ratio computed for years 2011 and 2012 shows that during desert dust episodes a decrease of the fine PM fraction has been observed. During days characterized by concentrations higher than 80 µg/m^3, the fine fraction of PM$_{10}$ decreased in fact to values lower than 40%, indicating the probable natural origin of the aerosol. This features of measured PM concentrations is not clearly observable for year 2010, when the fine-to-coarse PM ratio showed values and time behavior that are different from the corresponding ones recorded during the other two years. The largest number of Sahara dust advection episodes has been identified during year 2010, when also the concentration levels occurred during the episodes resulted larger than those observed during the following years. The number of episodes identified for year 2012 is larger than the one of 2011, but their impact has been less intense in term of PM concentration peak values recorded by Malta monitoring network.

Two major dust episodes are illustrated in details in the following, to describe the advection conditions causing the major episodes and provide examples of the analysis method employed.

Figures 67 and 68 report the dust outbreak episodes occurred on 27-30/01/2011 and 13-18/03/2011. These two periods have been characterized by the highest PM$_{10}$ concentrations measured in both Malta and Gozo islands during year 2011. On 27/01/2011, model results indicate very high dust concentration over north-western Africa, in particular over Algeria, Tunisia and Libya. The back-trajectories indicate that dust is advected towards Malta from southern Tunisia

and the western Sirte gulf, as clearly confirmed by the dust plumes motion visible in the MODIS AQUA image (Figure 67). The presence of dust over the Mediterranean Sea surrounding Malta is confirmed by the AOD produced by the analysis of MODIS images. During the second period (13-18/03/2011) the movement of a low pressure system across the western Mediterranean basin caused advection of Saharan dust over large part of the Mediterranean Sea and southern Europe, as shown by the average MODIS AOD for 14-16/03/2011 (Figure 68). The direct impact of the dust plume over Malta on 15/03/2011 (characterized by the highest PM_{10} daily average concentrations measured during 2011, reaching 323 μg/m^3 in Msida) is shown by the plume shape indicated by OMI Aerosol Index and by the dust forecast models concentration maps. The back-trajectories calculated by the HYSPLIT model indicate that the path of air masses reaching Malta from desert areas spanned the Libya and Tunisia coastal area from eastern to western Sirte gulf at different heights over the sea level.
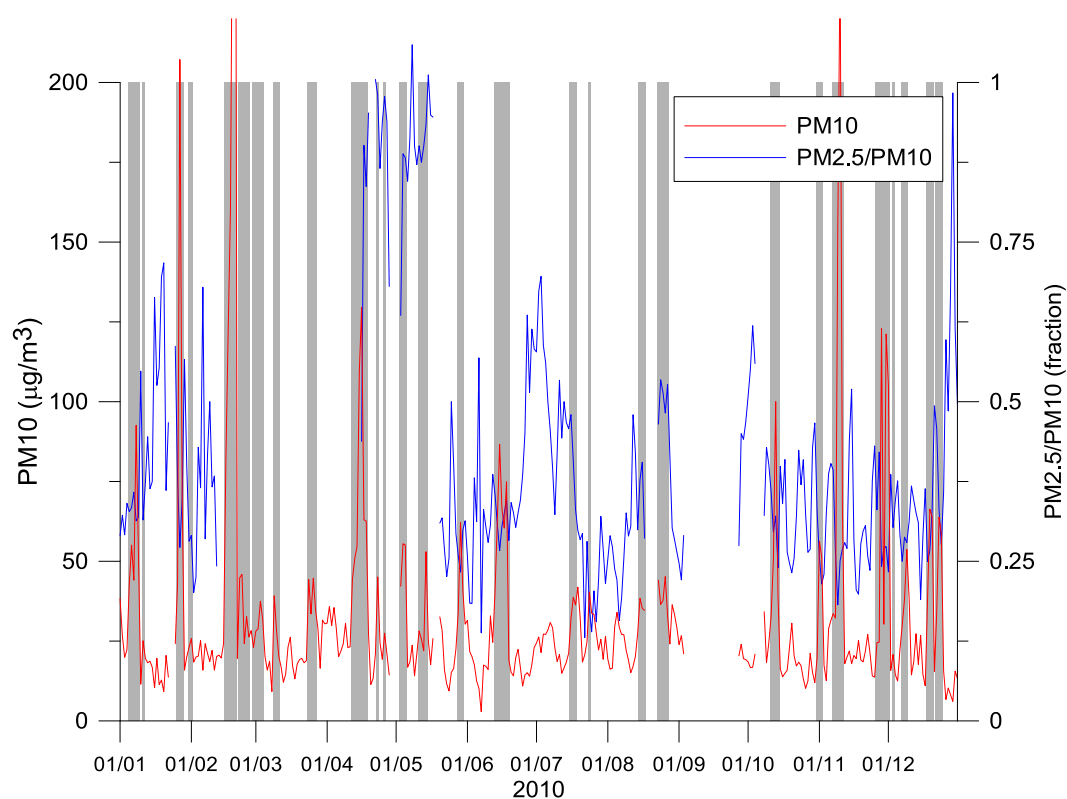
Figure 64. PM_{10} daily average concentrations (red line) and $PM_{2.5}/PM_{10}$ concentrations ratio (blue line) from measurements at Gharb station during year 2010, with superimposed (gray bars) the identified Saharan dust outbreak episodes.
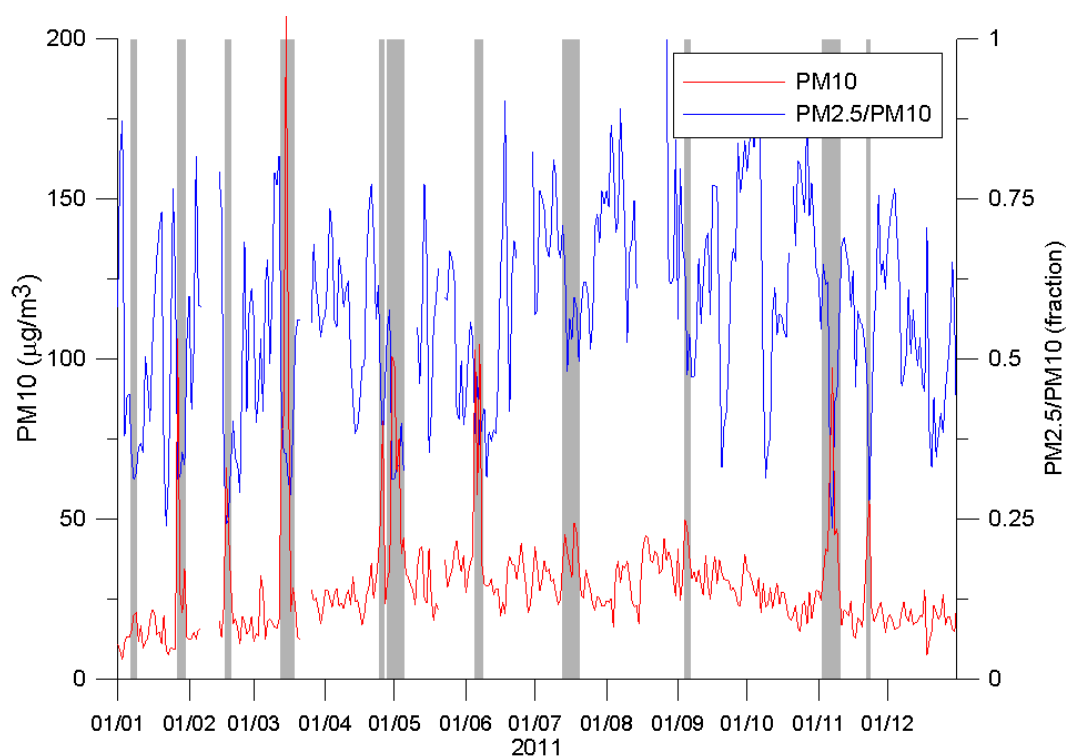
Figure 65. PM$_{10}$ daily average concentrations (red line) and PM$_{2.5}$/PM$_{10}$ concentrations ratio (blue line) from measurements at Gharb station during year 2011, with superimposed (gray bars) the identified Saharan dust outbreak episodes.
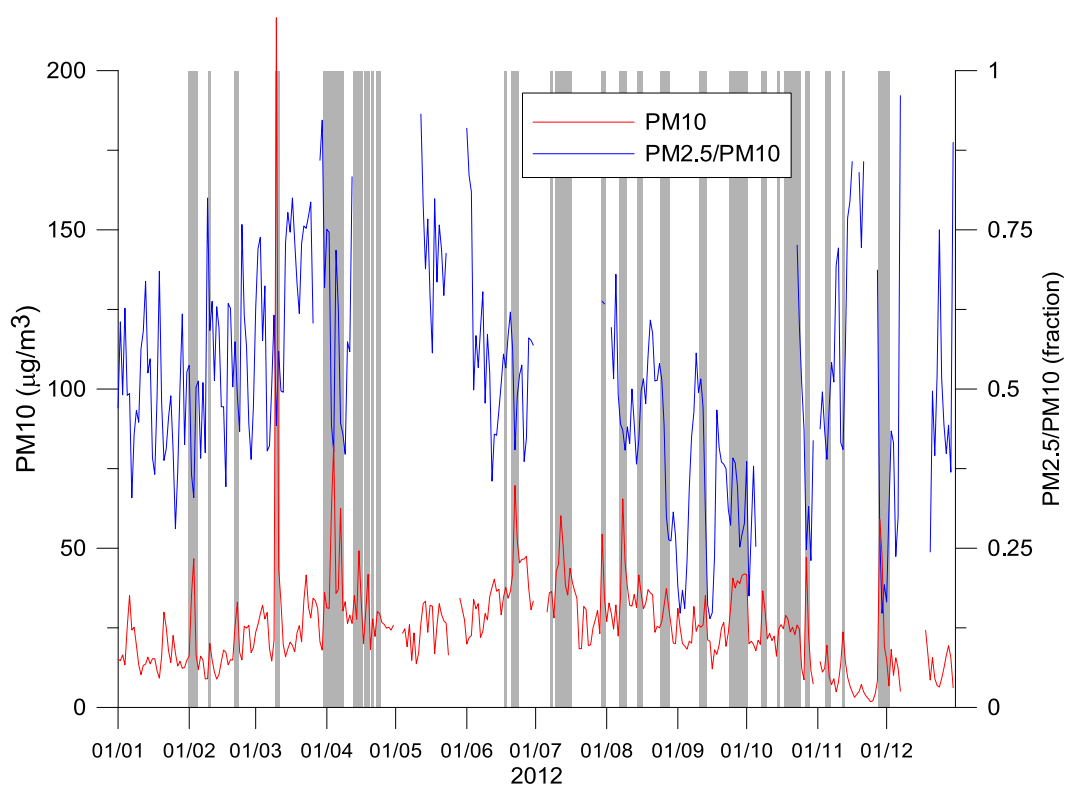
Figure 66. PM$_{10}$ daily average concentrations (red line) and PM$_{2.5}$/PM$_{10}$ concentrations ratio (blue line) from measurements at Gharb station during year 2012, with superimposed (gray bars) the identified Saharan dust outbreak episodes.

Figure 67. Average 550 nm Aerosol Optical Depth from MODIS-AQUA measured on 27/01/2011 (upper left panel); MODIS-AQUA image on 27/01/2011 (upper right panel); three days back-trajectories from HYSPLIT model for 27/01/2011 (lower left panel) and surface dust concentration forecast for 27/01/2011 at 12:00 UTC from BSC-DREAM model (lower right panel).
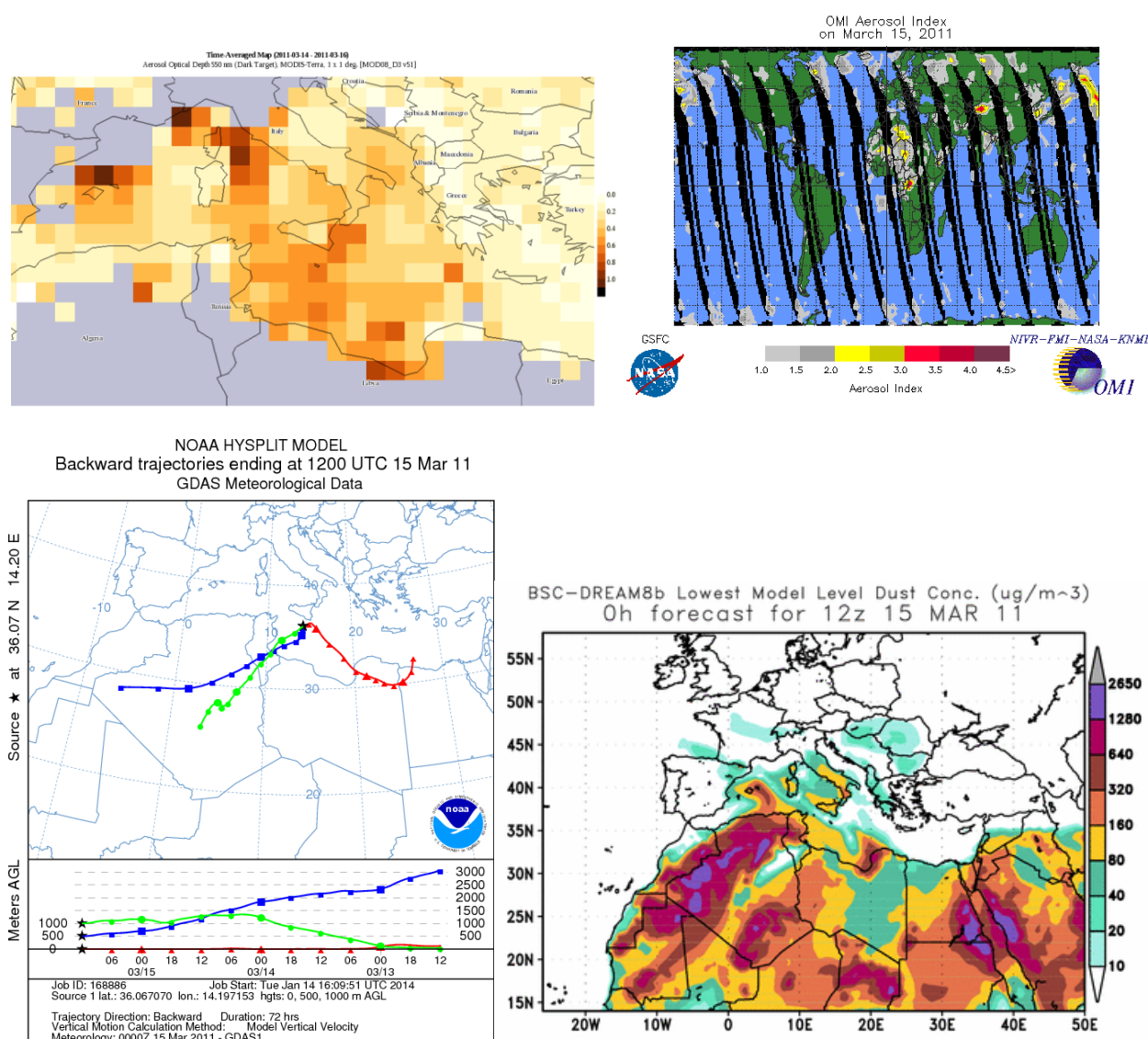
Figure 68. Average 550 nm Aerosol Optical Depth from MODIS-AQUA measurements on 14-16/03/2011 (upper left panel); OMI Aerosol Index for 15/03/2011 (upper right panel); three days back-trajectories from HYSPLIT model for 15/03/2011 (lower left panel) and surface dust concentration forecast for 15/03/2011 at 12:00 UTC from BSC-DREAM model (lower right panel).

Another short but very intense Sahara dust outbreak episode occurred on 10 March 2012, when dust was blown off the northern coast of Africa and over the Mediterranean Sea. The MODIS instrument on NASA's Terra satellite captured this event (Figure 69). The dust plumes blew off the coast of both eastern and western Libya. The eastern plume can be clearly observed in nearly clear sky conditions while the western plume appears mingled with clouds northwest of Tripoli. The main path of the dust plume is confirmed by both DREAM model results and by the back trajectories computed by HYSPLIT model (Figure 69). The AOD map computed from the MODIS observations illustrates the presence of aerosol over the Mediterranean basin from 10 to 11 March 2012. It is worth mentioning that the area between Sicily and Tunisia does not show high AOD values due to the masking effect of clouds, as can be seen from the MODIS image. The atmospheric circulation condition driving the dust advection is described by GFS model meteorological analyses, which illustrates the presence of an intense closed pressure minimum centered on the border between Tunisia and Libya on 10 March 2012 at 00:00 (Figure 70). PM_{10}

concentrations measured in Malta on 10 March 2012 ranged from 191 µg/m^3 at Zejtun to 286 µg/m^3 at Msida monitoring stations.

A less intense but longer lasting episode occurred between 28 October and 2 November 2012, when a deep and persisting low-pressure trough remained located over the western Mediterranean, between Spain, Morocco and Algeria, favoring dust transport in northeastward direction. Satellite observations clearly show a dust plume crossing the Mediterranean Sea over Southern Italy with maximum concentrations occurring over the Sicily channel, the Sirte gulf and the Ionian Sea (Figure 71). Dream model forecast and HYSPLIT back trajectories clearly indicate the plume path carrying dust from Algeria and Libya desert regions towards Malta. Maximum PM$_{10}$ concentrations have been recorded in Malta on 29 November 2012 ranging from 47 µg/m^3 in Kordin to 74 µg/m^3 in Zejtun.
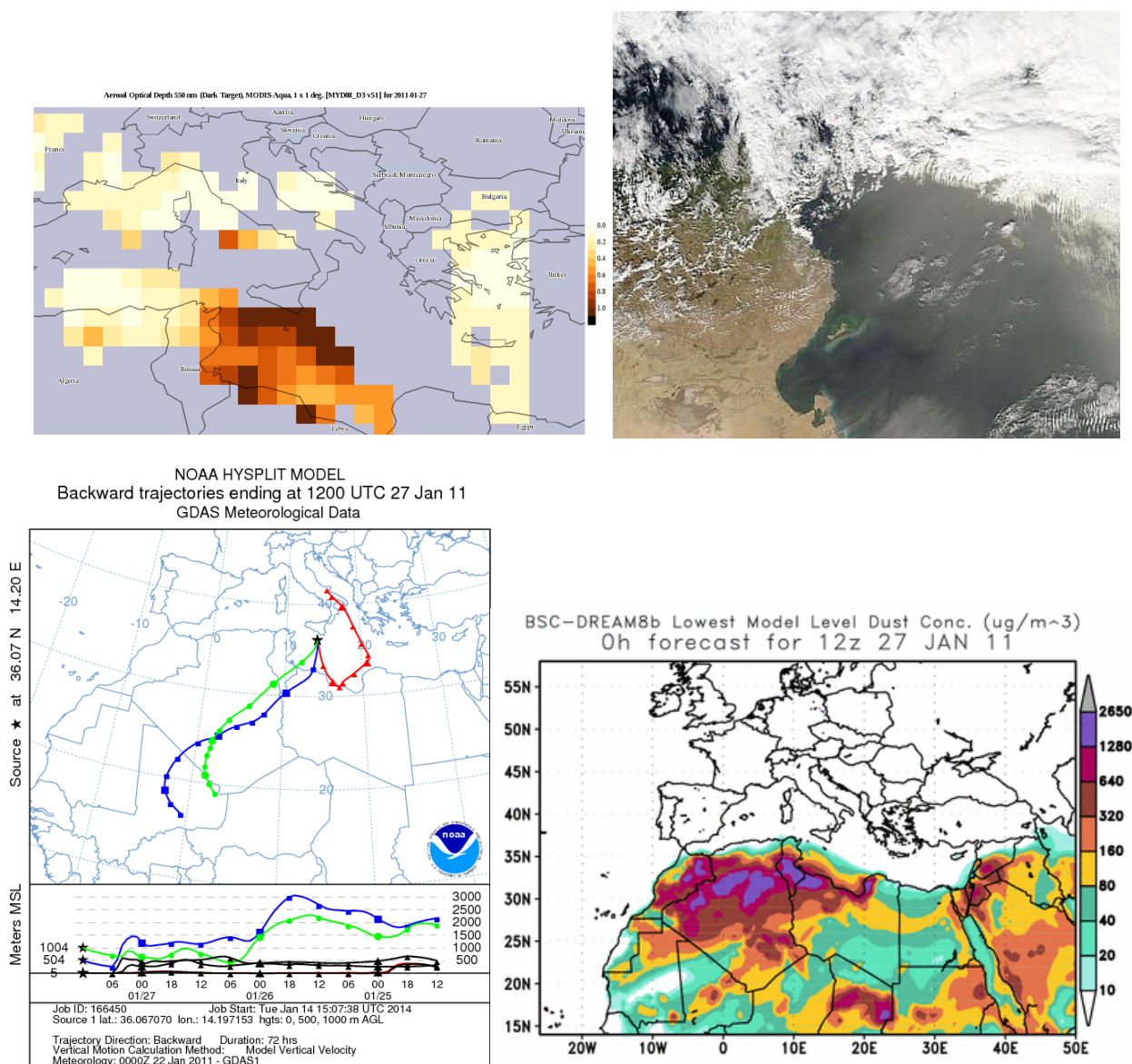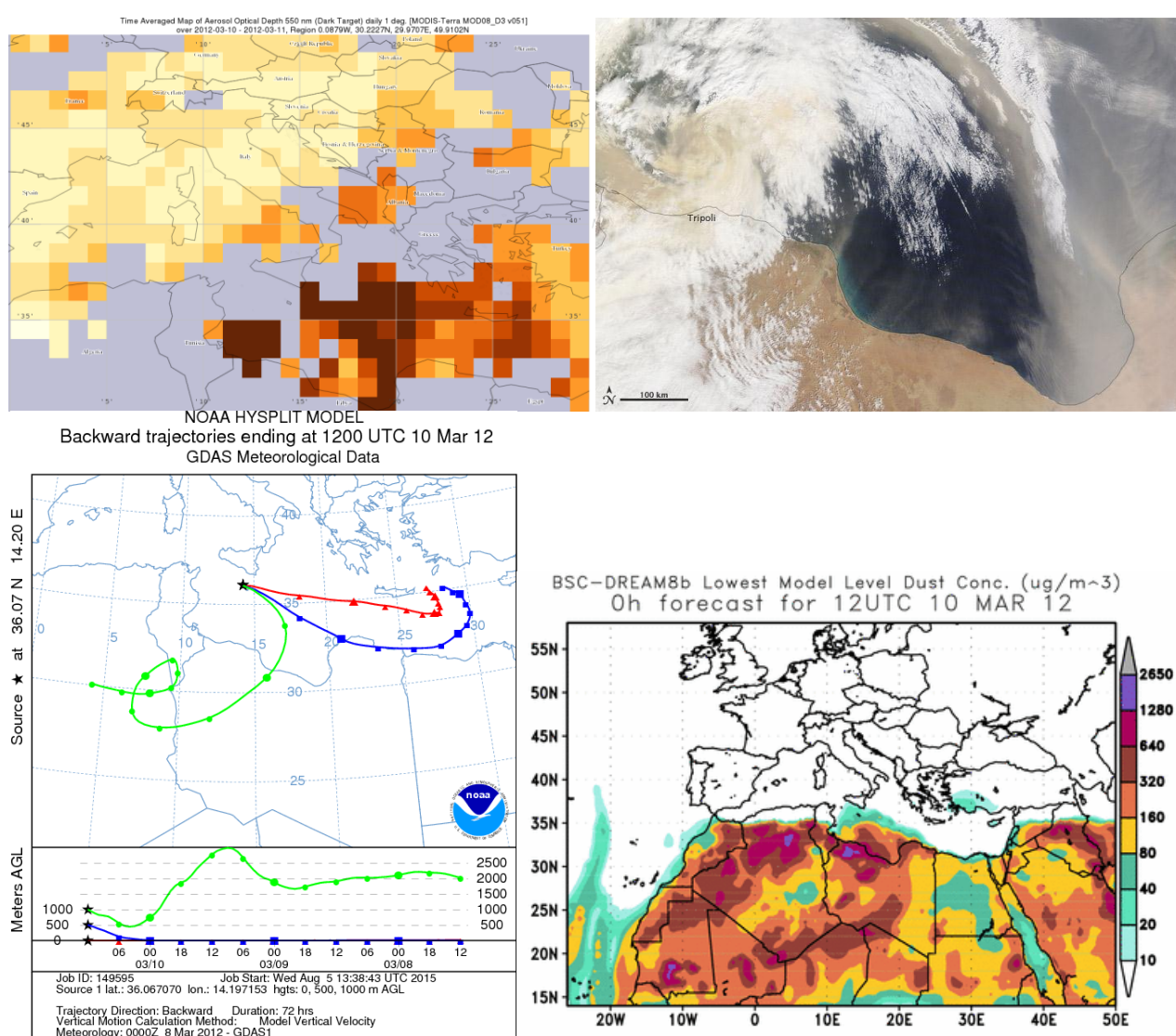

Figure 69. Average 550 nm Aerosol Optical Depth from MODIS-TERRA measured on 10-11/03/2012 (upper left panel); MODIS-TERRA image on 10/03/2012 (upper right panel); three days back-trajectories from HYSPLIT model for 10/03/2012 (lower left panel) and surface dust concentration forecast for 10/03/2011 at 12:00 UTC from BSC-DREAM model (lower right panel).
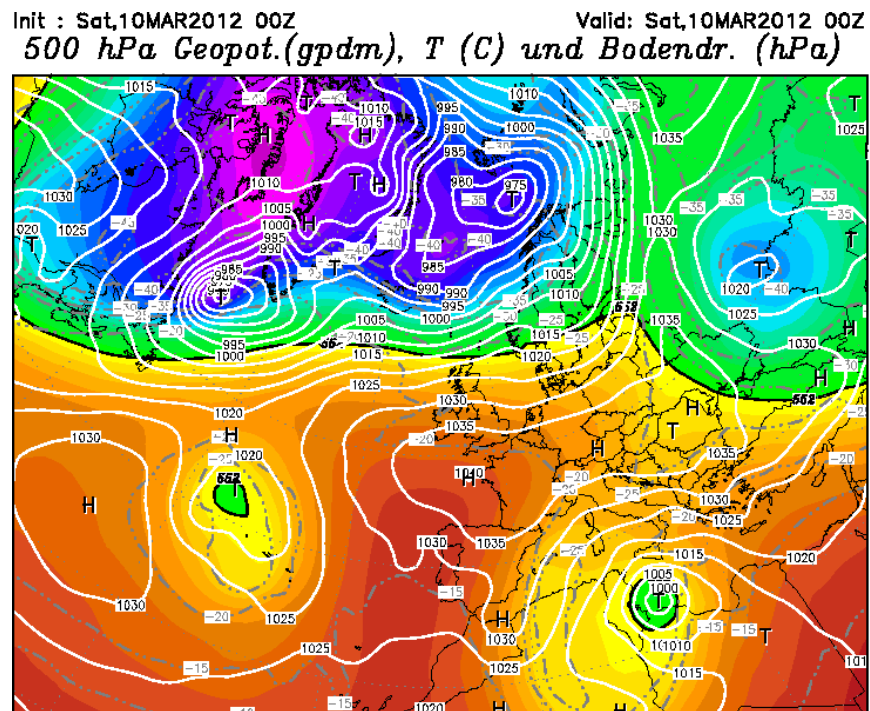
Figure 70. 500 hPa geopotential (color field) and sea level pressure described by NOAA GFS meteorological analysis for 10/03/2012 at 00:00.
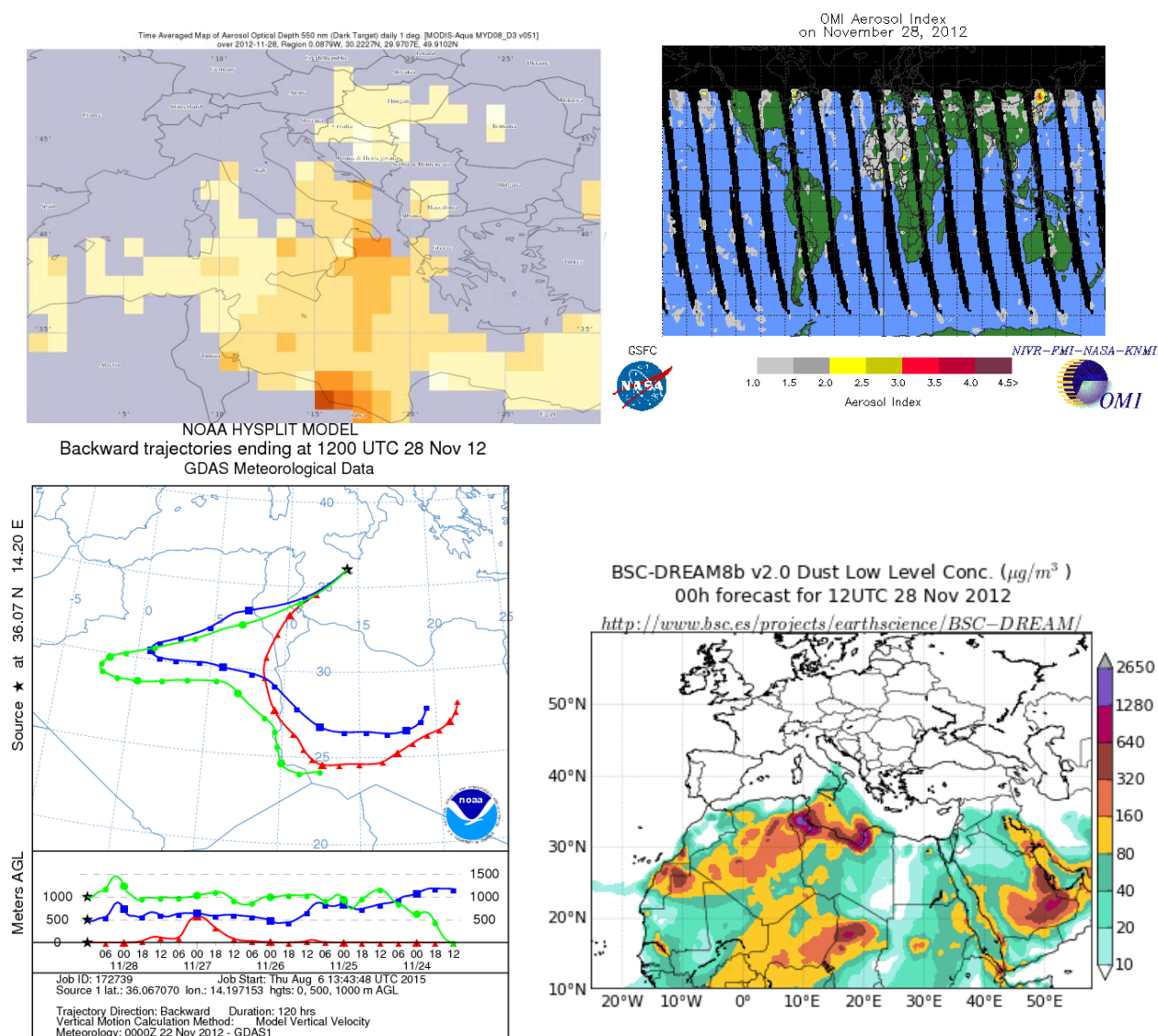
Figure 71. Average 550 nm Aerosol Optical Depth from MODIS-AQUA measurements on 28/11/2012 (upper left panel); OMI Aerosol Index for 28/11/2012 (upper right panel); five days back-trajectories from HYSPLIT model for 28/11/2012 (lower left panel) and surface dust concentration forecast for 28/11/2012 at 12:00 UTC from BSC-DREAM model (lower right panel).

Due to the limited extension of Malta territory and to the relatively large spatial scale that characterizes desert dust plumes advected northward, the desert dust contribution evaluated from the analysis of the time series of PM_{10} concentrations measured in Gharb can be considered representative for the whole Maltese archipelago. In particular, the urban traffic station of Msida is located at a distance of about 33 km from Gharb station. Msida station recorded a yearly average concentration of 45.3 µg/m^3 and 84 exceedancees of the daily average concentration limit during 2010, a yearly average concentration of 40.9 µg/m^3 and 48 exceedancees of the daily average concentration limit during 2011 and a yearly average concentration of 40.7 µg/m^3 and 54 exceedancees during 2012. The percentage of valid data has been respectively of about 93, 73 and 81% for years 2010, 2011 and 2012. Gharb station recorded a yearly average concentration of 32.4 µg/m^3 and 40 exceedancees of the daily average concentration limit during 2010, a yearly average concentration of 29.1 µg/m^3 and 18 exceedancees of the daily average concentration limit during 2011 and a yearly average concentration of 25.6 µg/m^3 and 11 exceedancees during 2012.

Following the European Commission Guidelines, the desert dust contribution has been identified comparing concentration measured in Gharb during desert dust episodes against the monthly moving 50th percentile values computed excluding all days identified as having Saharan dust influence. The list of days influenced by Saharan dust outbreaks identified for years 2010 (Figure 64) 2011 (Figure 65) and 2012 (Figure 66) are reported respectively in Tables 24, 25 and 26, together with the PM_{10} concentrations measured in Gharb and Msida, the desert dust contribution to PM_{10} and the concentrations at Msida after deduction of desert contribution. Concentrations exceeding the European limit are marked in red. The estimated desert contribution to PM_{10} daily average concentrations ranges between 1.8 and 346 µg/m^3 during year 2010 episodes, between 2 and 189 µg/m^3 during year 2011 ones and between 1.5 and 191 µg/m^3 during year 2012 ones. Days with estimated desert contribution below 1 µg/m^3 have been excluded from the selection of dust episodes.

As a result, the subtraction of desert contribution allows to eliminate all the exceedancees of the PM_{10} daily average concentration limit recorded in Gharb during years 2010, 2011 and 2012, while the number of exceedances in Msida are reduced from 84 to 45 (~46% reduction) for year 2010, from 48 to 34 (~29% reduction) for year 2011 and from 54 to 32 (~40% reduction) for year 2012. From the presented analysis, the resulting contribution to the PM_{10} yearly average concentration from Saharan dust episodes can be estimated in the range of 3.5-4.5 µg/m^3, if we keep into account the range of values obtained for years 2011 and 2012 and the values estimated at Gharb and Msida. During 2010, the Sahara dust impact on the PM_{10} yearly average concentration resulted to be roughly double, with contribution estimated to be 9 and 12.1 µg/m^3 at Msida and Gharb, respectively.

This evaluation of desert dust impact on the PM_{10} yearly average concentrations can be considered an underestimation of the possible actual value. The applied methodology considers in fact only desert dust contribution during major dust advection episodes, that can be more clearly identifiable, while the Maltese Islands can be expected to be affected also by minor dust contributions from the African continent, which cannot be clearly identified only through the air quality network measurements analysis prescribed by the European Commission Guidelines. It is anyway worth mentioning that the Sahara dust impact evaluation provided very similar results for years 2011-2012, even if they have been characterized by episodes of different intensity and time frequency, while a strong variation and a more relevant impact has been estimated for 2010 affecting especially yearly average PM concentrations.

Table 24. PM_{10} concentrations (µg/m^3) during Sahara dust outbreak episodes detected during year 2010: deduction of natural contribution. Numbers in red indicate exceedancees of the daily average concentration limit.

Date	Measured concentration at Msida	Measured concentration at Gharb	Sahara dust contribution	Msida concentration after deduction of dust contribution
05/01/2010	40.7	42.7	24.0	16.7
06/01/2010	58.6	55.1	36.0	22.7
07/01/2010	73.8	44.1	25.4	48.4
08/01/2010	83.1	92.6	73.9	9.2
09/01/2010	60.8	51.7	33.0	27.8
11/01/2010	44.2	25.1	6.0	38.3

26/01/2010	44.3	43.2	24.5	19.8
27/01/2010	206.0	207.2	188.6	17.4
28/01/2010	102.7	70.6	51.9	50.8
31/01/2010	22.7	23.1	3.1	19.6
01/02/2010	32.7	25.8	5.8	27.0
16/02/2010	87.9	81.9	61.7	26.3
17/02/2010	153.1	122.0	101.7	51.4
18/02/2010	n.a.	160.4	140.1	
19/02/2010	n.a.	283.3	263.1	
20/02/2010	n.a.	366.4	346.2	
22/02/2010	n.a.	44.8	24.9	
23/02/2010	n.a.	45.9	26.2	
24/02/2010	n.a.	24.2	4.3	
25/02/2010	42.6	32.7	13.0	29.6
26/02/2010	n.a.	26.3	6.6	
28/02/2010	41.1	23.0	3.4	37.7
01/03/2010	67.7	28.1	8.5	59.2
02/03/2010	36.1	28.9	10.2	25.9
03/03/2010	43.6	37.5	19.6	24.1
04/03/2010	46.4	31.8	14.0	32.4
09/03/2010	41.9	39.2	20.8	21.2
10/03/2010	47.4	28.4	10.0	37.5
11/03/2010	35.5	20.2	1.8	33.8
24/03/2010	47.5	44.3	22.4	25.1
25/03/2010	50.5	33.5	11.0	39.5
26/03/2010	48.2	44.7	21.7	26.5
27/03/2010	46.7	34.5	11.5	35.3
12/04/2010	41.8	44.3	20.2	21.6
13/04/2010	61.9	50.8	26.7	35.2
14/04/2010	62.8	54.7	31.1	31.8
15/04/2010	138.9	109.3	86.1	52.8
16/04/2010	185.5	129.5	106.4	79.1
17/04/2010	76.8	63.0	40.0	36.8
18/04/2010	63.1	62.6	40.2	23.0
23/04/2010	62.3	45.1	24.1	38.2
26/04/2010	46.7	27.5	8.2	38.5
03/05/2010	43.4	42.2	22.1	21.4
04/05/2010	65.7	55.5	36.2	29.5
05/05/2010	69.9	55.1	34.1	35.8
11/05/2010	42.4	28.2	10.6	31.8
12/05/2010	38.2	25.6	8.0	30.2
13/05/2010	37.7	22.0	4.0	33.8
14/05/2010	59.9	53.0	35.0	25.0
28/05/2010	n.a.	34.0	16.4	

29/05/2010	n.a.	62.2	44.6	
30/05/2010	n.a.	40.8	23.2	
13/06/2010	58.2	40.6	23.7	34.6
14/06/2010	92.8	62.7	45.6	47.2
15/06/2010	95.5	86.6	69.5	26.0
16/06/2010	109.4	66.5	49.4	60.0
17/06/2010	80.1	60.4	43.3	36.8
18/06/2010	89.4	74.9	57.8	31.6
19/06/2010	40.0	19.1	2.0	38.0
16/07/2010	65.0	31.9	6.3	58.7
17/07/2010	68.2	38.7	13.8	54.4
18/07/2010	50.6	36.3	11.4	39.2
24/07/2010	61.3	40.4	15.5	45.8
15/08/2010	46.7	38.4	13.9	32.9
16/08/2010	64.3	35.3	8.3	56.1
17/08/2010	49.0	34.6	7.6	41.5
23/08/2010	42.6	44.1	21.1	21.5
24/08/2010	39.8	36.5	12.6	27.2
25/08/2010	43.3	37.7	12.4	30.9
26/08/2010	48.5	45.2	18.5	30.0
27/08/2010	49.1	33.0	6.0	43.2
11/10/2010	65.3	32.8	14.4	50.9
12/10/2010	73.2	50.4	32.2	41.0
13/10/2010	120.1	100.0	81.8	38.3
14/10/2010	73.9	39.2	21.9	52.0
31/10/2010	33.5	19.8	2.2	31.4
01/11/2010	90.3	56.3	38.4	51.9
02/11/2010	111.3	51.3	33.2	78.2
07/11/2010	52.2	33.6	14.8	37.4
08/11/2010	30.0	32.2	12.9	17.1
09/11/2010	132.9	155.1	135.8	
10/11/2010	232.1	240.9	221.6	10.5
11/11/2010	96.4	66.5	47.0	49.4
26/11/2010	42.9	24.5	5.0	37.9
27/11/2010	32.2	24.7	5.2	27.0
28/11/2010	114.1	122.9	103.4	10.7
29/11/2010	50.2	30.3	11.2	39.0
30/11/2010	108.0	121.2	101.7	6.3
01/12/2010	107.0	105.0	85.9	21.1
03/12/2010	52.4	20.8	2.3	50.1
07/12/2010	75.5	30.0	14.6	60.9
08/12/2010	62.5	38.2	23.3	39.3
09/12/2010	87.4	53.7	38.3	49.1
18/12/2010	41.3	37.7	23.2	18.1

19/12/2010	99.3	66.3	51.4	48.0
20/12/2010	83.5	64.0	48.6	34.9
22/12/2010	60.3	34.1	19.2	41.2
23/12/2010	70.2	63.8	48.9	21.4
24/12/2010	77.6	58.6	43.7	34.0

Table 25. PM$_{10}$ concentrations (µg/m^3) during Sahara dust outbreak episodes detected during year 2011: deduction of natural contribution. Numbers in red indicate exceedancees of the daily average concentration limit.

Date	Measured concentration at Msida	Measured concentration at Gharb	Sahara dust contribution	Msida concentration after deduction of dust contribution
07/01/2011	94.8	15.3	2.5	92.3
08/01/2011	64.1	20.2	7.9	56.3
09/01/2011	58.7	20.8	8.9	49.8
27/01/2011	115.7	106.3	93.5	22.2
28/01/2011	44.6	27.2	14.3	30.3
29/01/2011	58.0	20.6	7.6	50.4
30/01/2011	65.0	34.4	21.4	43.6
17/02/2011	84.4	66.0	50.4	34.0
18/02/2011	47.4	47.1	31.2	16.3
19/02/2011	37.0	30.7	14.8	22.3
13/03/2011	66.7	75.1	57.3	9.5
14/03/2011	94.3	83.0	64.7	29.6
15/03/2011	323.0	207.0	189.2	133.9
16/03/2011	118.9	101.8	83.5	35.4
17/03/2011	38.9	21.2	2.6	36.4
18/03/2011	48.5	28.4	8.4	40.2
25/04/2011	51.7	50.9	23.1	28.6
26/04/2011	107.1	80.7	52.7	54.4
28/04/2011	30.8	31.4	2.4	28.4
29/04/2011	n.a.	34.0	5.0	
30/04/2011	n.a.	100.9	71.9	
01/05/2011	n.a.	98.2	68.7	
02/05/2011	n.a.	64.8	35.3	
03/05/2011	105.7	75.2	45.7	60.0
04/05/2011	47.4	39.0	9.5	37.9
05/05/2011	n.a.	44.2	14.7	
05/06/2011	n.a.	102.9	70.7	
06/06/2011	n.a.	57.4	24.7	
07/06/2011	n.a.	104.7	72.0	
08/06/2011	n.a.	35.5	2.8	
13/07/2011	n.a.	36.5	6.1	
14/07/2011	60.1	45.2	14.8	45.3

15/07/2011	54.2	39.5	11.6	42.6
16/07/2011	57.0	36.0	8.5	48.5
17/07/2011	49.1	31.8	5.0	44.1
18/07/2011	73.3	48.8	22.3	51.0
19/07/2011	62.6	46.0	20.0	42.6
20/07/2011	68.8	35.5	10.3	58.5
04/09/2011	41.3	49.9	16.3	25.0
05/09/2011	47.0	47.2	13.8	33.2
06/09/2011	43.8	38.4	5.1	38.7
03/11/2011	n.a.	32.1	11.6	
04/11/2011	n.a.	40.7	20.2	
05/11/2011	n.a.	39.8	19.5	
06/11/2011	n.a.	70.8	50.5	
07/11/2011	n.a.	97.3	76.3	
08/11/2011	57.2	45.2	23.9	33.3
09/11/2011	n.a.	47.2	25.9	
10/11/2011	48.2	27.9	7.6	40.7
22/11/2011	74.6	43.6	24.3	50.3
23/11/2011	83.7	55.6	36.3	47.4

Table 26. PM$_{10}$ concentrations (μg/m^3) during Sahara dust outbreak episodes detected during year 2012: deduction of natural contribution. Numbers in red indicate exceedancees of the daily average concentration limit.

Date	Measured concentration at Msida	Measured concentration at Gharb	Sahara dust contribution	Msida concentration after deduction of dust contribution
01/02/2012	28.6	16.2	1.8	26.8
02/02/2012	57.6	35.2	20.7	36.9
03/02/2012	57.9	46.7	32.2	25.7
04/02/2012	34.0	16.5	2.0	32.0
10/02/2012	29.2	20.1	5.7	23.5
21/02/2012	35.3	25.6	8.0	27.4
22/02/2012	52.3	33.1	15.5	36.9
10/03/2012	286.2	216.6	191.7	94.5
11/03/2012	65.9	43.8	18.9	47.0
31/03/2012	n.a.	36.1	8.9	
01/04/2012	n.a.	31.3	3.2	
02/04/2012	n.a.	31.1	3.0	
03/04/2012	n.a.	62.1	33.6	
04/04/2012	n.a.	82.3	53.3	
05/04/2012	n.a.	35.8	5.8	
06/04/2012	66.9	37.0	8.0	58.9
07/04/2012	80.7	62.5	34.0	46.8
08/04/2012	31.4	30.3	2.2	29.2
13/04/2012	43.3	35.2	9.0	34.3

14/04/2012	34.3	27.7	1.5	32.8
15/04/2012	69.1	49.2	23.1	46.0
16/04/2012	54.0	33.2	7.1	46.9
18/04/2012	39.6	30.4	4.3	35.3
19/04/2012	60.2	41.8	15.9	44.4
21/04/2012	36.6	27.8	2.3	34.3
23/04/2012	42.0	30.1	4.6	37.4
24/04/2012	n.a.	29.5	4.5	
18/06/2012	33.5	37.7	3.0	30.5
21/06/2012	40.6	42.0	6.4	34.2
22/06/2012	58.8	69.7	33.3	25.5
23/06/2012	50.8	52.4	16.0	34.9
08/07/2012	42.8	36.4	2.1	40.7
10/07/2012	47.9	42.8	11.1	36.8
11/07/2012	54.7	45.0	14.2	40.5
12/07/2012	81.4	60.2	29.5	51.9
13/07/2012	59.8	50.7	20.2	39.6
14/07/2012	39.5	38.3	8.3	31.2
15/07/2012	36.9	35.3	6.6	30.4
16/07/2012	46.1	43.7	15.0	31.2
30/07/2012	66.9	54.4	23.8	43.2
31/07/2012	38.2	34.4	3.8	34.5
07/08/2012	48.8	34.6	3.5	45.4
08/08/2012	69.4	65.5	34.4	35.1
09/08/2012	59.2	45.3	14.2	45.1
15/08/2012	38.7	41.6	9.7	29.1
16/08/2012	40.1	35.8	4.0	36.1
25/08/2012	42.5	27.0	1.8	40.8
26/08/2012	35.9	32.0	6.8	29.2
27/08/2012	39.0	37.3	12.3	26.7
28/08/2012	40.0	31.5	6.5	33.5
11/09/2012	54.3	25.2	4.4	49.9
12/09/2012	53.6	25.9	5.1	48.5
13/09/2012	66.5	35.1	14.6	51.9
24/09/2012	45.8	31.1	10.3	35.5
25/09/2012	55.6	40.6	19.8	35.8
26/09/2012	54.2	37.5	16.7	37.5
27/09/2012	47.5	39.8	19.0	28.5
28/09/2012	47.2	38.9	18.0	29.2
29/09/2012	51.8	41.5	20.7	31.1
30/09/2012	48.8	41.9	21.1	27.7
01/10/2012	56.1	41.7	20.7	35.4
08/10/2012	n.a.	36.6	15.5	
09/10/2012	39.4	30.5	9.4	30.0

15/10/2012	n.a.	24.7	3.9	
18/10/2012	n.a.	28.9	9.1	
19/10/2012	n.a.	27.7	9.9	
20/10/2012	n.a.	23.7	7.6	
21/10/2012	n.a.	25.2	10.0	
22/10/2012	n.a.	22.9	7.7	
23/10/2012	n.a.	25.9	11.5	
24/10/2012	n.a.	24.6	11.3	
27/10/2012	n.a.	47.2	35.3	
28/10/2012	n.a.	22.5	10.8	
05/11/2012	33.7	19.5	11.2	22.5
06/11/2012	28.3	9.5	1.6	26.7
12/11/2012	41.4	23.7	16.5	24.9
28/11/2012	56.5	59.0	54.0	2.5
29/11/2012	49.9	48.0	43.1	6.9
30/11/2012	47.9	19.2	14.3	33.6
01/12/2012	60.7	15.1	10.2	50.6
02/12/2012	21.2	6.8	1.8	19.4

5.2.3 Urban background

To estimate the urban background, the FARM model has been run on the background domain at 1 km resolution over a whole year, fed by hourly meteorology (the one reconstructed for year 2011) and the emissions from all sources illustrated in § 4.1.2, also modulated at hourly level. Boundary conditions for PM have been assigned using EMEP modeled concentrations, while for all other species the boundary conditions have been extracted from QualeAria modelling system.

Two runs have then been conducted, one with all emission sources inside the domain, and a second without all the emissions from Maltese sources. The urban background (ie. the contribution from all Maltese sources, excluded DPS and MPS) has then been estimated as the difference between the concentrations computed with the two runs. Figure 72 shows the maps of the urban background estimated for NO_2, PM_{10} and $PM_{2.5}$ (bottom, right) annual average concentrations. For NO_2, the estimated contribution is above 10 µg/m^3 around the Valletta and Sliema agglomeration main urbanized area (where it reaches a maximum of 20 µg/m^3) and the airport area, with minima in the northwestern part of Gozo in the order of 1 µg/m^3. PM_{10} is estimated to be above 3 µg/m^3 (2 µg/m^3 for $PM_{2.5}$) over most of Malta island and the central part of Gozo, and above 5 µg/m^3 (3.5 µg/m^3 for $PM_{2.5}$) over the main urbanized area, where the its maximum reaches 8 µg/m^3 (near 6 µg/m^3 for $PM_{2.5}$); the minimum values in the northwestern part of Gozo are around 1.5 µg/m^3 for $PM_{2.5}$ and 1 µg/m^3 for $PM_{2.5}$.
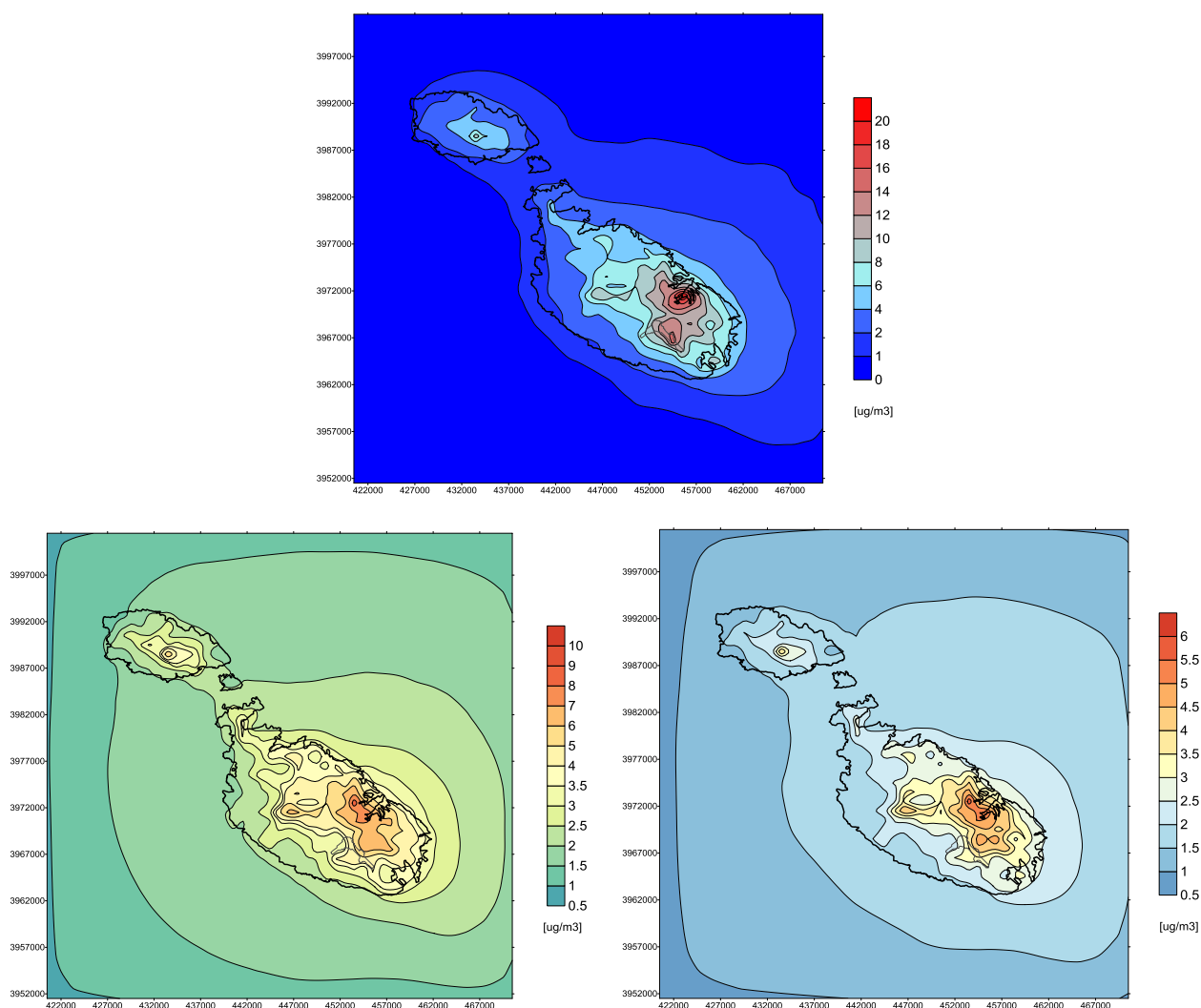
Figure 72. Maps of urban background estimated for NO$_2$ (top), PM$_{10}$ (bottom, left) and PM$_{2.5}$ (bottom, right) annual average concentrations.

5.2.4 Comparison with observations

The modeled concentrations have been compared with the data collected from the continuous monitoring stations (Table 22), at the time of the study available for the years 2010 and 2011.

The Zejtun monitoring station is situated on the south-easterly edge of the Valletta and Sliema agglomeration is the closest to DPS, although due to the prevailing wind direction on the Maltese Islands (NW) is mostly affected by anthropogenic air pollution sources from the agglomeration. This site is representative of the "urban background". Kordin station is characterised as "industrial", since it is situated within an industrial estate; it is also meant to monitor possible ground-level pollution plumes coming from the Marsa power plant. Gharb monitoring station is located close to the northwestern coast of Gozo island, away from the direct influence of nearby sources, so it is characterized as a station representative of the "rural background". Msida station is situated at about four metre distance from a road in an area where several traffic arteries merge (with approximately 40,000 cars passing by the station every day), so it is characterized as "traffic" station.

This study is focused on the assessment of DPS impact on air quality, considering also the contribution of all other major sources that may affect background concentration levels. The comparison of modeled concentrations against the observations from continuous monitoring stations has been performed for the sites of Zejtun, Kordin and Gharb. The Msida station has not been considered in the comparison, since a realistic reconstruction of roadside concentration levels requires specific modelling effort that is beyond the scope of this study.

Figure 73 shows the comparison of modeled annual average concentrations from DPS and all the other sources considered against the observed data collected by continuous monitoring stations for years 2010 and 2011. The comparison must be examined also by considering the underlying different operating conditions of Enemalta power plants. For the dispersion modeling, the emissions at the "transitional operating conditions" of power plants at the time of the study have been assumed, in fact derived from actual data monitored by CEMS for year 2013. Most importantly, respect to the years for which the ambient air quality observations are available, some MPS units, burning residual (heavy) fuel oil with gases emitted from relatively low stacks, have been progressively shut down. This means that the observations for the available years still include a contribution that has not considered anymore in the modelling.

The comparison for NO_2 shows that the model correctly reconstruct the differences in concentration levels at the different sites, with the highest value in Kordin industrial station and the lowest in Gharb rural background station.

The differences among the concentrations averages recorded at the stations are otherwise much less pronounced for PM, possibly reflecting a series of factors: a non-negligible secondary component, the absence of dominant individual sources (usually reflected by an increase of primary PM at nearby locations), and relevant background contributions across the Maltese Islands. The latter may be attributed to a combination of long-range transport from anthropogenic sources and natural sources, as discussed in § 5.2.1 and § 5.2.2. The modeled concentrations reflect this behavior, with lower differences among stations and the magnitude of concentration values correctly represented. The larger underestimation of PM10 at Kordin could be also attributed to the effect of emissions from MPS, that were more consistent during the years corresponding to the observations than in the transitionaloperating conditions considered in this study.

Given also these considerations, the modelling uncertainty fulfill the requirements given by the European legislation (Directive 2008/50/EC).

In the second phase of the study the comparison will be also extended to include the monitoring data of year 2012, as well a full list of the data that will be utilized.
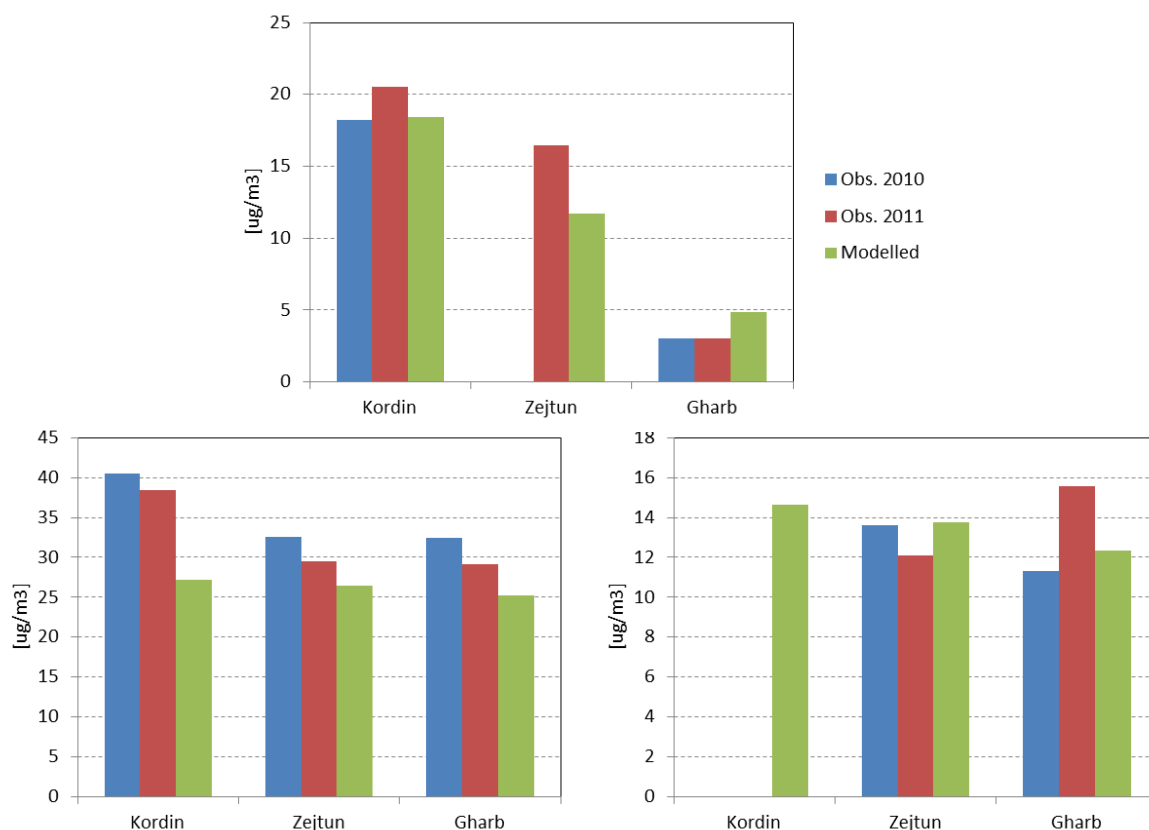
Figure 73. Comparison of modeled annual average concentrations from all sources (year 2011 meteorology) against data from continuous monitoring stations of years 2010 and 2011: NO$_2$ (top), PM$_{10}$ (bottom, left) PM$_{2.5}$ (bottom, right).

5.3 Sensitive receptors

The modelled concentrations have been also computed on a series of sensitive receptor points, corresponding to hospitals and health cares, cultural heritage sites, sport facilities and other public buildings (Table 27). Their location is depicted in Figure 74.

Table 27. List of sensitive receptors considered.

Receptor name	Type	x (UTM33)	y (UTM33)
Cottonera Sports Complex	public building	457324	3971118
Ghar Dalam Cave and Museum	public building	457282	3966157
Grand Harbour	UNESCO heritage	456269	3972739
Hagar Qim Temples	cultural heritage	449676	3965165
Hal Saflieni Hypogeum	cultural heritage	454889	3969477
Karin Grech Hospital	health care	454555	3972663
Malta National Pool	sports facility	453785	3973514
Marsa Sports Club	public building	453847	3970596
Mater Dei Hospital	health care	452920	3973361
Mnajdra Neolithic Temples	cultural heritage	449616	3965239
Sir Paul Boffa Hospital	health care	455761	3972409
St. Aloysius Sports & Recreational Complex	sports facility	451183	3972610
St. Vincent De Paul Residence	public building	453364	3969749
Tarxien Temples	cultural heritage	456089	3969746
Valletta	UNESCO heritage	456126	3973008

Figure 74. Location of sensitive receptors.

The contribution from DPS emissions in TOC and NOC configurations to annual average NO_2 and PM_{10} concentrations at the receptors is reported in Table 28, as the maximum values simulated for the three meteorological years considered (2010, 2011, 2012).

Table 28. Contribution of DPS in TOC and NOC configurations to annual average NO$_2$ and PM$_{10}$ concentrations at sensitive receptors: maximum values (µg/m^3) among the three meteorological years considered (2010, 2011, 2012).

Receptor	TOC scenario		NOC scenario	
	NO$_2$	PM$_{10}$	NO$_2$	PM$_{10}$
Cottonera Sports Complex	0.76	0.04	0.43	0.03
Ghar Dalam Cave and Museum	2.36	0.13	1.24	0.11
Grand Harbour	1.00	0.05	0.47	0.04
Hagar Qim Temples	0.50	0.03	0.29	0.02
Hal Saflieni Hypogeum	0.63	0.04	0.37	0.04
Karin Grech Hospital	0.49	0.03	0.33	0.03
Malta National Pool	0.40	0.02	0.22	0.02
Marsa Sports Club	0.54	0.03	0.30	0.03
Mater Dei Hospital	0.41	0.02	0.24	0.02
Mnajdra Neolithic Temples	0.50	0.03	0.30	0.02
Sir Paul Boffa Hospital	0.70	0.04	0.36	0.03
St. Aloysius Sports & Recreational Complex	0.32	0.02	0.19	0.02
St. Vincent De Paul Residence	0.54	0.03	0.31	0.03
Tarxien Temples	0.77	0.04	0.46	0.04
Valletta	0.55	0.03	0.35	0.03

5.4 *Comparison with limits in legislation*

The limit and target values currently in force are summarized in Tables 29 and 30.

Table 29. Pollutants limit values.

Pollutant	Averaging period	Limit value
NO$_2$	calendar year	40 µg/m^3
NO$_2$	one hour	200 µg/m^3, not to be exceeded more than 18 times in a calendar year
PM$_{10}$	calendar year	40 µg/m^3
PM$_{10}$	one day	50 µg/m^3, not to be exceeded more than 35 times in a calendar year
Lead	calendar year	0.5 µg/m^3

Table 30. Pollutants target values.

Pollutant	Averaging period	Target value
PM$_{2.5}$	calendar year	24 µg/m^3
Arsenic	calendar year	6 ng/m^3
Cadmium	calendar year	5 ng/m^3
Nickel	calendar year	20 ng/m^3

For what concern vanadium, the WHO in its Air Quality Guidelines for Europe (WHO, 2000) indicates a guideline value for the 24-hours averages of 1 µg/m^3.

The compliance with the limits and targets on ambient concentrations of the contributions from DPS emissions in both its "transitional"and "new" operating conditions is recapitulated in Tables 31-33, for all three meteorological year considered. For both scenarios, the compliance is respected for all pollutants and meteorological years.

When compared against ambient air monitoring and the background contributions from all other sources (in Malta and outside it), the contribution from DPS, although below the limits/targets, can be anyway considered worth of attention in the case of NO_2 (a few exceedances per year of the hourly limit in the worst meteorological year, even if over a very limited area surrounding DPS) and nickel.

Table 31. DPS in "transitional" and "new" operating conditions: compliance with the limit values, considering different meteorological years (: in compliance; : not in compliance).

Air quality limit	Meteorological year		
	2010	2011	2012
NO_2 annual			
NO_2 hourly			
PM_{10} annual			
PM_{10} 24 hour			
Pb annual			

Table 32. DPS in "transitional" and "new" operating conditions: compliance with the target values, considering different meteorological years (: in compliance; : not in compliance).

Air quality target	Meteorological year		
	2010	2011	2012
$PM_{2.5}$ annual			
As annual			
Cd annual			
Ni annual			

Table 33. DPS in "transitional" and "new" operating conditions: compliance with vanadium WHO guideline, considering different meteorological years (: in compliance; : not in compliance).

Air quality guideline	Meteorological year		
	2010	2011	2012
V one day			

6 Limitations of study

The main limitations of this study can be ascribed to the following groups of factors.

Scope: the study is focused on the impact assessment of DPS on air quality; all other main sources, either inside Maltese Islands or outside them, are included in the analysis to estimate the background contributions, and put in a correct perspective the impact of DPS in its current and

upcoming configuration. Therefore, a detailed impact assessment of some of those other sources categories may require a more detailed analysis.

Data availability and quality: realistic and up-to-date data are a crucial aspect of any assessment study. For what concern the main subject of the study, DPS, the availability and direct use of hourly data collected by the continuous emission monitoring systems installed at the stacks contributes to the trustworthiness of the current model application. Instead, heavy metals emissions are monitored only discontinuously, by means of period sampling activities, so of the continuation of the monitoring plan could add confidence in the information available until now, and of the related assessment. The inventory of the other emission sources could also be further improved. Road traffic is probably the sector of first importance, probably calling for a targeted study, involving more detailed information. Also, particulate emissions do not take into account the contribution from resuspension (emission from ambient material deposited on the road, which relevance grows during wind calm and dry meteorological conditions): although potentially important, there is still a high level of uncertainty in the estimation of this fraction. Also more information allowing to better describe the international maritime activities around Malta would probably be of interest.

Model uncertainty: even when made with state-of-the-art tools, as all model-based assessments this study reflects the limitations inherent in the assumptions, parametrizations and configuration of the employed models. Among them, it is worth to cite the limitations associated to the adopted spatial resolution the time frame, which also depends from the availability of realistic input data. The model reliability could increase if performed on a continuous basis, either periodically or in real-time, contributing to the interpretation of monitoring activities and the consistency of the emission inventory.

7   Conclusions and recommendations

The study has assessed the contribution from DPS in two different configurations to ambient air concentration levels, updating the air dispersion study carried out by Enemalta in 2011 as part of IPPC obligations. The configurations considered for DPS have been the current operating conditions at the end of year 2013 (a scenario referred as "transitional operating conditions - TOC") and the "new operating conditions - NOC" at the middle of year 2015, after the commissioning of the submarine cable interconnector and shut down of MPS.

This has been evaluated employing the state-of-the-art SPRAY Lagrangian particle model, which is 3D and dynamic in nature, run over three years fed by hourly meteorological data and, most importantly, by hour-by-hour emissions directly monitored at the stacks by continuous emission monitoring systems. Contributions from other relevant emission sources inside Malta as well from natural sources and long-range transport has been also considered, by mean of FARM Eulerian 3D model.

The modelling analyses assess the likelihood that respect to the ones from other sources, for both scenarios (TOC and NOC) the contribution from DPS in exceeding the limits and targets on ambient concentrations of NO_2 and metals is limited, and very limited in the case of particulate matter. For all considered pollutants, concentration indicators for NOC scenario are somewhat lower than the corresponding ones for TOC scenario, as the result of lower emissions from DPS units, considered as a whole.

The study also indirectly confirms that, discounting the contributions from natural sources, the road transport sector is likely to be the major contributor to the exceedance of PM10 concentrations in ambient air, as indicated by (MEPA, 2010). In this perspective, road traffic could be the subject of a more detailed evaluation of the initiatives envisaged to ensure Malta's compliance with the European Directives limits.

The conclusions of the 2011 air dispersion study, using information on planned DPS extension and on MPS working at its previous conditions, stated that "DPS by itself … does not violate any limit/target values and contributes very marginally to target value violations". Such conclusions are so substantially confirmed by this study, even using hour-by-hour actual emission data from the plants at their current conditions and 3D dynamic models: the contribution from DPS is below the limits/targets, except for few exceedances per year of the hourly limit in the case of NO_2 (although happening in the worst meteorological year, over a very limited area surrounding DPS). .

8 References

Ecoserv and Cada (2013) *Report of the first session of sampling and analysis at Marsa and Delimara Power Stations, carried out in July and August 2013 for Quarter 2/2013.* Ecoserv report ref. 133-13, September 2013.

Escudero M. , Querol X. , Pey J. , Alastuey A. , Pérez, N. Ferreira F. , Alonso S. , Rodríguez S. , Cuevas E. (2007) A methodology for the quantification of the net African dust load in air quality monitoring networks. Atmospheric Environment 41, 5516–5524.

EMEP (2012) *Transboundary air pollution by main pollutants (S, N, O3) and PM in 2010 – Malta.* MSC-W Data Note 1/2012, Norwegian Meteorological Institute, July 2012.

European Commission (2011) *Commission Staff Working Paper. Establishing guidelines for demonstration and subtraction of exceedances attributable to natural sources under the Directive 2008/50/EC on ambient air quality and cleaner air for Europe* (SEC 2011, 208 final).

European Union (2008) Directive of the European Parliament and of the Council on ambient air quality and cleaner air for Europe. Directive 2008/50/EC, 28 March 2008.

Kukkonen J., T. Olsson, D. M. Schultz, A. Baklanov, T. Klein, A. I. Miranda, A. Monteiro, M. HirtlV. Tarvainen, M. Boy, V.-H. Peuch, A. Poupkou, I. Kioutsioukis, S. Finardi, M. Sofiev, R. Sokhi, K.E.J. Lehtinen, K. Karatzas, R. San Jose, M. Astitha, G. Kallos, M. Schaap, E. Reimer, H. Jakobs, K. Eben (2012) A review of operational, regional-scale, chemical weather forecasting models in Europe. *Atmospheric Chemistry and Physics* **12**, 1-87.

MEPA (2010) *The Air Quality Plan for the Maltese Islands.* Malta Environment and Planning Authority, January 2010.

MEPA (2010b) *Justification report on the contribution of natural events to the PM10 daily limit value (reference to assessment questionnaire form 23a).* Report to the EC, February 2010.

MEPA (2013) Informative Inventory Report for Malta. Malta Environment and Planning Authority, March 2013.

Ministry for Infrastructure, Transport and Communications (2009) *Air Quality Plan - Proposed traffic measures as part of the plans and programmes in compliance with Directive 1996/62/EC*. Valletta, September 2009.

Transport Malta (2010) *3rd National Household Travel Survey*, Transport Malta.

WHO (2000) *Air Quality Guidelines for Europe - Second Edition*. WHO Regional Publications, European Series, No. 91. World Health Organization, Regional Office for Europe, Copenhagen.

APPENDIX A – Modelling system description

A.1 ARIA Industry/Regional overview

A.1.1 Features

The **ARIA Industry** and **ARIA Regional** packages are integrated software suites for atmospheric dispersion modelling, allowing the manipulation, presentation, modification and visualisation of several data classes (geographic site data, emission data, meteorological data, air pollution data, receptor data). In such packages, all simulation models access topography, maps, emissions, meteorology, through the same procedures (or methods), and the visualisation tools are common to all models.

The software suites comprises several modules for:

- **site data**: cartography, topography, land use, sensors,

- **meteorological data**: ground and upper air measurement data, output from large-scale NWP (ECMWF, NCEP, Local Agency)

- **emission inventory**: linear, large point sources, diffuse area sources by category

- **3D meteorological fields computation**: wind, temperature, atmospheric turbulence

- **3D dispersion**: calculation of primary pollutant concentrations

- **3D reactive Dispersion**: calculation of primary and secondary pollutants

- **3D display and animation**: the module visualizes all data and compares observed and computed concentration levels.

The next figure presents a flowchart for **ARIA Regional**, where the names of some of the main modules are reported. This chart may help the reader in following the short presentation of the functions of each module.
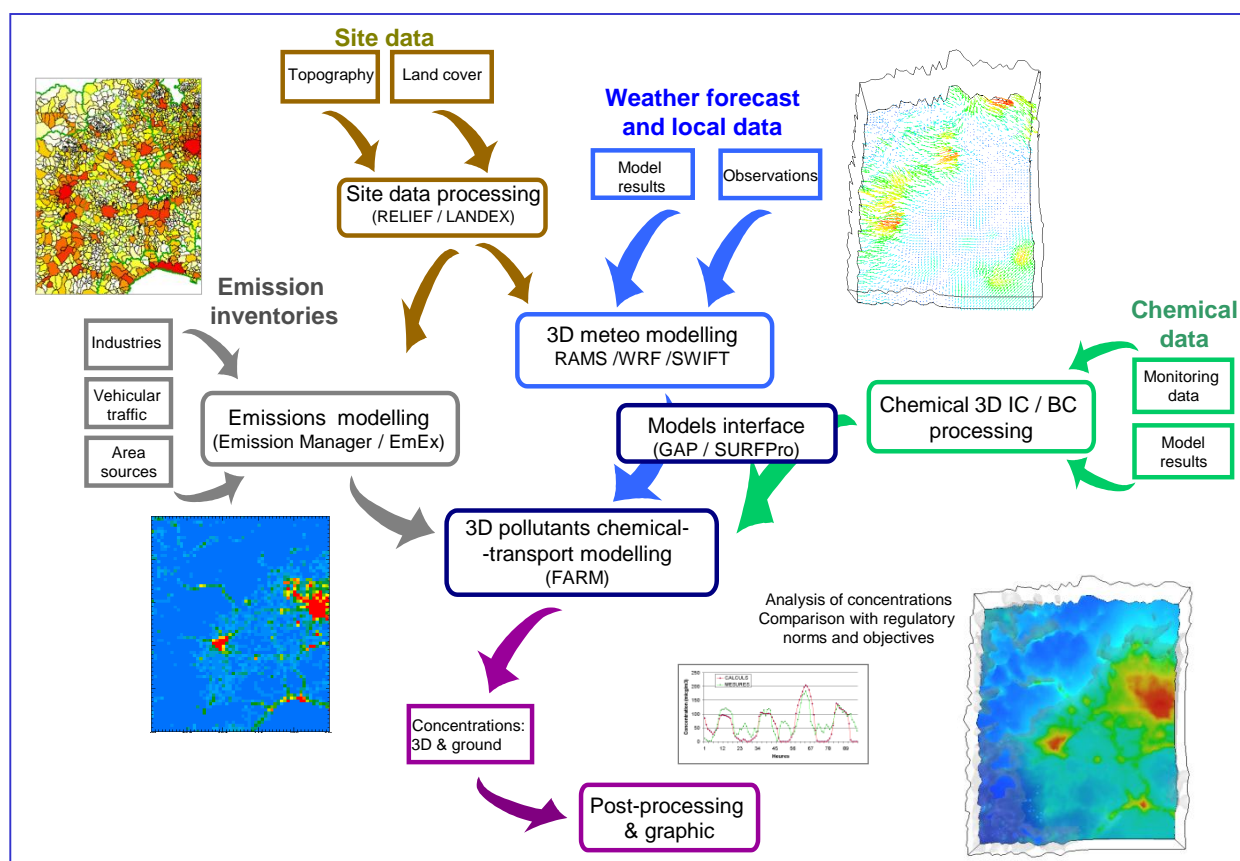
A.2 SPRAY 3D Lagrangian model

SPRAY (Tinarelli, 1994, 2007) is a three-dimensional model for the simulation of airborne pollutant dispersion, taking into account either spatial or temporal variations of the mean flow and turbulence.

A.2.2 Features

The code is able to reproduce concentration and dry/wet deposition fields deriving from point, line, area or volume sources. The airborne pollutant is simulated by means of 'virtual' particles, whose motion is defined both by local mean wind and by stochastic velocities that reproduce the atmospheric turbulence statistical behavior. In this way different parts of the emitted plume can deal with different details of the atmospheric flow, thus allowing more realistic simulations in complex meteorological conditions, which are usually difficult to reproduce with traditional models (presence of vertical shear, low wind speed, temperature inversion due to the altitude, flow over complex topography, presence of topographical discontinuities such as sea-land or town-countryside). This version of the code reproduces the transport, dispersion, dry and wet deposition of chemically inert species. Each particle motion is reproduced by means of the following equations:

$$x(t + \Delta t) = x(t) + u_x(t) \cdot \Delta t \quad ; \quad u_x(t) = \overline{U_x}(t) + u_x'(t)$$

$$y(t + \Delta t) = y(t) + u_y(t) \cdot \Delta t \quad ; \quad u_y(t) = \overline{U_y}(t) + u_y'(t)$$

$$z(t + \Delta t) = z(t) + u_z(t) \cdot \Delta t \quad ; \quad u_z(t) = \overline{U_z}(t) + u_z'(t)$$

in which x, y, z are the Cartesian coordinates of each single particle in the three-dimensional domain and u_x, u_y, u_z are the velocity components, divided in mean component and turbulent fluctuation. The mean component is obtained by MINERVE/SWIFT model in a *terrain-following* reference frame *x,y,s*, in which vertical coordinate s is defined as:

$$s = \frac{z - z_g}{z_{top} - z_g}$$

where z is the vertical geometric coordinate, z_{top} is the height of the computational domain and $z_g(x,y)$ is the height of topography. Particles linearly interpolate the wind value in the x,y,z point where they are located just using the values found in these arrays. SPRAY can simulate unstable conditions by means of a linear temporal interpolation between the values of two subsequent arrays.

Turbulent fluctuations u'_x, u'_y and u'_z, leading to diffusion, are determined by solving Langevin stochastic differential equations:

$$u_i^{'}(t + \Delta t) = a_i(\vec{x}, \vec{u}(t), t) + b_i(\vec{x}, \vec{u}(t), t)\Delta\xi \quad ; \quad i = x, y, z$$

where a and b are functions of each single particle position and velocity of, depending on the turbulence characteristics as well as on the chosen solving scheme. SPRAY refers to Thomson's schemes (1984, 1987).

A.2.3 Input data

In order to perform a dispersion simulation SPRAY model basically uses:

- three-dimensional wind fields provided by MINERVE/SWIFT meteorological model;

- two-dimensional turbulence fields z_0, H_{mix}, u_*, L, w_* , and species-dependent dry deposition velocities (for each of the species to be considered in the simulation), given by the SURFPro code;

- species dependent washout coefficient and two dimensional fields of precipitation rates in mm/h used by the wet deposition schemes;

- emission data, consisting in a sequence of time-varying data on spatial location and geometry of the emitting volumes linked to point / line / era sources, their thermodynamic parameters and the emission rates for each polluting species (gas / aerosol); SPRAY can dynamically simulate the plume rise of hot buoyant emissions.

A.2.4 Output

Three-dimensional Lagrangian particle models, when fed by realistic meteorological fields assimilating local topographic features and data, are superior to traditional and hybrid straight-plume Gaussian models. This is especially important in situations with complex terrain, including over stretches of sea coastal sites, presenting sea breezes regimes with transition situations, where the Gaussian formulation can not fully follow evolving meteorological conditions and can hardly reproduce the interaction of plumes with orography.

The following display illustrates these capabilities, where the impact of multiple stacks in the Fos-Berre area (near Marseille, on the Mediterranean coast) is simulated during a sea-breeze reversal process.
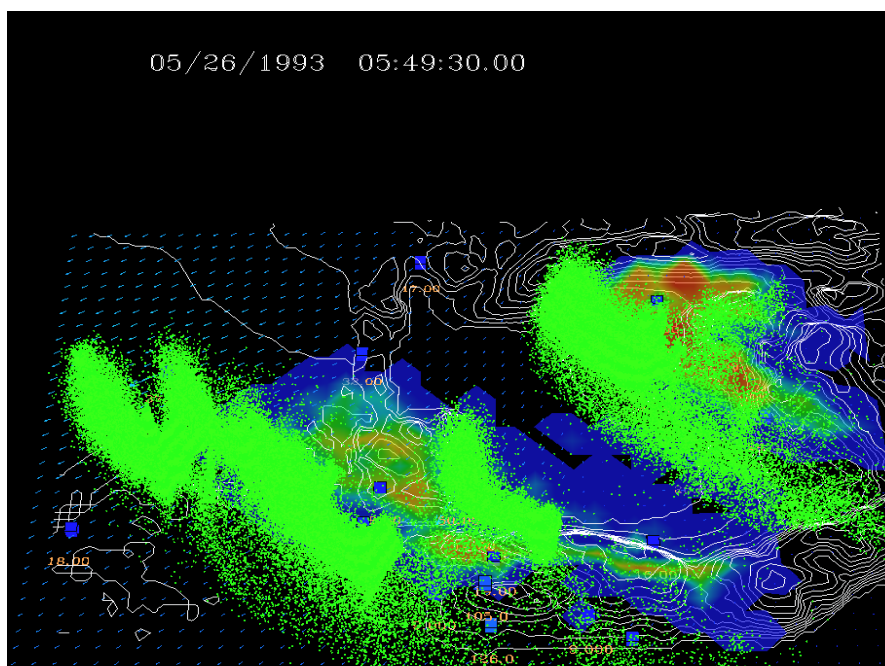
Dispersion of SO$_2$ plumes on the Fos-Berre area (white isolines: topography; clouds of SPRAY computational particles in green; ground level color shading: computed ground concentrations).

SPRAY is present in the **European Model Documentation System** (MDS, http://acm.eionet.europa.eu/databases/MDS/index_html), collecting information and descriptions about the most relevant meteorological/dispersion models available in Europe.

SPRAY is the result of more than twenty years of continuous development efforts, documented by a large number of scientific publications concerning its theoretical formulation, verifications in controlled experiments and real-world applications, documenting its levels of accuracy and output data reliability. Applications include short- and long-term impact assessment of power plants and industrial sites, episodic studies, urban and regional applications, pollution traffic studies, real-time control of sources, accidental releases.

Providing that the model is fed by 3D meteorological fields embedding mesoscale and local features (e.g. through local representative measurements), the SPRAY Lagrangian particle model is the **most accurate solution for complex configurations of sources and terrain features** at scales ranging from tens of km down to meters.

The inadequacy of Gaussian straight plume models to fully describe the dispersion in **coastal sites** as well as the transition situations is well represented in the following figures, showing the comparison of yearly average concentrations computed by a Gaussian model and SPRAY for thermal power plants at Fusina and Porto Marghera (near Venice):

- on top panels (yearly average concentrations computed by both models) the straight line approximation of the Gaussian models is clearly visible;

- the bottom panel (differences between concentrations computed by SPRAY and the Gaussian model), evidences that the transition regimes (the most common situation in that area) are missed by the Gaussian model.

Gaussian plume (ISCST3)

SPRAY 3D Lagrangian

straight concentrated plumes

SPRAY - ISC3 differences

most common situations (transitions) are missed
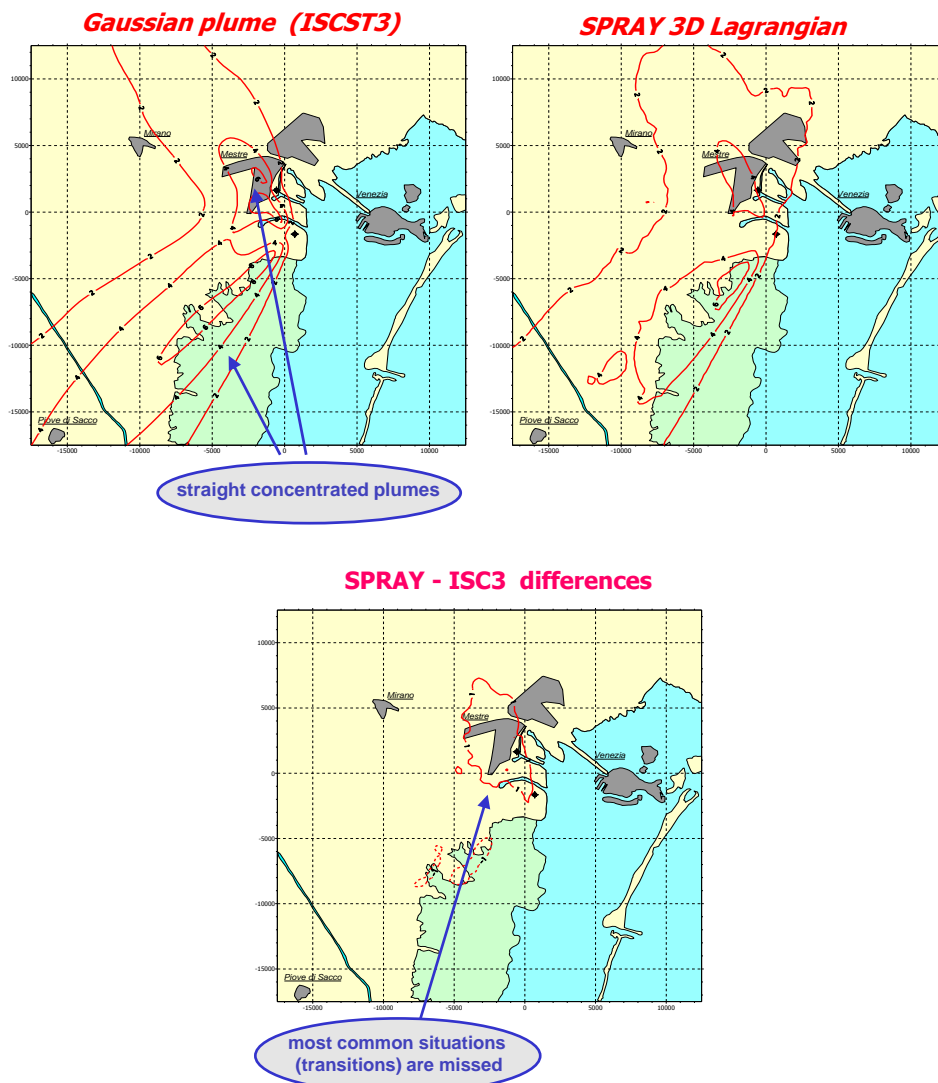
A further example in coastal sites with **complex orography**, is given in the following figures, showing summer average concentrations computed by dispersion models originating from the ENEL thermal power plant at Vado Ligure (Mediterranean coast): it is very clear that even on average concentrations, the two patterns are completely different.

Gaussian plume (ISCST3)   **SPRAY 3D Lagrangian**
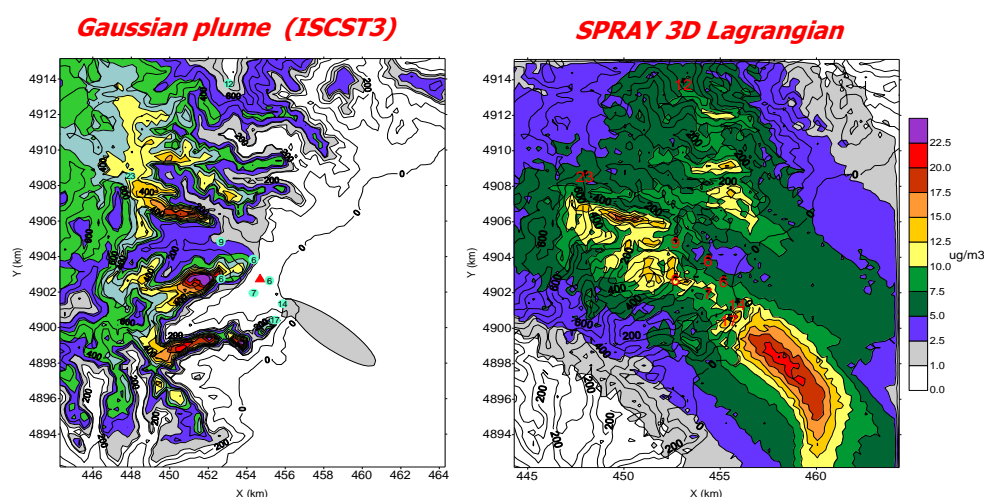
A.2.5   Scientific references

Brusasca G., Tinarelli G., Anfossi D., Zannetti P. (1987) : "Particle modeling simulation of atmospheric dispersion using the MC-LAGPAR package", Environmental Software 2,151-158.

Anfossi D., **Brusasca G., Tinarelli G.** (1988) : "Sensitivity analysis of a Monte Carlo atmospheric diffusion model", Il Nuovo Cimento C 11, 13-28.

Brusasca G., Tinarelli G., Moussafir J., Biscay P., Zannetti P., Anfossi D. (1988) : "Development of a portable FORTRAN 77 code for Monte Carlo particle modelling of atmospheric diffusion (MC-LAGPAR II) - Validation against analytical solution and tracer experiments", Proc. of Envirosoft '88, Porto Carras (Greece) 27-29 September: Computer Technique in Environmental studies, Computational Mechanics Pub., Springer-Verlag, 431-450.

Brusasca G., **Tinarelli G.**, Anfossi D. (1989) : "Comparison between the results of a Monte Carlo atmospheric diffusion model and tracer experiments", Atmospheric Environment 23, 1263-1280.

Anfossi D., **Brusasca G.**, **Tinarelli G.** (1990) : "Simulation of atmospheric diffusion in low windspeed meandering conditions by a Monte Carlo dispersion model". Il Nuovo Cimento C 13, N. 6, 995 1006.

Anfossi D., **Brusasca G.**, **Tinarelli G.** (1990) : "Results from a random walk dispersion model in low windspeed stable conditions", Proc. of 9th Symposium on Turbulence and Diffusion, American Meteorological Society, Roskilde (Denmark), April 30 - May 3, 6.1, 160-163.

Brusasca G., Morselli M.G., Anfossi D. (1990) : "Particle diffusion model evaluation against tracer experiments", Proc. of the 18th CCMS-NATO meeting, Vancouver (Canada), 13-17 May, Air Pollution Modelling and its Application VIII, Plenum Press, 625-626.

Anfossi D., **Brusasca G.**, **Tinarelli G.** (1991) : "Modello lagrangiano di dispersione di inquinanti in atmosfera a scala locale", Bollettino Geofisico XIV, 1, 23-33.

Finzi G. e **G. Brusasca** (1991) : "La Qualità dell'Aria: Modelli Previsionali e Gestionali", Chap. 4 "Modelli di diffusione a particelle", MASSON Ed., pp. 346.

Anfossi D., Ferrero E., **Brusasca G.**, **Tinarelli G.**, Tampieri F., Trombetti F., Giostra U. (1992) : "Dispersion simulation of a wind tunnel experiment with Lagrangian particle models", Il Nuovo Cimento C 15, 139-158.

Anfossi D., **Brusasca G.** Ferrero E. (1992): "Modelli per la dispersione degli inquinanti in atmosfera", Le Scienze n. 288, 38-49.

Brusasca G., **Tinarelli G.**, Anfossi D. (1992): "Particle model simulation of diffusion in low windspeed stable conditions", Atmospheric Environment 26, 707-723.

Giostra U., Tampieri F., **Brusasca G.**, **Tinarelli G.**, Anfossi D., Ferrero E. (1992): "Sulla applicazione di modelli di dispersione Lagrangiani a condizioni di turbolenza non omogenea", 9° Convegno Nazionale GNFAO, Roma 8-9-10 giugno, Bollettino Geofisico XV, N. 1, 90-91.

Tampieri F., C. Scarani, U. Giostra, **G. Brusasca, G.**Tinarelli, D. Anfossi, E. Ferrero(1992): "On the application of random flight dispersion models in inhomogeneous turbulent flows", Annales Geophysicae, 10, 749 758.

Tinarelli G., Giostra U., Ferrero E., Tampieri F., Anfossi D., **Brusasca G.**, Trombetti F. (1992) : "SPRAY, a 3-D particle model for complex terrain dispersion", Proc. of 10th Symposium on Turbulence and Diffusion, American Meteorological Society, Portland, Oregon (USA), 29-Sept. - 2 Oct, P2.9, 147-150.

Anfossi D., Ferrero E., **Brusasca G.**, Marzorati A., **Tinarelli G.** (1993): "A simple way of computing buoyant plume rise in Lagrangian stocastic dispersion models", Atmospheric Environment 27A, 1443-1451.

Brusasca G., **Tinarelli G.**, Anfossi D., Ferrero E., Castelli G., Centemeri M., Finzi G. (1993): "Software presentation of LAMBDA Code", Air Pollution Modelling and its Applications IX, S.E. Gryning ed., Plenum Press, New York

Brusasca G., Morselli M.G., Anfossi D. (1993): "Model evaluation criteria on tracer experimental data". Proceeding of the Manno workshop "Intercomparison of advanced practical short-range atmospheric dispersion models" August 30- September 3 1993, Manno, Switzerland 131-140.

Brusasca G., Marzorati A., Nadalutti M., Sguarnieri S., **Tinarelli G.**, Zardetto G. (1993): "Nodo Intelligente per il monitoraggio ambientale dell'area industriale di Porto Marghera e Fusina", atti del convegno internazionale ANIPLA, Milano, 23-25 Novembre 1993, 797-811.

Tinarelli G., Anfossi D., **Brusasca G.**, Ferrero E., Morselli M.G., Moussafir J. (1993): "A complete 3-D Lagrangian particle model to simulate the dispersion of non-reacting airborne pollutants over complex terrain". Proceedings of the Manno workshop "Intercomparison of advanced practical short-range atmospheric dispersion models" August 30- September 3 1993, Manno, Switzerland 103-111.

Boznar M., **Brusasca G.**, Cavicchioli C., Faggian P., **Finardi S.**, Mlakar P., Morselli M.G., Sozzi R., **Tinarelli G.** (1994): "Application of advanced and traditional diffusion models to an experimental campaign in complex terrain". Reprint of Second International Conference "Air Pollution 1994", 27-29 Sept 1994, Barcelona, Spain, pp. 159-166.

Brusasca G., **Tinarelli G.**, Anfossi D., Ferrero E., Tampieri F., F. Trombetti (1994) "Development of a Lagrangian stochastic model for dispersion in complex terrain", Air Pollution Modelling and its Applications X, S.E. Gryning and M.M. Millan eds., Plenum Press, New York, 329-337

Nanni A., Riva M., **Tinarelli G.**, **Brusasca G.** (1994): "Particle model simulation of pollutants dispersion from a line source in complex terrain", Proc. of 5th International Symposium on Highway and Urban Pollution, Copenhagen, 22-24 May 1994. Pubblicato su The Science of the total Environment, Elsevier 189/190, 301-309 (1996).

Tinarelli G., Anfossi D., **Brusasca G.**, Ferrero E., Giostra U., Morselli M.G., Moussafir J., Tampieri F., Trombetti F (1994): "Lagrangian particle simulation of tracer dispersion in the lee of a schematic two-dimensional hill", Journal of Applied Meteorology, Vol. 33, N. 6, 744-756.

Anfossi D., Sacchetti D., Trini Castelli S. 1995: "Development and sensitivity analysis of a Lagrangian particle model for long range dispersion", Environmental Software 10, 263-287.

Brusasca G., Ferrero E., Anfossi D., Desiato F., **Tinarelli G.**, Morselli M.G., **Finardi S.**, Sacchetti D. (1995): "Intercomparison of 3-D flow and particle models with Transalp 1989 meteorological and tracer data", Proc. of the 21st CCMS-NATO meeting, Baltimore, 6-10 November, 1995, 386-394. Air Pollution Modelling and its Application XI, Plenum Press, 559-567.

Ferrero E., Anfossi D., **Brusasca G.**, **Tinarelli G.** (1995): "Lagrangian Particle Model: Evaluation against Tracer Data", Int. J. Environment and Pollution, Vol. 5, N. 4-6, 360-374.

Tampieri F., U. Giostra, F. Trombetti, D. Anfossi, E. Ferrero, G.Tinarelli(1995): "Flux gradient relationships for turbulent dispersion in complex terrain", Nonlinear Processes in Geophysics, 2, 89-100.

Ferrero E., Anfossi D., **Brusasca G.**, **Tinarelli G.**, Alessandrini S., Trini Castelli S. (1996): "Simulation of atmospheric dispersion in convective boundary layer: comparison between different Lagrangian particle models", 4th Workshop on Harmonisation within Atmospheric Dispersion Modelling for Regulatory Purposes, Oostende, 6-9 May 1996, 67-74. Pubblicato su Int. J. Environment and Pollution, Vol 8, Nos. 3-6, 315-323.

E. Ferrero, F. Desiato, **G. Brusasca**, D.Anfossi, **G. Tinarelli**, M.G. Morselli, S. Finardi, D. Sacchetti (1996) "Intercomparison of 3-D flow and particle models with TRANSALP 1989 meteorological and tracer data". Air

Pollution Modelling and its Applications XI, S.E. Gryning and F. Schiermeier eds., Plenum Press, New York, 559-567

E. Ferrero, F. Desiato, **G. Brusasca**, D.Anfossi, **G. Tinarelli**, M.G. Morselli, S. Finardi, D. Sacchetti (1996) "Intercomparison of 3-D flow and particle models with TRANSALP 1989 meteorological and tracer data". Air Pollution Modelling and its Applications XI, S.E. Gryning and F. Schiermeier eds., Plenum Press, New York, 559-567

Anfossi D., E. Ferrero, **G. Tinarelli**, S. Alessandrini (1997): "A simplified version of the correct boundary conditions for skewed turbulence in Lagrangian particle models", Atmospheric Environment, 31, 2, 301-308.

Bacci P., **Brusasca G.**, Morselli M.G. (1997):: "Modellistica dell'inquinamento atmosferico prodotto da impianti industriali in condizioni meteo-diffusive complesse", SIDISA – Simposio internazionale di ingegneria sanitaria ambientale, Revello 3-7 giugno 1997.

Brusasca G. (1997): "La modellistica di dispersione degli inquinanti in atmosfera", Giornate di Studio "Progettare la qualità dell'aria", 25-27 Settembre, Lipari (ME).

Ferrero E., D.Anfossi, **G. Tinarelli**, S. Trini Castelli (1997): "An intercomparison of two turbulence closure schemes and four parameterizations for stochastic dispersion models", Nuovo Cimento, 20 C, 315-329, Editrice Compositori, Bologna

Ferrero E., D.Anfossi, **G. Brusasca, G. Tinarelli**, Alessandrini S., S. Trini Castelli (1997): "Simulation of atmospheric dispersion in convective boundary layer: comparison between two Lagrangian particle models", Int. J. Environment and Pollution, 8, 315-323

Pacitti, M. P. Mensio, **G. Brusasca, G. Tinarelli, G.** Genon, F. Marchese, G. Nobile, G. Malvasi (1997): "Global evaluation of the activity of toxic and hazardous waste landfills using monitoring and modeling integrated system". Proc. of 5th International Conference "Air Pollution 1997", 16-18 September, Bologna, Italy. Air Pollution V, modelling, monitoring and management, 517-526, Computational Mechanics Publications.

Stefani A., **Brusasca G.**, Grigolon E., Martinelli U., Marzorati A. (1997): "Integrazione di un sistema di supervisione ambientale nel sistema informativo della Centrale Termoelettrica di Fusina", Atti del 97° convegno AEI - Baveno (VB) 7-9 Maggio 1997, 65-70.

Trini Castelli S., Anfossi D. (1997): "Intercomparison of 3-D turbulence parameterizations for dispersion models in complex terrain derived from a circulation model", Nuovo Cimento, 20 C, 287-313, Editrice Compositori, Bologna

Anfossi D., F. Desiato, **G. Tinarelli, G. Brusasca**, E. Ferrero, D. Sacchetti, (1997): "TRANSALP 1989 Experimental Campaign - part II: Simulation of a tracer experiment with Lagrangian particle models.", Atmospheric Environment, 32, 7, 1157-1166.

Anfossi D., Trini Castelli S., Ferrero E., **Brusasca G.**, **Tinarelli G.**(1998) : "Confronto tra modelli stocastici Lagrangiani di dispersione nello strato limite convettivo basati su diverse PDF", Convegno di Meccanica Stocastica, Lampedusa, 1-3 giugno 1998.

Bacci P., **Brusasca G.**, Morselli M.G., Negri A., **Tinarelli G.** (1998): "Modellistica di diffusione per la gestione dei rifiuti", RICICLA '98, Rimini, 17-20 settembre 1998.

Degrazia G., Anfossi D., Fraga de Campos Velho H., Ferrero E., (1998) "A Lagrangian decorrelation time scale for non-homogeneous turbulence", Boundary-Layer Meteorology, 86, 525-534.

Degrazia G., D.Anfossi (1998) : "Estimation of the Kolmogorov constant C0 from classical statistical diffusion theory", Atmospheric Environment, 32, 3611-3614. Pergamon Press, Oxford

Desiato F., Anfossi D., Trini Castelli S., Ferrero E., **Tinarelli G.** (1998) , "The role of wind field, mixing height and horizontal diffusion investigated through two Lagrangian particle models", Atmospheric Environment, 32, 4157-4165.

Ferrero E., Anfossi D., **Tinarelli G.**, Tamiazzo M. (1998) "Intercomparison of Lagrangian stochastic models based on two different PDF's", 5th International Conference on Harmonisation within Atmospheric Dispersion Modeling for Regulatory Purposes, Rhodes, Greece, 18-21 May 1998.

Ferrero E., D. Anfossi (1998) : "Comparison of PDFs, closures schemes and turbulence parameterizations in Lagrangian Stochastic Models", Int. J. Environment and Pollution, 9, 384-410

Ferrero E., D. Anfossi (1998) : "Sensitivity analysis of Lagrangian Stochastic models for CBL with different PDF's and turbulence parameterizations". Air Pollution Modelling and its Applications XII, S.E. Gryning and N. Chaumerliac eds., Plenum Press, New York

Tinarelli G., Anfossi D., Bider M., Ferrero E., Trini Castelli S. (1998)   : "A new high performance version of the Lagrangian particle dispersion model SPRAY, some case studies", Preprints of the 23rd CCMS-NATO meeting, Varna, 28 September - 2 October 1998, 343-350. DEMETRA publications.

Anfossi D., Bellasio R., Bianconi R., Bider M., Canepa E., Modesti F., Mosca S., Ratto C., **Tinarelli G.**, Trini Castelli S. (1999) : "A prototype integrated system of models simulating accidental releases and atmospheric dispersion in a topographically complex area". 4th International Congress "Energy, Environment and Technological Innovation", Rome, September 20-24, 1999.

Carvalho J., G. Degrazia, D.Anfossi, S. Trini Castelli (1999) : "Simulation of Copenhagen tracer diffusion experiment by means of a Lagrangian particle model", Hybrid Methods in Engineering, 1, 309-327

Ferrero E., Anfossi D., **Tinarelli G.** (1999) : "Simulation of atmospheric dispersion in urban stable boundary layer". 6th International Conference on Harmonisation within Atmospheric Dispersion Modeling for Regulatory Purposes, Rouen, France, 11-14 October 1999.

Ferrero E., Tamiazzo M., Anfossi D., **Tinarelli G.** (1999) .: "Lagrangian stochastic models applied to urban atmospheric dispersion". 4th International Congress "Energy, Environment and Technological Innovation", Rome, September 20-24, 1999.

Sansigolo Kerr A., Anfossi D., Carvalho J., Trini Castelli S. (1999) : "A dispersion study of the aerosol emitted by fertilizer plants in the region of Serra do Mar Sierra, Cubatao, Brazil". 6th International Conference on Harmonisation within Atmospheric Dispersion Modeling for Regulatory Purposes, Rouen, France, 11-14 October 1999.

Sansigolo Kerr A., Anfossi D., Aparecida Do Nascimiento S. (1999) : "Analysis of the atmospheric aerosol impact on Serra do Mar Sierra, Cubatao, Brazil", 2nd International Conference - Urban Air Quality, Madrid, 3-5 March, 1999.

Anfossi D., G. Degrazia, E. Ferrero, S.E. Gryning, **M.G. Morselli**, S. Trini Castelli (2000): "Estimation of the Lagrangian structure function constant C0 from surface layer wind data", Boundary-Layer Meteorology, 95, 249-270

Anfossi D. (2000):, "Short Review of Lagrangian Stochastic Models for the Simulation of the Atmospheric Pollutant Dispersion", Hybrid Methods in Engineering, 2, 261-279

Anfossi D., G. Degrazia, E. Ferrero, S.E. Gryning, **M.G. Morselli**, S. Trini Castelli: (2000): "Estimation of Kolmogorov constant C0 from sonic anemometer measurements in the Atmospheric Surface Layer". Air Pollution Modelling and its Applications XIII, S.E. Gryning and E. Batchvarova eds., Kluwer Academic / Plenum Press, New York, 631-639

Carvalho J., Degrazia G., Anfossi D., Trini Castelli S. (2000):, "Simulacão da dispersão de poluentes na camada limite planetaria utilizando um sistema de modelos", Ciencia e Natura, Volume Especial 2000, 9-43.

Ferrero E., Anfossi D., **Tinarelli G.**, Tamiazzo M. (2000):, "Intercomparison of Lagrangian stochastic models based on two different PDF's", Int. J. Environment and Pollution, 14, 225-234

Sansigolo Kerr A., Anfossi D., Trini Castelli S., Nascimiento S. (2000): "Investigation of inhalable aerosol dispersion at Cubatão by means of a modelling system for complex terrain", Hybrid Methods in Enginnering, 2, 389-407

Tinarelli G., D.Anfossi, M. Bider, E.Ferrero, S. Trini Castelli (2000): "A new high performance version of the Lagrangian particle dispersion model SPRAY, some case studies". Air Pollution Modelling and its Applications XIII, S.E. Gryning and E. Batchvarova eds., Kluwer Academic / Plenum Press, New York, 499-507.

Brusasca G., Carboni G., **Finardi S.**, Sanavio D., **Tinarelli G.**, Toppetti A. (2001): "Comparison of a Gaussian (ISC3) and a Lagrangian Particle Model (SPRAY) for Regulatory applications in Flat and Complex Terrain Sites Representative of Typical Italian Landscape", presented to the 7th International Conference on Harmonization within Atmospheric Dispersion Modelling for Regulatory Purposes, Belgirate, Italy, May 28-31, 2001.

Carvalho J., Degrazia G. , Anfossi D. , Trini Castelli S. (2001): "Study of the transport and diffusion process in the PBL using the RAMS and SPRAY models: application to the TRACT experiment". Air Pollution

Modelling and its Applications XIV, S.E. Gryning and F.A. Schiermeier eds., Kluwer Academic / Plenum Press, New York.

Carvalho J., Anfossi D., Trini Castelli S., Degrazia G.A. (2001): "Application of a model system for the study of transport and diffusion in complex terrain to the TRACT experiment", Atmospheric Environment, 36, 1147-1161

Cuffini S., Pavone F., Anfossi D., **Nanni A.**, **Tinarelli G.** (2001): "Metodologie integrate per il controllo della qualità dell'aria in aree ad alta urbanizzazione". Proceedings of the congress "Arie di città" – Bologna 28-30 Novembre 2000

Ferrero E., Anfossi D., **Tinarelli G.**, Trini Castelli S. (2001): "Lagrangian Particle Simulation of an EPA Wind Tunnel Tracer Experiment in a Schematic Two-Dimensional Valley". Air Pollution Modelling and its Applications XIV, S.E. Gryning and F.A. Schiermeier eds., Kluwer Academic / Plenum Press, New York

Ferrero E., D.Anfossi, **G. Tinarelli** (2001): "Simulation of atmospheric dispersion in urban stable boundary layer", Int. J. Environment and Pollution, 16 (1-6), 1-8.

Finardi S., **Tinarelli G.**, **Nanni A.**, Anfossi D., Ferrero E., Trini Castelli S. (2001): "In situ diagnostic or nested prognostic meteorological models to drive dispersion simulations in complex area: a comparison in a real application". Air Pollution Modelling and its Applications XIV, S.E. Gryning and F.A. Schiermeier eds., Kluwer Academic / Plenum Press, New York

Sansigolo Kerr A., Anfossi D., Carvalho J., Trini Castelli S. (2001): "A dispersion study of the aerosol emitted by fertilizer plants in the region of Serra do Mar Sierra, Cubatao, Brazil", Int. J. Environment and Pollution, 16, 251-263

Sansigolo Kerr A., Anfossi D., Jonas da Costa Carvalho, **Finardi S.**, Trini Castelli S. (2001) "Analysis of the Middle Range Transport of tha Aerosol from Cubatão by means of a Modelling System for Complex Terrain". Proceedings of the 7th International Conference on Harmonization within Atmospheric Dispersion Modelling for Regulatory Purposes, Belgirate, Italy, May 28-31, 2001, 405-409.

Tinarelli G., Alessandrini S., D. Anfossi, F. Pavone, S. Cuffini (2001) "Assessment of pollution impact over Turin suburban area using integrated methods". Proceedings of the 25th NATO/CCMS International Technical Meeting on Air Pollution Modelling and its Application, Louvaine la Neuve 15-19 Oct 2001.

Breznik B., Boznar M., Mlakar P., **Tinarelli G.**, (2002). Dose protectionusing dispersion models. 8th Conference on Harmonization within Atmospheric Dispersion Modeling for Regulatory Purposes. Sofia, 14-17 October, 409-413.

Carvalho J., Degrazia G., Anfossi D., Jacondino de Campos C., Roberti D.R., Sansigolo Kerr A., (2002). "Lagrangian stochastic dispersion modelling for the simulation of the release of contaminants from tall and low sources", Meteorologische Zeitschrift, 11, 89-97.

Finardi S., **Brusasca G.**, **Calori G.**, **Nanni A.**, **Tinarelli G.**, Agnesod G., Pession G., Zublena M. (2002). "Integrated air quality assessment of an alpine region: evaluation of the Mont Blanc tunnel re-opening effects" 8th Conference on Harmonization within Atmospheric Dispersion Modeling for Regulatory Purposes. Sofia, Bulgaria, 14-17 October, 404-408.

Maro, D., M. Bouzom, F. Bompay, C. Lac and D. Herbert (2002) Comparison of Lagrangian atmospheric dispersion models (DIFPAR, SPRAY) with krypton 85 measurements taken around La Hague spent fuel reprocessing plant 8th Conference on Harmonization within Atmospheric Dispersion Modeling for Regulatory Purposes. Sofia, Bulgaria, 14-17 October, 404-408

Nanni A., **Brusasca G.**, **Calori G.**, **Finardi S.**, **Silibello C.**, **Tinarelli G.**, Zublena M., Agnesod G., Pession G., Savoye M. (2002). "Integrated assessment of traffic impact in an Alpine region", Seventh Highway & Urban Pollution Symposium, Barcelona (Spain), 20-23 May.

Trini Castelli S., Ferrero E., Anfossi D. (2002) "Turbulence statistics estimation and dispersion simulation scenarios in urban environment". Proceedings of 8th Workshop on Harmonisation within Atmospheric Dispersion Modeling for Regulatory Purposes, Sofia, Bulgaria, 14-17 October 2002

Calori G., De Maria R., M. Clemente, F. Lollobrigida, S. Finardi, **G. Tinarelli** (2003) "Air quality integrated assessment in Turin urban area using atmospheric transport and dispersion models" 4th International Conference on Urban Air Quality Measurement, Modelling and Management. Prague, 25-27 March 2003, 214-217.

Ferrero E., Trini Castelli S., Anfossi D. (2003), "Turbulence fields for atmospheric dispersion models in horizontally non-homogeneous conditions", Atmospheric Environment, 37, 2305-2315 .

Trini Castelli S., Ferrero E., Anfossi D. (2003), "Atmospheric dispersion in non-homogeneous conditions – simulation of a wind tunnel tracer experiment". Proceedings of PHYSMOD2003: International Workshop on Physical Modelling of Flow and Dispersion Phenomena. 3-5 September 2003, Prato, Italy.

Trini Castelli S., Anfossi D., Ferrero E. (2003) "Evaluation of the environmental impact of two different heating scenarios in urban area", Int. J. Environment and Pollution, 20, 207-217.

Armand P., Achim P., Commanay J., Chevallaz-Perrier R., Moussafir J, Moon D., Albergel A. (2004) "Mesoscale dispersion of Xenon along the Rhone Valley in France – Results of a modelling system chaining ADAS, MM5,MINERVE and SPRAY" 9th International Conference on Harmonisation within Atmospheric Dispersion Modelling for Regulatory Purposes, Garmisch 1-4 June 2004.

Armand P., Achim P., Commanay J., Monfort M.., Carrere J, Oldrini O., Commanay J. Albergel A. 2004 "Simulation of the plume Gamma Exposure Rate With 3D Lagrangian Particle model SPRAY and Post-processor Cloud-Shine" 9th International Conference on Harmonisation within Atmospheric Dispersion Modelling for Regulatory Purposes, Garmisch 1-4 June 2004.

Gariazzo C., Pelliccioni A., Bugliolo M.P., Scalisi G. 2004 "Evaluation of a Lagrangian Particle Model (SPRAY) to assess environmental impact of an industrial facility in complex terrain", Water Air and Soil Pollution, 155, 137-158

Moussafir J., Oldrini O., **Tinarelli G**, Sontowski J, Dougherty C. 2004: "A new operational approach to deal with dispersion around obstacles : the MSS (Micro-Swift-Spray) software suite", 9th International Conference on Harmonisation within Atmospheric Dispersion Modelling for Regulatory Purposes Garmisch 1-4 June 2004.

Tinarelli G., **Brusasca G.**, Oldrini O., Anfossi D., Trini Castelli S., Moussafir J. (2004): "Micro-Swift-Spray (MSS) a new modelling system for the simulation of dispersion at microscale, general description and validation", Proc. of the 27th CCMS-NATO meeting, Banff (CANADA), 25-29 Oct 2004.

Albergel, A.,Fresneau A., Commanay J. , Lacome J.M., Moussafir J. (2004) "Operational on-line modelling tool: evaluation of the three common techniques (Gaussian puff, Eulerian and Lagrangian). Application on Fos-Berre area" 9th International Conference on Harmonisation within Atmospheric Dispersion Modelling for Regulatory Purposes Garmisch 1-4 June 2004.

Anfossi D., Physick W., (2004) "Lagrangian Particle Models", Chapter 11 of Air Quality Modeling - Theories, Methodologies, Computational Techniques, and Available Databases and Software. Vol. II - Fundamentals (P. Zannetti, Editor). Published by The EnviroComp Institute and the Air & Waste Management Association

Brusasca G., **Tinarelli G.**, Oldrini O., Anfossi D., Trini Castelli S., Moussafir J. (2005), Micro-Swift-Spray (MSS) a new modelling system for the simulation of dispersion at microscale. General description and validation. Air Pollution Modelling and its Applications XVII, C. Borrego and D. Steyn eds., Kluwer Academic / Plenum Press, in press

D. Anfossi, **G. Tinarelli**, S. Trini Castelli, E. Ferrero, D. Oettl, G. Degrazia (2005) "Well mixed condition verification in windy, low wind speed conditions" 10th International Conference on Harmonisation within Atmospheric Dispersion Modelling for Regulatory Purposes, Sissi (Malia), Creta, 17-20 Oct 2005

Armand P., Achim P., Monfort M., Carrère J., Oldrini O., Commanay J., Albergel A. (2005) : "Simulation of the plume gamma exposure rate with 3D lagrangian particle model SPRAY and post-processor CLOUD_SHINE", 10th International Conference on Harmonisation within Atmospheric Dispersion Modelling for Regulatory Purposes, Sissi (Malia), Creta, 17-20 Oct 2005

Armand P., Commanay J., Nibart M., Albergel A., Achim P. (2007) : "3D simulations of pollutants atmospheric dispersion around the building of an industrial site. Comparison of Mercure CFD approach with Micro-Swift-Spray semi-empirical approach", 11th International Conference on Harmonisation within Atmospheric Dispersion Modelling for Regulatory Purposes, Cambridge, UK. 2-5 July 2007

D. Anfossi, **G. Tinarelli**, S. Trini Castelli, G. Belfiore (2007) "Proposal Of A New Lagrangian Particle Model For The Simulation Of Dense Gas Dispersion" 11th International Conference on Harmonisation within Atmospheric Dispersion Modelling for Regulatory Purposes, Cambridge, UK. 2-5 July 2007

Castelli S.T., Reisin T. **G. Tinarelli G.** "Comparison of RAMS, RMS and MSS Modelling Systems for High Resolution Simulations in Presence of Obstacles for the MUST Field Experiment" NATO Science for Peace

and Security Series C: Environmental Security, 1, Volume 4, Air Pollution Modeling and its Application XXI, Part 1, Pages 9-14

Tinarelli G., Anfossi D., Trini Castelli S., Albergel A., Ganci F., Belfiore G., Moussafir J. (2007) : "Development of a lagrangian particle model for dense gas dispersion in urban environment",29th NATO/SPS International Technical Meeting on Air Pollution Modelling and its Application, 24-28 September 2007, University of Aveiro, Aveiro, Portugal

Gariazzo, C., Papaleo, V. , Pelliccioni, A., **Calori, G., Radice, P., Tinarelli, G.** (2007) Application of a Lagrangian particle model to assess the impact of harbour, industrial and urban activities on air quality in the Taranto area, Italy, Atmospheric Environment, 41, 6432-6444.

Tinarelli G., **Brusasca G.**, Oldrini O., Anfossi D., Castelli S.T., Moussafir (2007) "Micro-Swift-Spray (MSS): A New Modelling System for the Simulation of Dispersion at Microscale. General Description and Validation" Air Pollution Modeling and Its Application XVII 2007, 5, 449-458, DOI: 10.1007/978-0-387-68854-1_49

Armand, P., Olry, C., Albergel, A., Duchenne, C.(2008) "3D simulation of the dispersion in the urban environment in case of an explosion using TESATEX pre-processor, Micro-SWIFT-SPRAY modelling system" 12th International Conference on Harmonisation within Atmospheric Dispersion Modelling for Regulatory Purposes, Cavtat, Croatia, October 6-9, 2008.

Anfossi, D., **Tinarelli, G.**, Trini Castelli, S., Commanay, J., Nibart, M. .(2008) « MicroSpray simulation of dense gas dispersion in complex terrain" 12th International Conference on Harmonisation within Atmospheric Dispersion Modelling for Regulatory Purposes, Cavtat, Croatia, October 6-9, 2008

Tinarelli, G., Piersanti, A., Radice, P., Clemente, M., De Maria, R. (2009) Microscale Modelling Simulations for the site characterization of air quality stations in an urban environment, *Radiation Protection Dosimetry*, doi: 10.1093/rpd/ncp225.

Trini Castelli, S., Anfossi, D., **Finardi, S**. (2010) Simulations of the dispersion from a waste incinerator in the Turin area in three different meteorological scenarios, *Int. J. Environment and Pollution*, 40, 10–25.

C. Duchenne, P. Armand, H. Dupont (2010) « Development of a 3D modelling suite from the global scale to the urban Anfossi, D., **Tinarelli, G.**, Trini Castelli, S., Nibart, M., Olry, C., Commanay, J. (2010) A new Lagrangian particle model for the simulation of dense gas dispersion, Atmospheric Environment, 44, 753-762.

Anfossi, D., **Tinarelli,G.**, Trini Castelli, S., Ferrrero, E., Oettl, D., DeGrazia, G.A. (2010) Well Mixed Condition verification in windy and low windspeed condition, *International Journal of Environment and Pollution*, 40, 49-61.

scale using MM5 and Micro-SWIFT-SPRAY. Application to the dispersion of a toxic release in New York City. 13th International Conference on Harmonisation within Atmospheric Dispersion Modelling for Regulatory Purposes, Paris, FRANCE. 1-4 June 2010

S. Trini Castelli, L. Mortarini, **G. Tinarelli**, D. Anfossi (2010) "Development and application of the microscale Lagrangian particle dispersion model MicroSpray for the simulation of hydrogen accidental releases" . 13th International Conference on Harmonisation within Atmospheric Dispersion Modelling for Regulatory Purposes, Paris, FRANCE. 1-4 June 2010

M. Z. Boznar, P. Mlakar, B. Grasic, **G. Tinarelli** (2010) "Environmental impact assessment of new Thermal Power Plant Šoštanj Block 6 in highly complex terrain" 13th International Conference on Harmonisation within Atmospheric Dispersion Modelling for Regulatory Purposes, Paris, FRANCE. 1-4 June 2010

C. Olry, J. Moussafir, P. Castanier, **G. Tinarelli**, O. Fourcault, A. Plassais (2010) « Applications of the MSS model (MICRO-SWIFT SPRAY) to photocatalytic coating simulations 13th International Conference on Harmonisation within Atmospheric Dispersion Modelling for Regulatory Purposes, Paris, FRANCE. 1-4 June 2010

S. Perdriel, J. Moussafir, C. Dérognat, J. Cortinovis (2010) Simulation of SO2 episodes exceeding EU regulations in the industrial area of Le Havre with the MM5, SWIFT and SPRAY models 13th International Conference on Harmonisation within Atmospheric Dispersion Modelling for Regulatory Purposes, Paris, FRANCE. 1-4 June 2010

Moussafir J., Olry Ch, Castanier P., **Tinarelli G.**, Perdriel S. (2010)"Applications Of The MSS (Micro-Swift-Spray) Model To Long-Term Regulatory Simulations Of The Impact Of Industrial Plants" 13th International

Conference on Harmonisation within Atmospheric Dispersion Modelling for Regulatory Purposes, Paris, FRANCE. 1-4 June 2010

Boštjan Grašič, Marija Zlata Božnar and Primož Mlakar (2011) "Validation Of Local Scale Prognostic And Diagnostic Air Pollution Modeling System In Extremely Complex Terrain" 14th International Conference on Harmonisation within Atmospheric Dispersion Modelling for Regulatory Purposes, Kos, GREECE. 2-6 October 2010

Primož Mlakar, Marija Zlata Božnar, Boštjan Grašič, Gianni Tinarelli (2011) "Zasavje Canyon Regional On-Line Air Pollution Modeling System In Highly Complex Terrain As A Support To Eu Directives" 14th International Conference on Harmonisation within Atmospheric Dispersion Modelling for Regulatory Purposes, Kos, GREECE. 2-6 October 2010

Primož Mlakar, Marija Zlata Božnar, Boštjan Grašič and Darko Popović (2011) Fireworks Air Pollution In Slovenia. 14th International Conference on Harmonisation within Atmospheric Dispersion Modelling for Regulatory Purposes, Kos, GREECE. 2-6 October 2010

Grazia Ghermandi, Sergio Teggi, Sara Fabbi, Alessandro Bigi and Marco Michele Zaccanti (2011) "Atmospheric Impact Of Power Plant Stack Emissions". 14th International Conference on Harmonisation within Atmospheric Dispersion Modelling for Regulatory Purposes, Kos, GREECE. 2-6 October 2010

Olivier Oldrini, Christophe Olry, Jacques Moussafir, Patrick Armand and Christophe Duchenne (2011) Development Of PMSS, The Parallel Version Of Micro-Swift-Spray. 14th International Conference on Harmonisation within Atmospheric Dispersion Modelling for Regulatory Purposes, Kos, GREECE. 2-6 October 2010

G. Pession, T. Magri, **G. Tinarelli** (2011) "Atmospheric Dispersion Of Asbestos Particles From Rural Building Roofs" 14th International Conference on Harmonisation within Atmospheric Dispersion Modelling for Regulatory Purposes, Kos, GREECE. 2-6 October 2010

Patrick Armand, Christophe Olry, Olivier Oldrini, Jérôme Carrère, Christophe Duchenne and Armand Albergel (2011) Simulation With Micro-Spray And Post-Processor Sprayshine Of The Irradiation Due To A Radioactive Plume And Its Deposition On All Accessible Surfaces In The Urban Environment 14th International Conference on Harmonisation within Atmospheric Dispersion Modelling for Regulatory Purposes, Kos, GREECE. 2-6 October 2010

Christophe Duchenne, Patrick Armand, Olivier Oldrini, Christophe Olry, Jacques Moussafir (2011) "Application Of PMSS, The Parallel Version Of Mss, To The Micro-Meteorological Flow Field And Deleterious Dispersion Inside An Extended Simulation Domain Covering The Whole Paris Area" 14th International Conference on Harmonisation within Atmospheric Dispersion Modelling for Regulatory Purposes, Kos, GREECE. 2-6 October 2010

Maxime NIBART, Patrick ARMAND, Christophe OLRY, Christophe DUCHENNE and Armand ALBERGEL (2011) "The Indoor / Outdoor Pollutant Transfer Of A Hazardous Release: Application To A Parisian Railway Station" 14th International Conference on Harmonisation within Atmospheric Dispersion Modelling for Regulatory Purposes, Kos, GREECE. 2-6 October 2010

L. Mortarini, G. Carlino, **G. Tinarelli**, L. Mauri, S. Trini Castelli and D. Anfossi (2011) "Development Of The Microscale Lagrangian Particle Dispersion Model Microspray For The Simulation Of Two-Phase Releases" 14th International Conference on Harmonisation within Atmospheric Dispersion Modelling for Regulatory Purposes, Kos, GREECE. 2-6 October 2010

Frédéric Tognet1, Cyrille Turmeau, Ti L. Ha, Eric Tarnaud, Laurence Rouïl, Bertrand Bessagnet, Enric Robine, Yannick Morel (2011) "Numerical Modelling Of Microorganisms Dispersion In Urban Area: Application To Legionella" 14th International Conference on Harmonisation within Atmospheric Dispersion Modelling for Regulatory Purposes, Kos, GREECE. 2-6 October 2010

Tinarelli G., Mortarini L., Trini Castelli S., Carlino G., Moussafir J., Armand P., Anfossi D. () Microspray, a Lagrangian Particle Model of Turbulent Dispersion. Review and Validation. Accepted for publication in the AGU book "Lagrangian Modeling of the Atmosphere".

A.3 FARM 3D Eulerian reactive AQM

FARM (Flexible Air quality Regional Model) is a three-dimensional Eulerian model that accounts for the transport, chemical conversion and deposition of atmospheric pollutants, used for policy support, forecast systems and impact studies.

It has been originally derived by ARIANET from STEM (G.R. Carmichael, Centre for Global and Regional Environmental Research, Univ. of Iowa), a model extensively used and tested during the past two decades (Kitada et al., 1984; Carmichael et al., 1986; Hong and Carmichael, 1986; Chang et al., 1990; Carmichael et al., 1991; Shim and Carmichael, 1991; Mathur et al., 1992; Carmichael et al., 1998).

Its development is currently carried out by ARIANET, with the support of ENEA, ARPA-Piemonte, CINECA supercomputing centre, and the involvement of experienced users in testing activities.

The current user community is mostly made by national and local authorities and research institutes (the following figure shows the main computational domains to date). It is worth to cite that FARM:

- is the core of the atmospheric component of the **MINNI Italian national modelling system** (Ministry of the Environment, the Land and the Sea), used for policies support, either directly or through its two-way link with GAINS-Italy model;

- is used by the Italian **Regional Environmental Protection Agencies** (ARPAs) of: Lombardia, Piemonte, Valle d'Aosta, Veneto, Lazio, Puglia, for operational forecasting, yearly air quality evaluations and policy scenarios assessment respect to EU legislation;

- has been also used in **regional scenarios and impact assessment studies** in: Campania and Naples, Sardegna (Cagliari), Lombardia, Veneto, Northern and Central Italy, as well as in several studies of major power and industrial plants and transport infrastructures;

- is being used in **urban zooming** applications in Tunisia, Morocco and Israel.

These applications consist or have consisted in:

- yearly air quality assessments according to European Directive on Ambient Air Quality
- assessment of future scenarios and policies (e.g. measures involved in regional air quality plans)
- assessment of the impact of major infrastructures

Moreover, FARM is a key component of the following **operational forecast/near-real-time (NRT)** systems:

- Lombardia (Milano)
- Piemonte region, with zooms on Turin and Novara
- Lazio region, with zoom on Rome
- Italian QualeAria system at national scale
- New Delhi
- Rio de Janeiro

The code can be configured to be used in a variety of applications, according to specific problem features, computational resources and data availability. The code is also embedded in ARIA Regional, a comprehensive regional atmospheric simulation system, including orography, land-use, meteorology, emissions and IC/BC pre-processors, as well as post-processors to extracts statistics from the results (hourly / eight-hour / daily / yearly averages, percentiles, etc.) and interfaces with visualization tools.

The documented applications show that when fed by proper 3D meteorological fields and emission inventories, FARM air quality model fulfills the accuracy requirements given by European legislation (Directive 2008/50/EC of the European Parliament and of the Council of 21 May 2008 on ambient air quality and cleaner air for Europe) and by Legal Notice 478 of 2010, at urban, regional and wider scales.

FARM is also present in the **European Model Documentation System** (MDS, http://acm.eionet.europa.eu/databases/MDS/index_html), collecting information and descriptions about the most relevant meteorological/dispersion models available in Europe, and in **COST Model Inventory** (http://www.mi.uni-hamburg.de/index.php?id=539) revising enhanced meso-scale meteorological and air pollution dispersion models.

Finally, FARM is also currently participating in the **EURODELTA3 model intercomparison project** at continental scale, managed by the European Joint Research Centre of Ispra, involving some of the main European regional modeling team.

FARM major features are listed in the following sections.

A.3.1 Features

FARM major features include:

- emission of pollutants from area and point sources, with plume rise calculation and mass assignment to vertical grid cells

- overall solution technique: operator splitting with adaptive fractional steps

- advection-diffusion - horizontal: Blackman cubic polynomials (Yamartino, 1993); vertical: hybrid semi-implicit Crank-Nicolson / fully implicit scheme (Yamartino et al., 1992).

- turbulence: ABL-scaling, using related pre-processors (SURFPRO or PROG2FARM, depending whether the meteo driver is diagnostic or prognostic)

- chemistry and aerosols: flexible mechanism, assigned through KPP chemical pre-processor, either:

  o a simplified gas-phase mechanism derived from the EMEP Lagrangian Acid Deposition Model (Hov et al., 1988; EMEP, 2003) coupled with a bulk aerosol module;

  o the SAPRC99 gas-phase chemical 121 mechanism (Carter, 2000) coupled with the aero3 aerosol module, implemented in the Community Multiscale Air Quality (CMAQ) modeling system (Binkowski, 1999)

- gas-phase solvers: LSODE and Rosembrock

photolysis rates, either:

- o adjusted according to local solar zenith angle and height; actinic flux reduction effect from clouds;

- o use of of TUV code to calculate the effects of aerosol particles and gaseous species on the photolysis rates, considering different wavelength grids

- estimation of aerosol optical depth from of aerosol species

- treatment of heavy metals and polycyclic aromatic hydrocarbons (PAHs), with gas-aerosol partitioning

- dry removal of pollutants on the basis of deposition velocities (from SURFPRO pre-processor) depending on land type, season, surface meteorology, surface wetness, by means of a "big leaf" resistance model after Walcek (1986) and Wesley (1989)

- precipitation scavenging based on Maul (1980)

- zooming possibility: on-line one- or two-way nesting with an arbitrary number of computational grids

- assimilation of sparse observed data by nudging methods

- parallel execution on various class of machines, using OpenMP, MPI and mixed paradigms

- integrated with a complete modelling system (ARIA Regional) for multiscale air quality simulations

A.3.2 Input data

Most input data are in the form of hourly 2D/3D gridded fields (netCDF or ADSO/bin format):

- Emissions: hourly SO_2, NO_x, NH_3, CO, speciated VOC, and PM emissions at each grid location and (optionally) at a set of point sources. Emissions from an arbitrary set of tracers can be also considered.

- Meteorology: hourly 2D/3D fields of wind, air temperature, pressure, relative humidity, cloud cover, precipitation, turbulent horizontal and vertical diffusivities, surface resistances and gas deposition velocities. Can be provided (through the GAP grid adaptor) by a wide series of diagnostic/prognostic meteorological models; among the others have been used: RAMS, MM5, WRF, Lokal-Modell, SWIFT/MINERVE, CALMET.

- Topography height for each grid cell.

- 3D fields of initial conditions, either from measurements or coarser model grid results, throught the use of companion pre-processors (ICBC and BOUNDER).

- Boundary conditions: time-varying concentrations at lateral and top boundaries, also either from measurements or coarser model grid results (currently: EMEP, CHIMERE, FARM itself).

A.3.3 Output

Output quantities, in the form of hourly 2D/3D gridded fields (netCDF or ADSO/bin format):

- concentrations (at the surface or 3D)
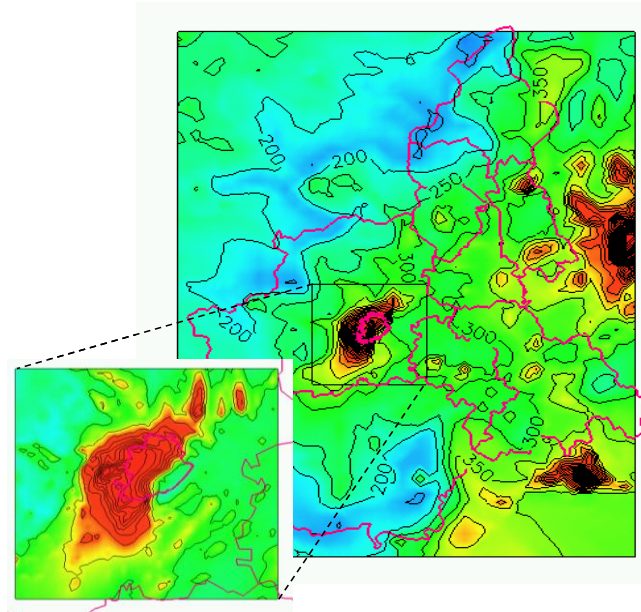
- deposition fluxes

As well as:

- domain balances and processes contributions

- restart file

- comprehensive logfile

The following figure shows an example of ground-level CO concentration fields computed by FARM on two nested grids (Piemonte Region and Torino metro area).

The following is a 3D plot of NO_2 concentration computed by FARM over Rio de Janeiro at 1 km resolution.
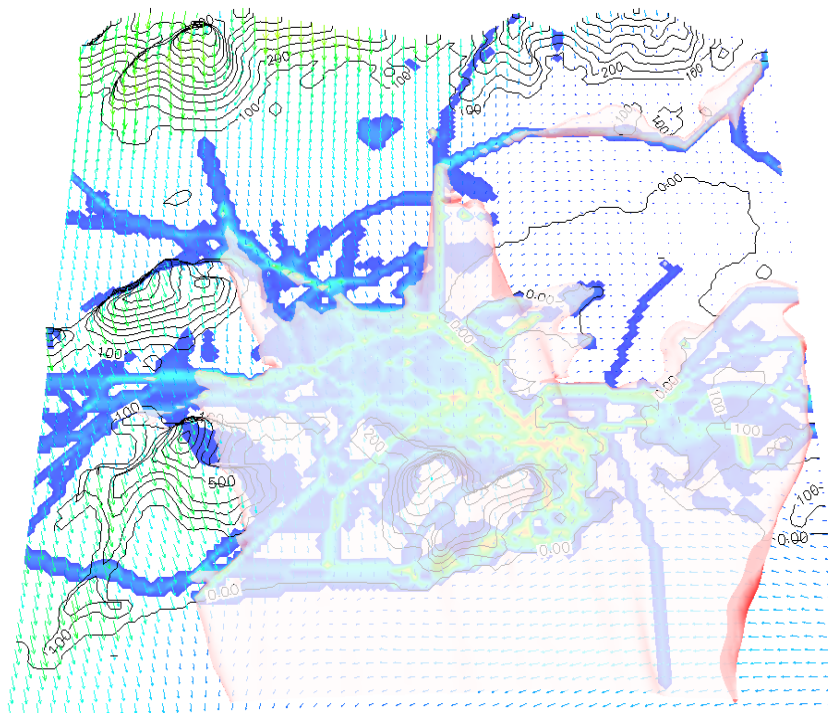
A.3.4 Scientific references

STEM

Carmichael G. R., Peters L. K., Saylor R. D. (1991) The STEM-II Regional Scale Acid Deposition and Photochemical Oxidant Model-I. An Overview of Model Development and Applications. Atmos. Environ., 25A, 10, 2077-2090.

Carmichael G.R., Peters L.K., Saylor R.D. (1990) The STEM-II regional scale acid deposition and photochemical oxidant model - I. An overview of model development and applications. Atmospheric Environment 25A, 2077-2090.

Carmichael, G. R., Uno I., Phadnis M. J., Zhang Y. and Sunwoo, Y. (1998) Tropospheric ozone production and transport in the springtime in east Asia, *J. Geophysical Research*, 103, 10649-10671.

Chang Y.-S., Carmichael G.R., Ueda H., Kurita H. (1990) Diagnostic evaluation of the components of the STEM-II model. *Atmos. Environ.*, **24A**, 2715-2731.

Hong M.-S., Carmichael G.R. (1986) Examination of a subgrid-scale parametrization for the transport of pollutants in a nonprecipitating cumulus cloud ensemble. *Atmos. Environ.*, **20**, 2205-2217.

Kitada T., Carmichael G.R., Peters L. (1984) Numerical simulation of the transport of chemically reactive species under land and sea breezes circulation, *J. Clim. App. Met.*, **23**, 1153-1172.

Mathur R., Saylor R.D., Peters L-K. (1992) The STEM-II regional-scale acid deposition and photochemical oxidant model - IV. The impact of emission reductions on mesoscale acid deposition in the lower Ohio River Valley. *Atmos. Environ.*, **26A**, 841-861.

Shim S.-G., Carmichael G.R. (1991) The STEM-II acid deposition and photochemical oxidant model - II. A diagnostic analysis of mesoscale acid deposition. *Atmos. Environ.*, **25B**, 25-45.

FARM formulation

Binkowski F. S. (1999) The aerosol portion of Models-3 CMAQ. In Science Algorithms of the EPA Models-3 Community Multiscale Air Quality (CMAQ) Modeling System. Part II: Chapters 9-18. D.W. Byun, and J.K.S.

Ching (Eds.). EPA-600/R-99/030, National Exposure Research Laboratory, U.S. Environmental Protection Agency, Research Triangle Park, NC, 10-1-10-16.

Binkowski F. S. (1999) The aerosol portion of Models-3 CMAQ. In Science Algorithms of the EPA Models-3 Community Multiscale Air Quality (CMAQ) Modeling System. Part II: Chapters 9-18. D.W. Byun, and J.K.S. Ching (Eds.). EPA-600/R-99/030, National Exposure Research Laboratory, U.S. Environmental Protection Agency, Research Triangle Park, NC, 10-1-10-16.

Binkowski, F.S. and U. Shankar (1995) The regional particulate matter model, 1. Model description and preliminary results. J. Geophys. Res., 100, 26191-26209.

Carter W.P.L. (1990) A detailed mechanism for the gas-phase atmospheric reactions of organic compounds. Atmospheric Environment 24A, 481-518.

Carter W.P.L. (2000) Documentation of the SAPRC-99 Chemical Mechanism for VOC Reactivity Assessment. Final Report to California Air Resources Board, Contract 92-329 and 95-308, SAPRC, University of California, Riverside,CA.

Chock D.P., Winkler S.L., Sun P. (1994) A comparison of stiff chemistry solvers for air quality modelling. Paper presented at the *Air & Waste Management Association 87*[th] *Annual Meeting*, Cincinnati, OH, June 19-24.

Geleyn J.-F. (1981) Some diagnostics of the cloud/radiation interaction in ECMWF forecasting model. ECMWF Workshop on radiation and cloud-radiation interaction in numerical modelling, 15-17 Oct. 1980, ECMWF, 135-162.

Hov O., Eliassen A., Simpson D. (1988) Calculation of the distribution of NOx compounds in Europe. In Isaksen I.S.A. (ed.) Troposheric ozone. Regional and global scale interactions, pp.239-262, Dordrecht D. Reidel.

Huang H-C., Chang J.S. (2001) On the performance of numerical solvers for a chemistry submodel in three-dimensional air quality models. I. Box model simulations. J. Geophys. Res. 106, 20175-20188.

Kumar N., Lurmann F.W., Carter W.P.L. (1995) Development of the Flexible Chemical Mechanism Version of the Urban Airshed Model. Final Report STI-94470-1508-FR, California Air Resources Board.

Maul P.R. (1980) Atmospheric transport of sulfur compound pollutants. Central Electricity Generating Board, MID/SSD/80/0026/R, Nottingham, England.

Marras, G.F., **Silibello, C.**, **Calori G.** (2012) A Hybrid Parallelization of Air Quality Model with MPI and OpenMP. *Recent Advances in the Message Passing Interface. Lecture Notes in Computer Science*, 7490, 235-245.

Sun P., Chock D.P., Winkler S.L. (1994) An implicit-explicit hybrid solver for a system of stiff kinetic equations. Air & Waste Management Association 87th Annual Meeting, Cincinnati, OH, June 19-24.

Yamartino R.J. (1993) Nonnegative, conserved scalar transport using grid-cell-centered, spectrally constrained Blackman cubics for applications on a variable-thickness mesh. Mon. Wea. Rev. 121, 753-763.

Yamartino R.J., Scire J.S., Carmichael G.R., Chang Y.S. (1992) The CALGRID mesoscale photochemical grid model - I. Model formulation. Atmospheric Environment 26A, 8, 1493-1512.

FARM recent applications

Baklanov A., Lawrence M., Pandis S., Mahura A., **Finardi S.**, Moussiopoulos N., Beekmann M., Laj P., Gomes L., Jaffrezo J.-L., Borbon A., Coll I., Gros V., Sciare J., Kukkonen J., Galmarini S., Giorgi F., Grimmond S., Esau I., Stohl A., Denby B., Wagner T., Butler T., Baltensperger U., Builtjes P., van den Hout D., van der Gon H. D., Collins B., Schluenzen H., Kulmala M., Zilitinkevich S., Sokhi R., Friedrich R., Theloke J., Kummer U., Jalkinen L., Halenka T., Wiedensholer A., Pyle J., and Rossow W. B. (2010) MEGAPOLI: concept of multi-scale modelling of megacity impact on air quality and climate, Adv. Sci. Res., 4, 115-120, 2010, www.adv-sci-res.net/4/115/2010/, doi:10.5194/asr-4-115-2010. (http://www.adv-sci-res.net/4/115/2010/asr-4-115-2010.pdf)

Baklanov, A., Hänninen, O., Slørdal, L. H., Kukkonen, J., Bjergene, N., Fay, B., **Finardi, S.**, Hoe, S. C., Jantunen, M., Karppinen, A., Rasmussen, A., Skouloudis, A., Sokhi, R. S., Sørensen, J. H. (2007) Integrated systems for forecasting urban meteorology, air pollution and population exposure, Atmos. Chem. Phys., 7, 855–874.

Calori G., **Finardi S.**, **Nanni A.**, **Radice P.**, Riccardo S., Bertello A., Pavone F. (2005) Long-term air quality modelling in Ivrea and Torino areas: sources contribution and scenario analysis. Proc. of 5th *Int. Conf. on Urban Air Quality*, Valencia (Spain), 29-31 March 2005.

Calori, G., Clemente, M., De Maria, R., **Finardi, S.**, Lollobrigida, F., **Tinarelli, G.** (2006) Air quality integrated modelling in Turin urban area, *Environmental Modelling and Software*, 21/4, 468-476.

Calori, G., **Finardi, S.**, **Nanni, A.**, **Radice, P.**, Riccardo, S., Bertello, A., Pavone, F. (2007) Long-term air quality assessment: modeling sources contribution and scenarios in Ivrea and Torino areas, Environmental Modelling and Assessment, 13, 329–335

De Maria R., Cascone C., Motta F., Picollo M.E., Clemente M., Bande S., Muraro M., Lollobrigida F., **Silibello C.** (2005) Simulation of a summer ozone episode: influence of emission resolution and initial/boundary conditions. Proc. of 5th *Int. Conf. on Urban Air Quality*, Valencia, Spain, 29-31 March 2005.

Finardi S., **D´Allura A.**, **Calori G.**, **Silibello C.**, De Maria R., Cascone C., Lollobrigida F. (2005) Deterministic air quality forecasting system for Torino urban area: verification on winter and summer episodes. Proc. of 5th *Int. Conf. on Urban Air Quality*, Valencia (Spain), 29-31 March 2005.

Finardi, S., De Maria, R., **D'Allura, A., Calori, G.**, Cascone, C., Lollobrigida, F. (2008) A Deterministic Air Quality Forecasting System For Torino Urban Area, Italy, *Environmental Modelling and Software*, 23, 344-355.

Gariazzo, C., Hänninen, O., Amicarelli, A., Pelliccioni, A., **Silibello, C.**, Sozzi, R., Jantune, M. (2011) Integrated model for the estimation of annual, seasonal, and episode PM10 exposures of children in Rome, Italy, *Air Quality, Atmosphere & Health*, 4, 169-178.

Gariazzo, C., **Silibello, C., Finardi, S., Radice, P., Piersanti, A., Calori, G.**, Cecinato, A., Perrino, C., Nussio, F., Pelliccioni, A., Gobbi, G.P. and Di Filippo, P. (2007) A gas/aerosol air pollutants study over the urban area of Rome using a comprehensive chemical transport model, Atmospheric Environment, 41, 7286–7303.

Kukkonen, J., Olsson, T., Schultz, D. M., Baklanov, A., Klein, T., Miranda, A. I., Monteiro, A., Hirtl, M., Tarvainen, V., Boy, M., Peuch, V.-H., Poupkou, A., Kioutsioukis, I., **Finardi, S.**, Sofiev, M., Sokhi, R., Lehtinen, K. E. J., Karatzas, K., San Jose´, R., Astit, M. (2012) A review of operational, regional-scale, chemical weather forecasting models in Europe, *Atmospheric Chemistry and Physics*, 12, 1-87.

Silibello C., Calori G., Arduino G., Contardi C., Sordi F. (2005) Model based yearly air quality evaluation on Piemonte region. Accepted at 10th *International Conference on Harmonisation within Atmospheric Dispersion Modelling for Regulatory Purposes*, Sissi (Malia), Crete, Greece 17-20 October, 2005.

Silibello C., **Calori G.**, **Brusasca G.**, Giudici A., Angelino E., Fossati E., Peroni E., Buganza E., Degiarde E. (2005) Modelling of PM10 concentrations over Milano urban area: validation and sensitivity analysis of different aerosol modules. Proc. of 5th *Int. Conf. on Urban Air Quality*, Valencia, Spain, 29-31 March 2005.

Silibello C., Calori G., Finardi S., Pirovano G. (2001) Sensitivity of Ozone Predictions to Prognostic and Diagnostic Generated Meteorological Fields. Proc. of *A Changing Atmosphere - 8th European Symposium on the Physico-Chemica Behaviour of the Atmospheric Pollutants*, Torino, 17-20 September 2001.

Silibello C., Calori G., Pirovano G., Carmichael G.R. (2001) Development of STEM-FCM (Flexible Chemical mechanism) modelling system – Chemical mechanisms sensitivity evaluated on a photochemical episode. Proc. of *APMS'01*, Parigi 9-13 aprile 2001.

Silibello, C., Calori, G., Brusasca, G., Giudici, A., Angelino, E., Fossati, G., Peroni, E., Buganza, E. (2008) Modelling of PM10 Concentrations Over Milano Urban Area Using Two Aerosol Modules, *Environmental Modelling and Software*, 23, 333-343.

Silibello, C., Calori, G., Costa, M. P., Dirodi, M., Mircea M., **Radice, P.**, Vitali L., Zanini G. () Benzo[a]pyrene modelling over Italy: comparison with experimental data and source apportionment. In publication in the Special Issue "Science in Support of International Treaties on POPs" of *Atmospheric Pollution Research*.

Zanini G., Monforti F., Ornelli P., Pignatelli T., Vialetto G., **Brusasca G.**, **Calori G., Finardi S., Radice P., Silibello C.** (2004) The MINNI project. 9th *Conference on Harmonisation within Atmospheric Dispersion Modelling for Regulatory Purposes*, 1-4/6/2004, Garmisch-Partenkirchen (D).

APPENDIX B – Data sources used in the study

Purpose / use	Data Type	Source
Preparation of emission input for modelling	Data regarding DPS and MPS: • details of each plant • stack parameters • information regarding the type of fuel used • operating times and conditions (over past periods and foreseen for new operating conditions) • information regarding pollution control equipment, including its efficiency	Enemalta Corporation
	Data from continuous emission monitoring systems (CEMS) installed at DPS and MPS: NOx, CO, SO2, dust and flow, from 2010 to 2014	Enemalta Corporation
	Discontinuous stack emissions monitoring data: measurements of lead, cadmium, arsenic, nickel and vanadium emissions to air mate at DPS and MPS from 2011 to 2014	Enemalta Corporation
	Statistics about shipping movements at Valletta harbour	Valletta Port Authority
	Statistics about shipping movements at Marsaxlokk harbour	Malta Freeport
	Statistics on aircrafts movements	Malta International Airport
	Capacity/movement data for 31st March 1979 fuel storage & Wied Dalam Depot	Enemalta Corporation
	Capacity/movement data for Oil Tanking Malta and San Lucian Oil Company fuel depots	Oiltanking website
	Road traffic emissions from National Emission Inventory for 2011	MEPA
	Road network maps: OpenStreetMap (www.openstreetmap.org)	OpenStreetMap
	Time modulation data from the National Travel Survey	Transport Malta
	Emissions related to fishing activities: from National Emission Inventory for 2011	MEPA
	Emissions from international shipping routes: EMEP database	EMEP
	Emissions from Marsa Thermal Treatment Facility: WasteServ website (http://statistics.wasteservmalta.com/scadamonthly.aspx)	WasteServ Ltd

	Other area emission sources: National Emission Inventory for 2011	MEPA
Preparation of emission input for modelling; meteorological modelling	CORINE Land Cover 2006 database (http://dataservice.eea.europa.eu/dataservice)	EEA
Meteorological modelling	Background meteorological output fields operationally produced by the Air Quality Modeling System (AQMS) QualeAria for years 2010-2012 (http://www.aria-net.eu/QualeAria/index_en.html)	ARIANET QualeAria
	USGS digital terrain model	USGS
Meteorological modelling verification	Meteorological data recorded at MEPA's monitoring stations for years 2009-2012	MEPA
NOx to NO2 estimation in local modelling	Hourly NOx and NO2 measurements from Msida monitoring station	MEPA
Ambient background level concentrations	NO2 rural background: QualeAria air quality modeling system results	ARIANET QualeAria
	PM rural background: EMEP model results	EMEP
Contribution of Sahara dust	PM10 measurements from continuous monitoring stations for year 2011	MEPA
Boundary conditions for background domain	Boundary conditions for gaseous species: QualeAria results	ARIANET QualeAria
	PM boundary conditions: EMEP model results	EMEP
Dispersion model verification	NO_2, PM_{10} and $PM_{2.5}$ data collected from continuous monitoring stations	MEPA